DOE/NASA/0114-80/1
NASA CR-159822
ELK P-1006

DESIGN STUDY OF FLAT BELT CVT FOR ELECTRIC VEHICLES

Emerson L. Kumm
Mechanical Engineer
Tempe, Arizona

March 1980

Prepared for
NATIONAL AERONAUTICS AND SPACE ADMINISTRATION
Lewis Research Center
Under Contract DEN 3-114

for
U.S. DEPARTMENT OF ENERGY
ELECTRIC AND HYBRID VEHICLE DIVISION
OFFICE OF TRANSPORTATION PROGRAMS

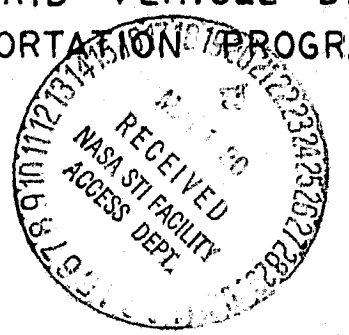

DOE/NASA/0114-80/1
NASA CR-159822
ELK P-1006

DESIGN STUDY OF FLAT BELT CVT FOR ELECTRIC VEHICLES

Emerson L. Kumm
Mechanical Engineer
Tempe, Arizona 85282

March 1980

Prepared for
National Aeronautics and Space Administration
Lewis Research Center
Cleveland, Ohio 44135
Under Contract DEN 3-114

for
U.S. DEPARTMENT OF ENERGY
Electric and Hybrid Vehicle Division
Office of Transportation Programs
Washington, D.C. 20545

EMERSON LAWRENCE KUMM
mechanical engineer

TABLE OF CONTENTS

LIST OF FIGURES

LIST OF TABLES

PROGRAM SCOPE

The basic objective of the work given in this report was to obtain an optimum arrangement of a continuously variable speed transmission (CVT) to couple the high speed output shaft of an energy storage flywheel to the drive train of an electric vehicle, together with a preliminary design layout of the complete CVT. All of the CVT components were required to be selected and sized based on specific design requirements and other criteria using engineering design studies. The design requirements were based on a representative vehicle weight of 1700 KG (3750 pounds) with the speed ratio of the CVT continuously controllable using an input speed of 14,000 to 28,000 RPM and output speed of 0 to 5,000 RPM. The CVT is required to transmit up to 75 KW (100 HP) on a transient basis as well as 450 N-m (330 lb- ft) at the point of wheel slip. In addition, the CVT is required to operate with 90 percent reliability for 2600 hours with an average output of 16 KW (22 HP) at 3,000 RPM and an average input of 21,000 RPM. Also, the CVT must provide for disengagement of the flywheel, be capable of absorbing the sudden shock loads and torques typical of automotive applications and permit bi-directional power flow. Other design criteria specified by NASA included special attention to maximizing the operating efficiency, and minimizing future production costs, size, and weight. Reliability and maintainability are stressed, as well as early consideration for reducing noise. Stable, reliable, responsive controls are required. The work program called for identification, analysis and recommended solutions to all technology advances required to develop the selected CVT to meet the specified design requirements and other criteria. Also, the recommended CVT concept was to be studied for its suitability for application to an alternate electric and a hybrid vehicle application. The work on these alternate applications was limited to identification of differences in CVT

arrangement, size, ratio, and other design variables and to any additional new technology requirement. The program also called for determining how the selected CVT would scale in size using larger or smaller maximum output design torques. This report was specified in the program to give sufficient detail and analysis that would enable verification that the design is credible and capable of meeting the required design specifications and criteria.

The approach taken by this contractor was to study the CVT design using technical consultants to help design gear train layouts and gears, to help specify bearings, to help make engineering design drawings, and to help with other areas, such as noise attenuation. While specific detailed engineering analyses were made to determine appropriate equipment sizes and arrangements, the potential overall installation arrangement and appropriate controls for an electric vehicle were also considered. The studies involved many design choices, so that it was necessary to use an iterated approach and, sometimes, to redirect or correct the design or analysis. The approach was taken that a prompt design choice, analysis and, if needed, subsequent redesign and analysis is usually preferable to long delays in making the initial engineering design choice. An effort was made to document the work in rather detailed monthly progress reports. Correspondence with equipment suppliers and solicitation of their cooperation was also regarded as an important part of the work effort. Considerable attention was given to organizing the work to permit a logical chronological sequence of the analyses and design.

I. EXECUTIVE SUMMARY

This report shows a novel flat belt continuously variable transmission (CVT) to be a very efficient, compact arrangement of reasonably low weight to transfer power between a high speed flywheel and/or an electric motor and the output shaft of an electrically powered vehicle. A flywheel energy storage element in the electric car provides the large power desirable for vehicle acceleration and passing and permits the efficient use of a much smaller electric motor. However, the flywheel decreases in speed as its energy is applied to increase the speed of the vehicle, thus making necessary a CVT.

The new flat belt pulley concept is used in the CVT shown in Figure I-1. The belt is positioned radially by drive elements located by guideways in the sideplates of the pulleys. Thus, the speed ratio of the two pulleys connected by the flat belt may be changed by varying the radial position of the belt in one pulley versus the other. This belt drive is used in combination with a differential gearing arrangement shown in Figure I-2, which allows the CVT to operate down to zero output speed. The preliminary design drawings of the CVT recommended by this study are shown in Figures I-3, I-4, and I-5. The overall dimensions of transmission are 602 by 301 by 484 mm (23.7 x 11.9 x 19.0 inches) with a calculated weight of 44.5 KG (98.0 pounds).

The CVT uses a conventional automotive type synchronizer to shift the transmission from a low speed to a high speed mode of operation, giving the complete speed range from zero to 5,000 RPM output as shown in Figure I-6 to be covered. A single lever speed control on the flat belt pulley is reversed simultaneously with the synchronizer shift, as indicated in Figure I-7, the speed control schematic. The power flow in the transmission passes through both the belt and

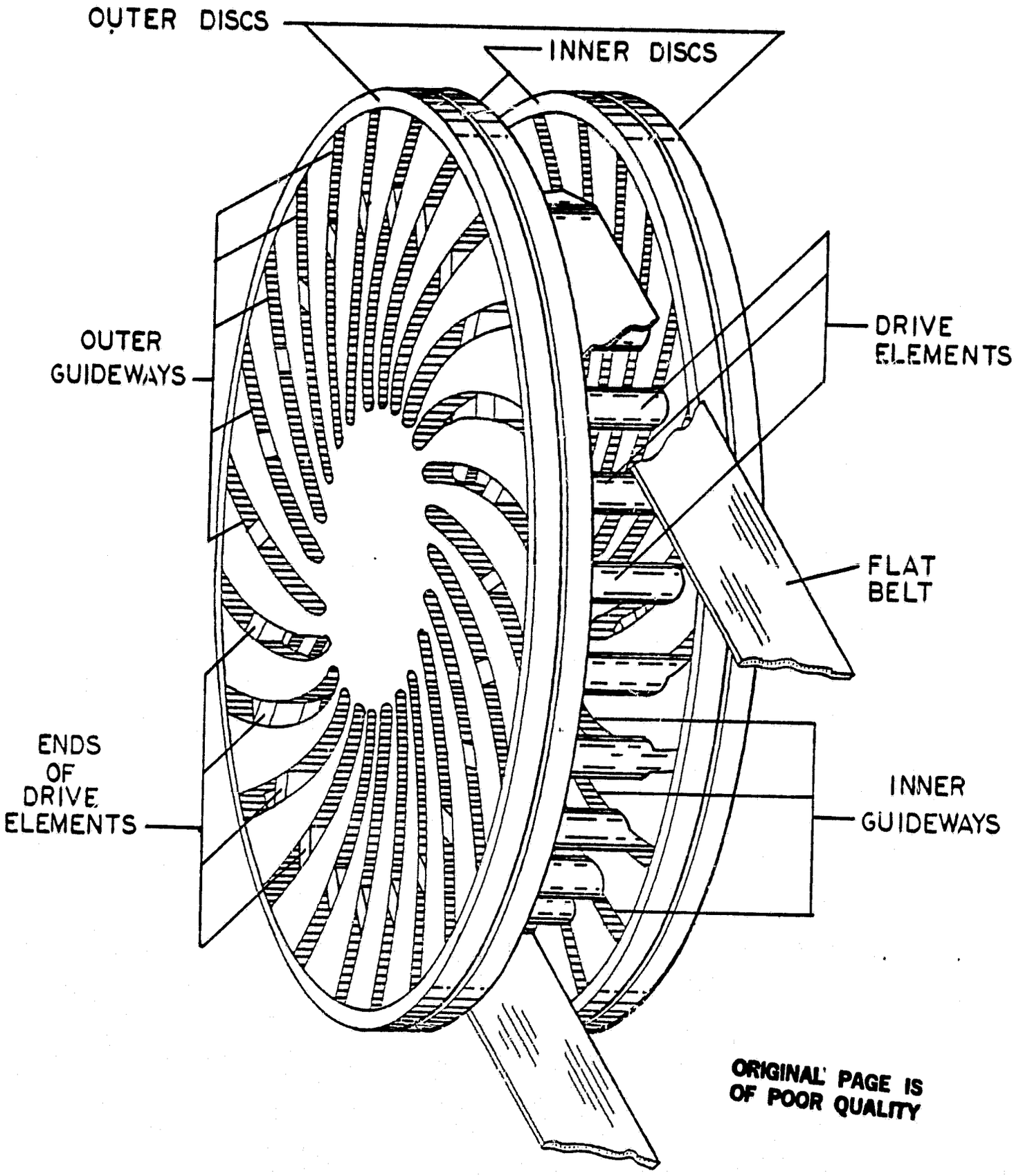

Figure I-1 — FLAT BELT ROTARY POSITIONING CONCEPT

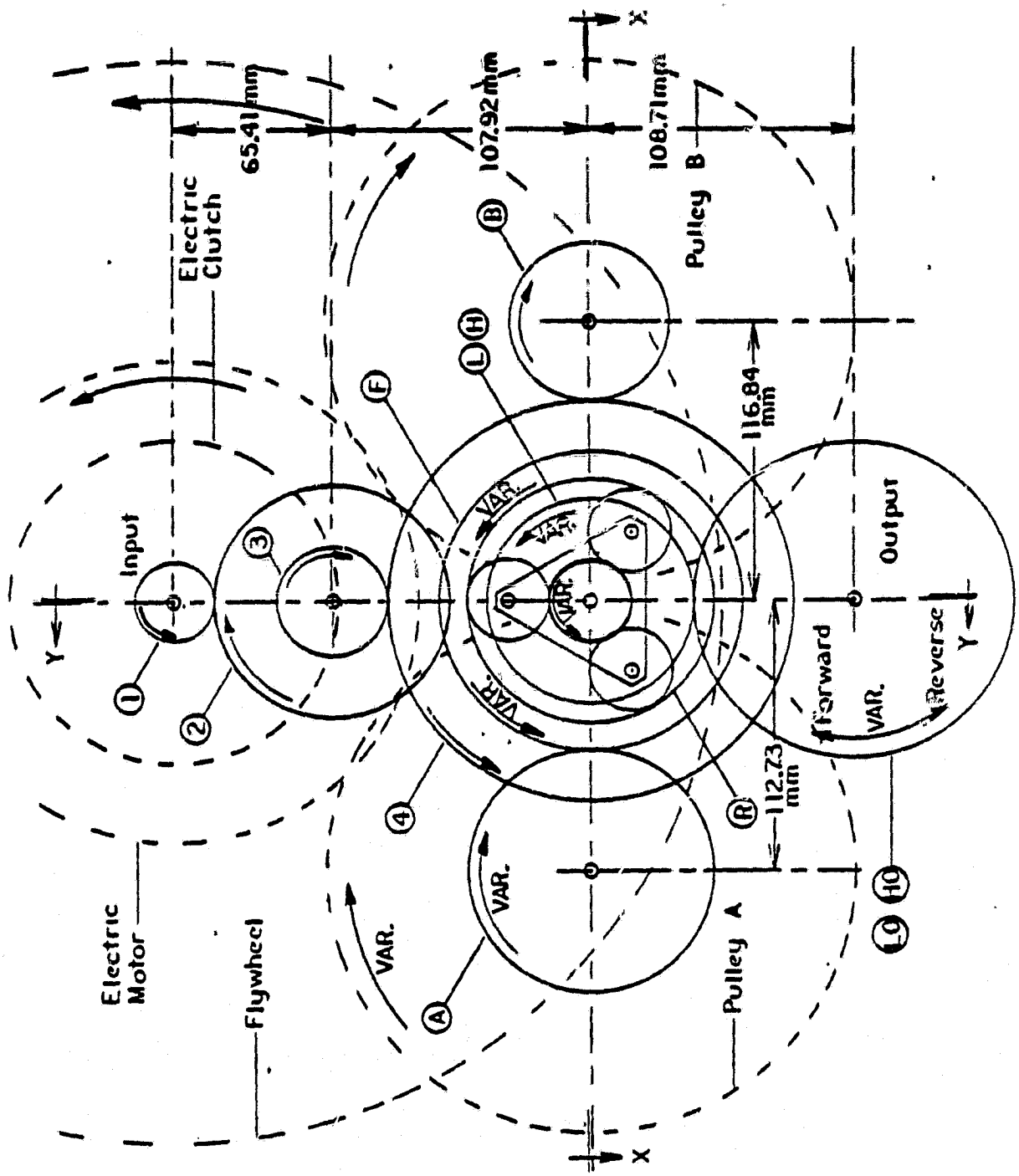

Figure I-2 — PLAN VIEW - TRANSMISSION GEARS

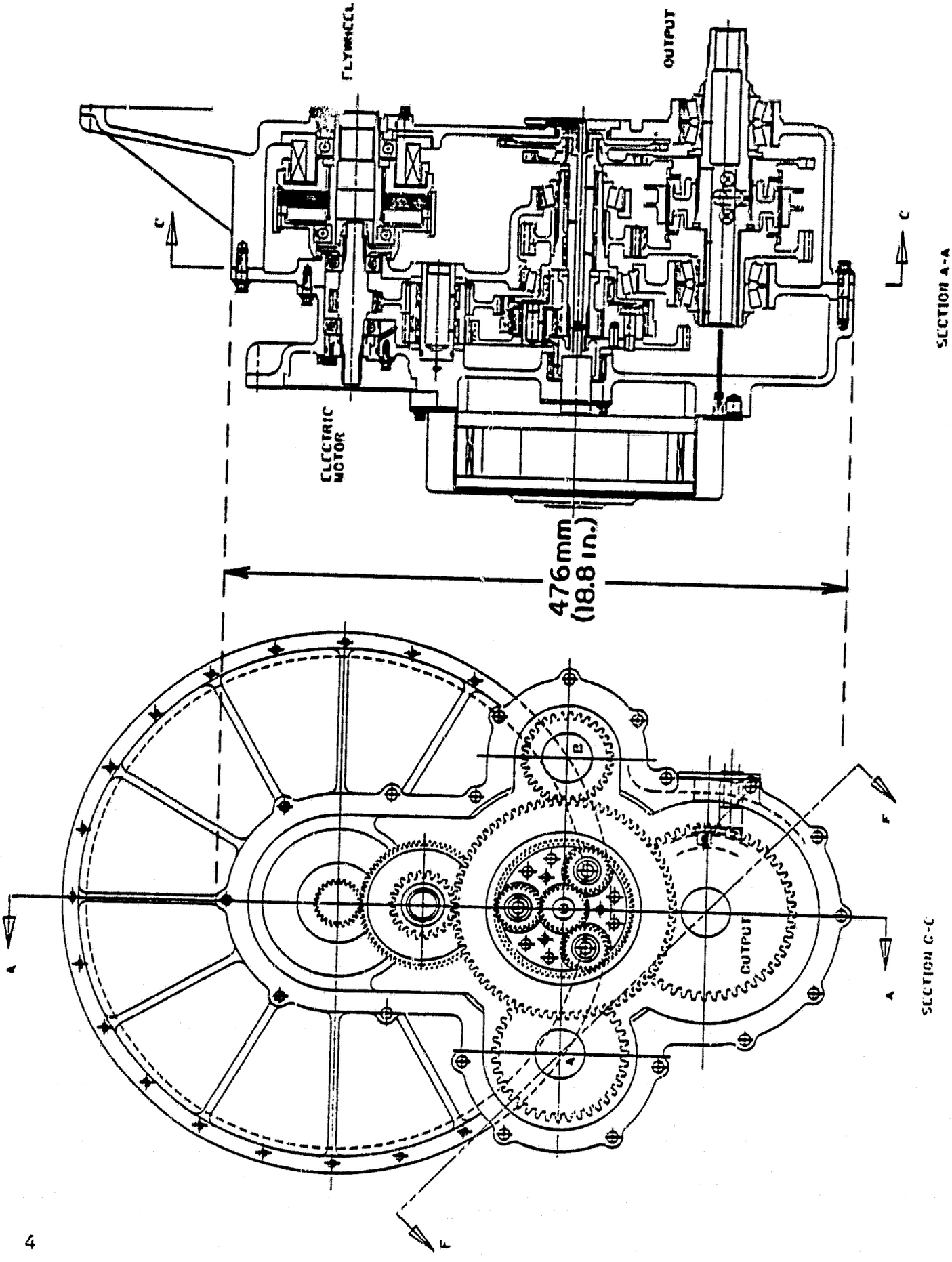

Figure I-3 — FLAT BELT TRANSMISSION - SHEET 1

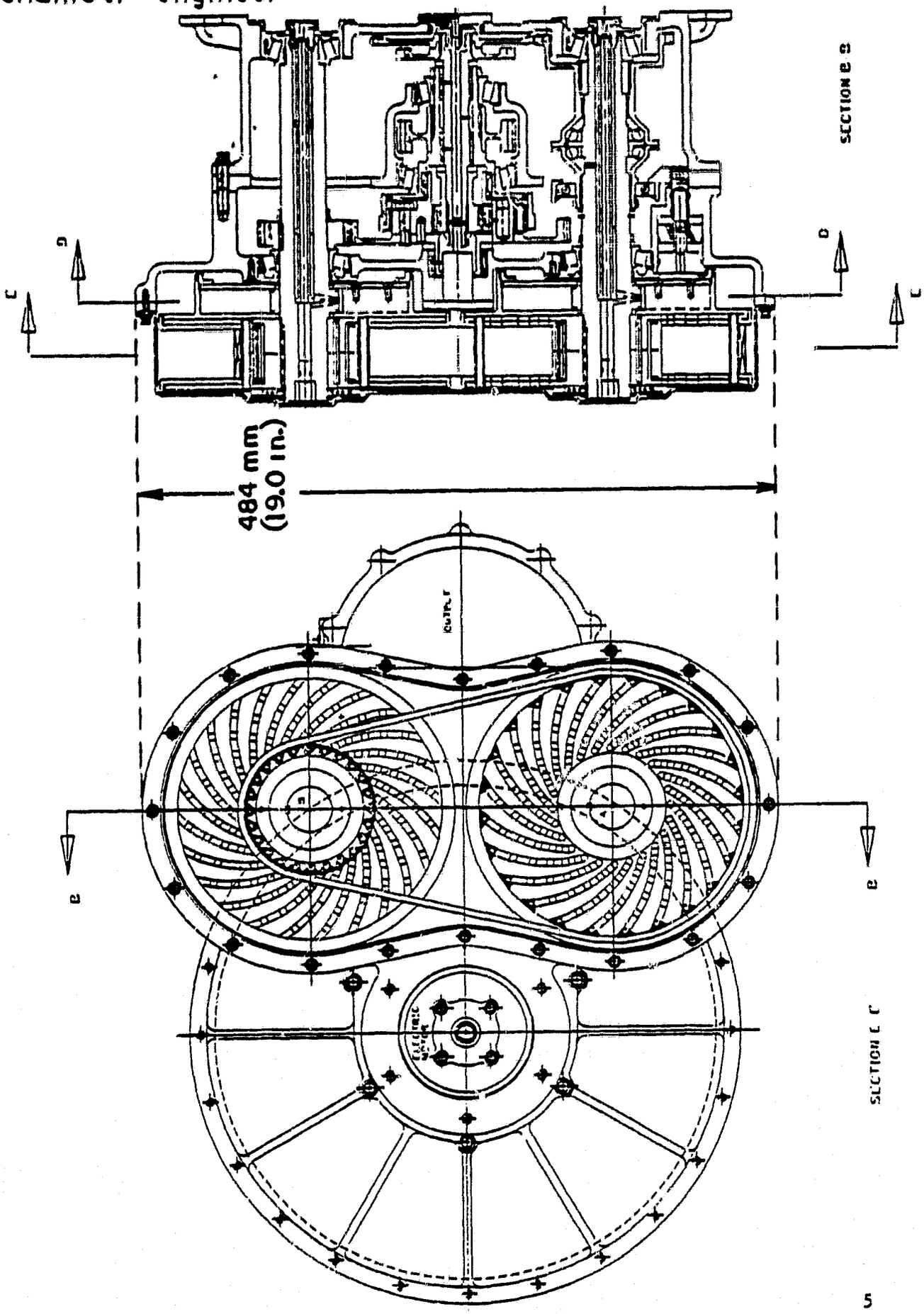

Figure I-4 — FLAT BELT TRANSMISSION - SHEET 2

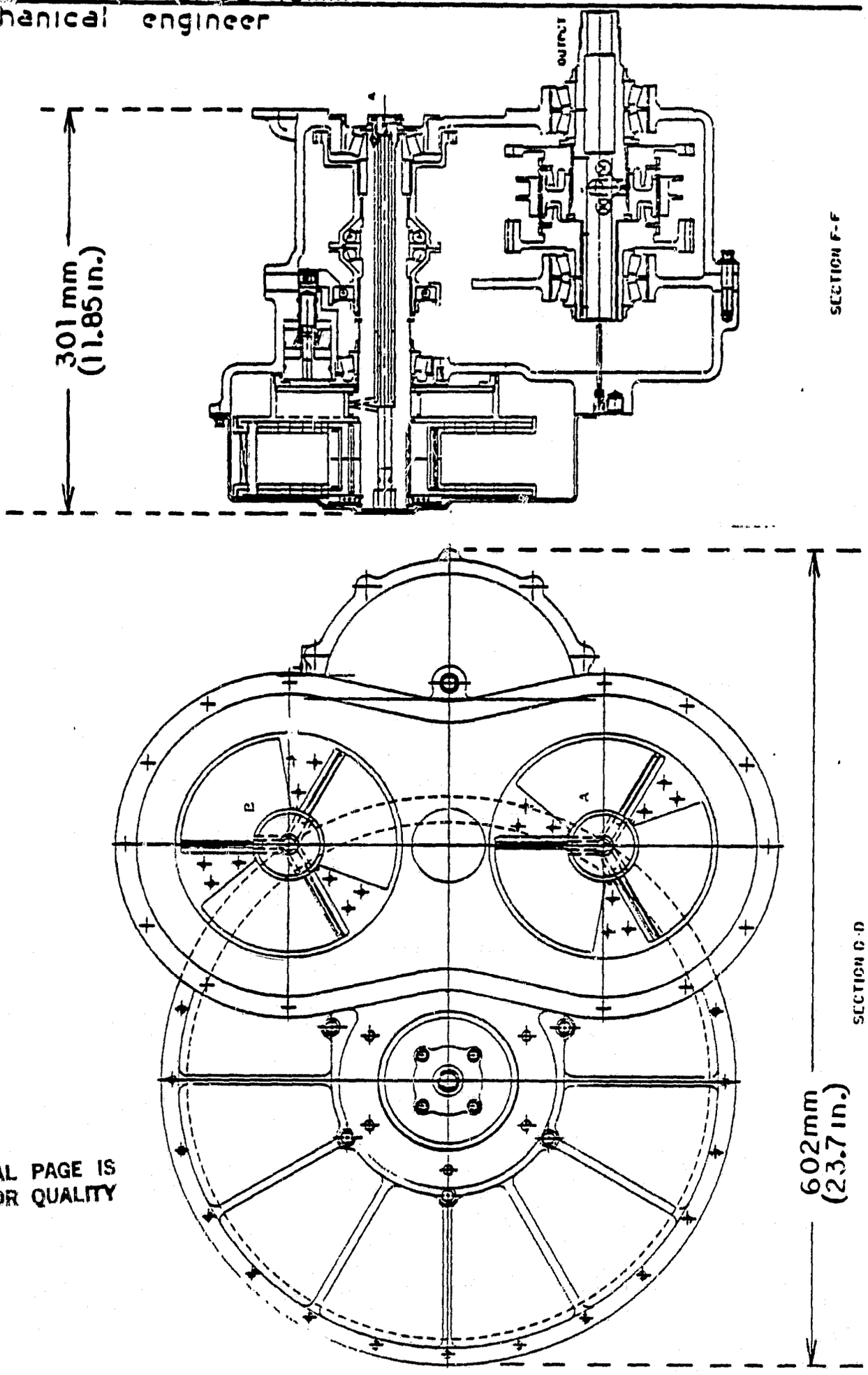

Figure 5 — FLAT BELT TRANSMISSION - SHEET 3

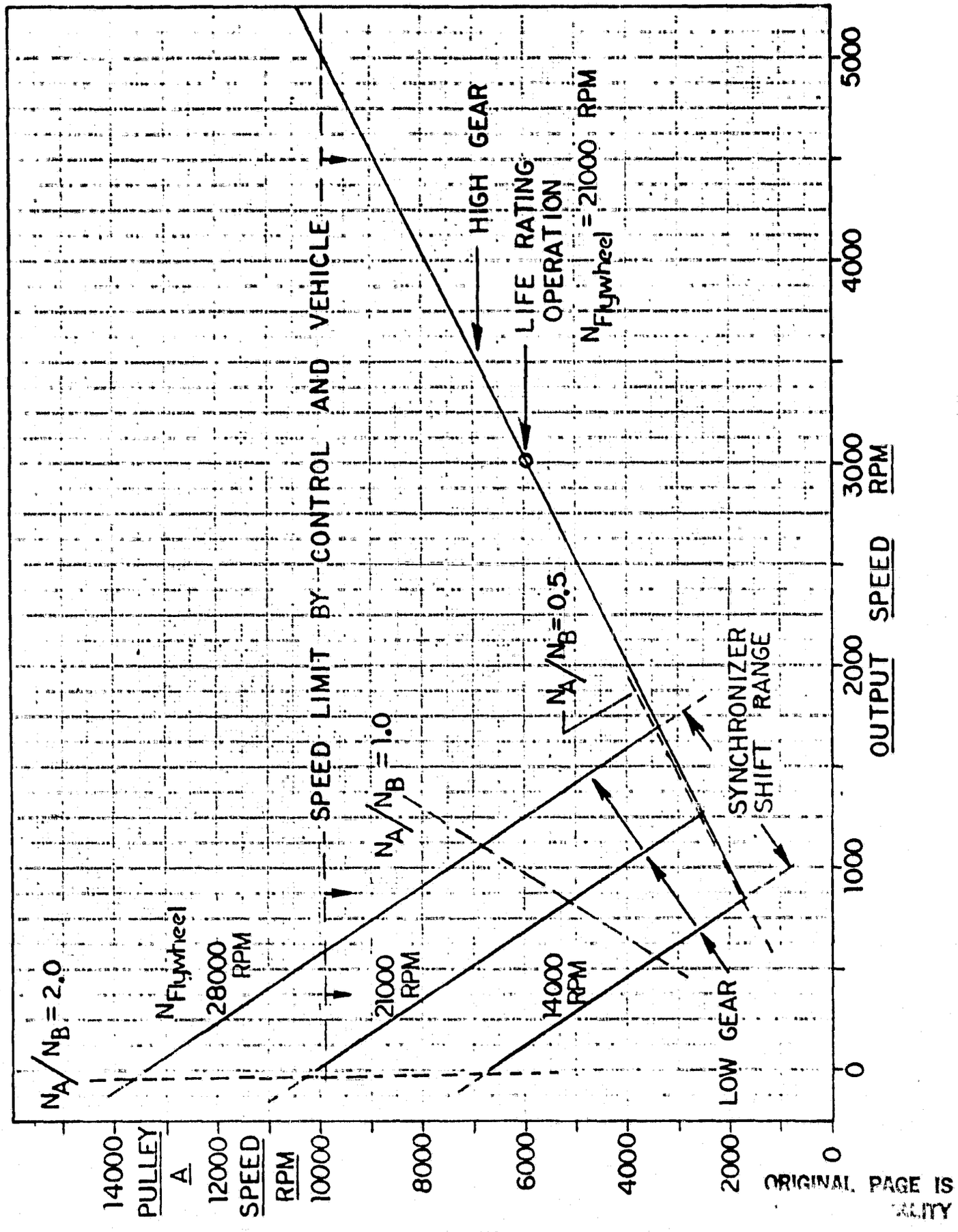

Figure 6 – PULLEY AND OUTPUT SPEEDS - FLAT BELT CVT

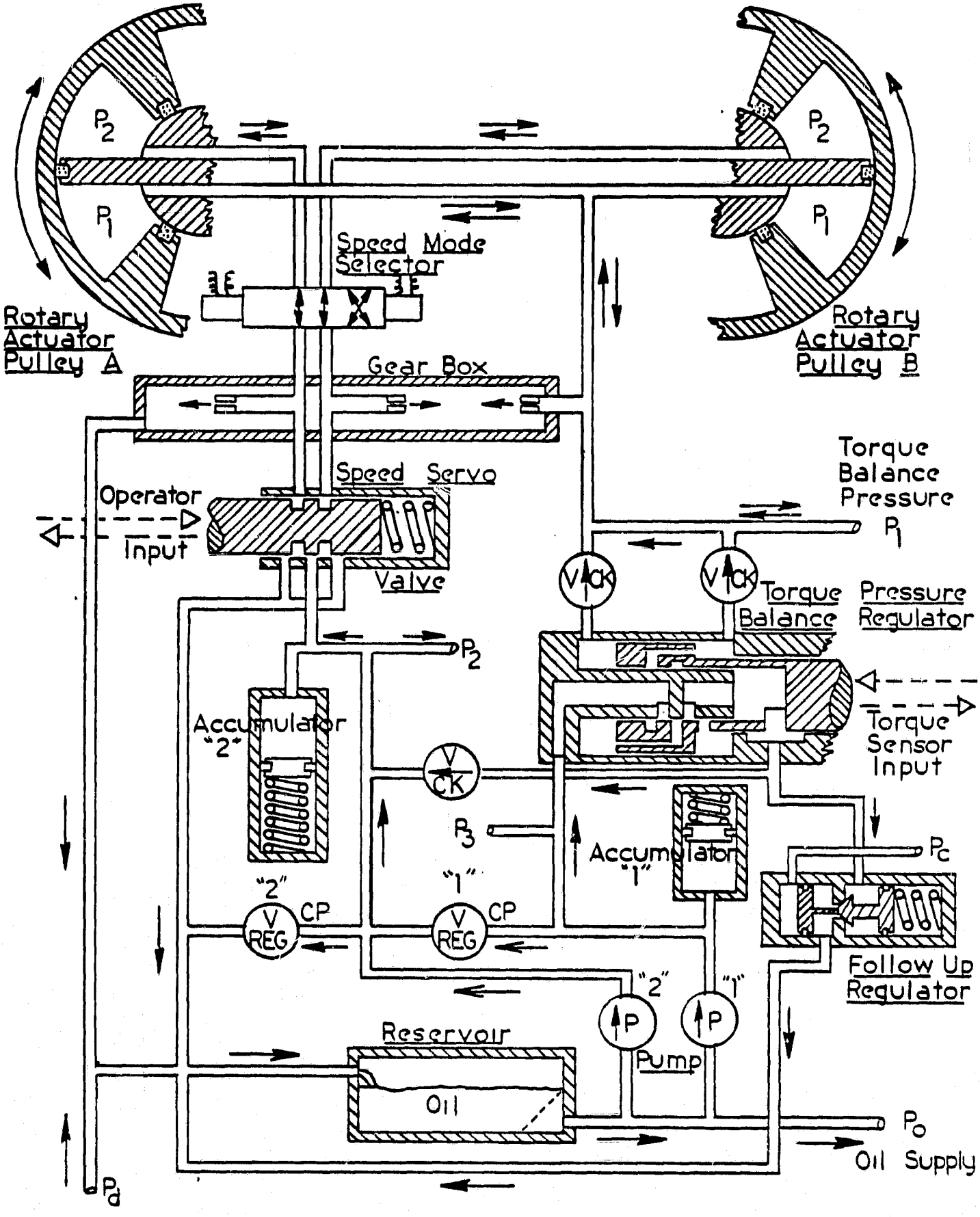

Figure I-7 — SPEED CONTROL

planetary differential gear in the low speed mode, but through only the belt in the high speed mode. The direction of power flow through the belt in the high speed mode is reversed from the power flow through the belt in the low speed mode. The transmission gearing arrangement incorporates a torque sensor which is used to load the rotary actuators in the pulleys to vary the tension of the flat belt only as needed to prevent it from slipping, thus maximizing transmission efficiency. The bearing selections and gear sizes were based on the loads specified by the design requirements of the study. Stresses and critical shaft speeds were calculated and parts designed to have adequate safety factors. The transmission power losses were examined in detail, resulting in the transmission efficiency curves, as given in Figures I-8, I-9, and I-10. The calculated efficiency varies from 95.2 - 93.2 percent at the rated design point as the input speed varies from 14,000 RPM to 28,000 RPM.

The required technology advancements were also examined and specified in this study. The current "state of art" was used substantially but several new improvements are proposed from these studies. A new electrically actuated clutch was designed which includes an integral balancing of components to permit very high speed operation. Integration of the transmission with operation of electric motors and their speed control resulted in an arrangement that would use the electric motor more efficiently at the high speed input with the flywheel. Accelerator clutches may also be incorporated in the transmission to provide additional transient power capability using the differential gearing in combination with the belt drive. Significant improvements also appear possible in the art of design of flat belts, although the "current state of art" was used to size the belts in the present preliminary design.

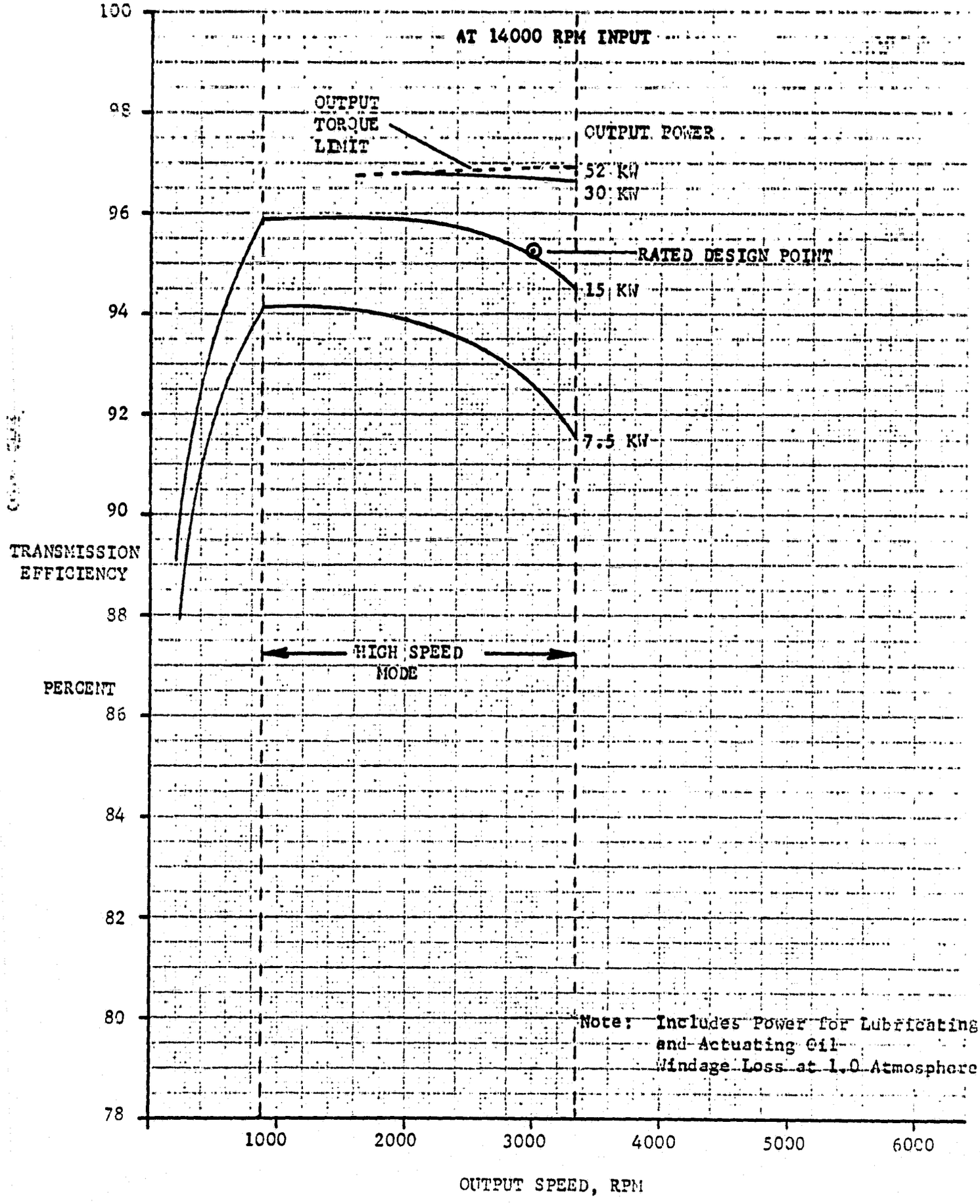

Figure I-8 — TRANSMISSION EFFICIENCY AT 14000 RPM INPUT

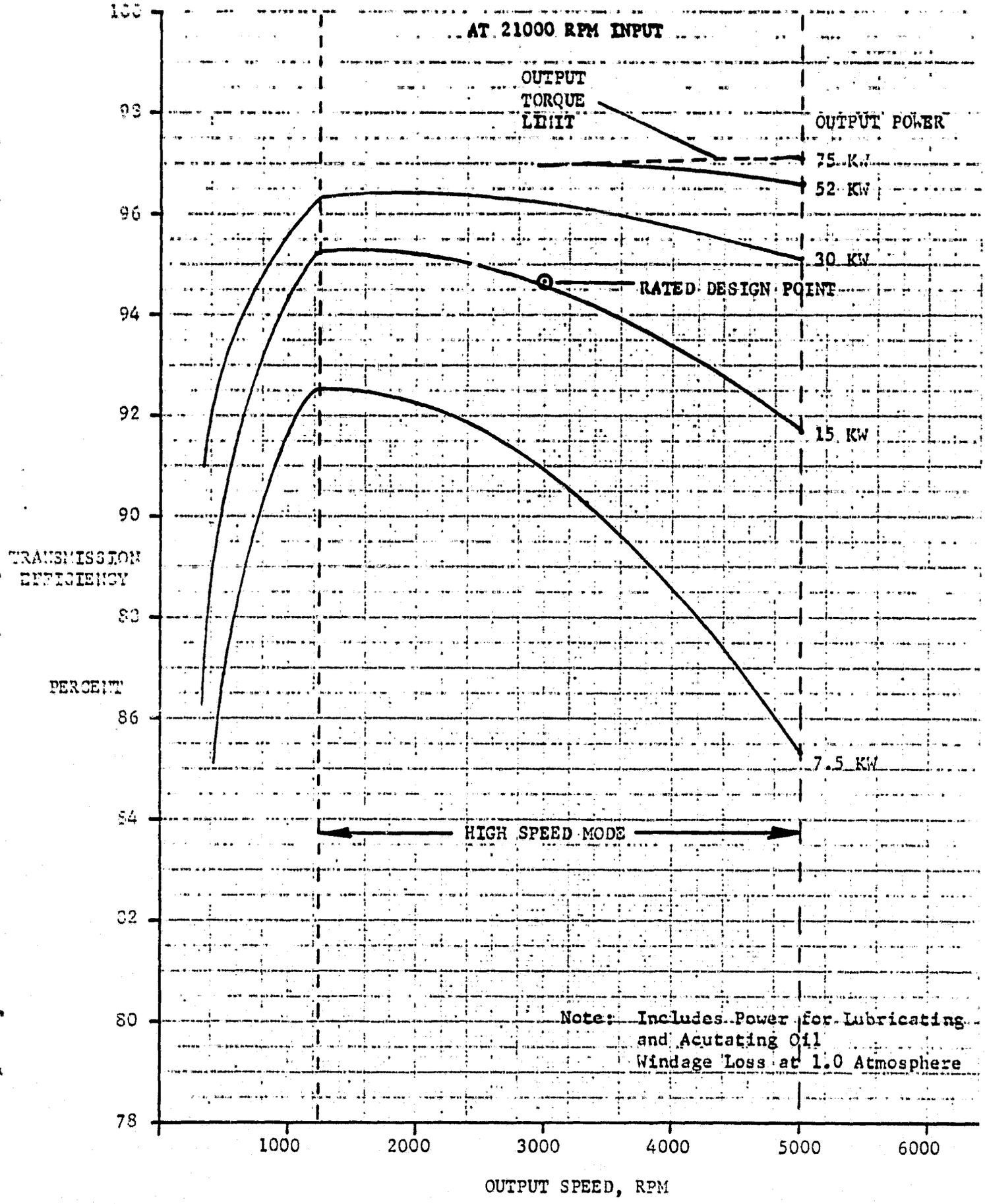

Figure I-9 — TRANSMISSION EFFICIENCY AT 21000 RPM INPUT

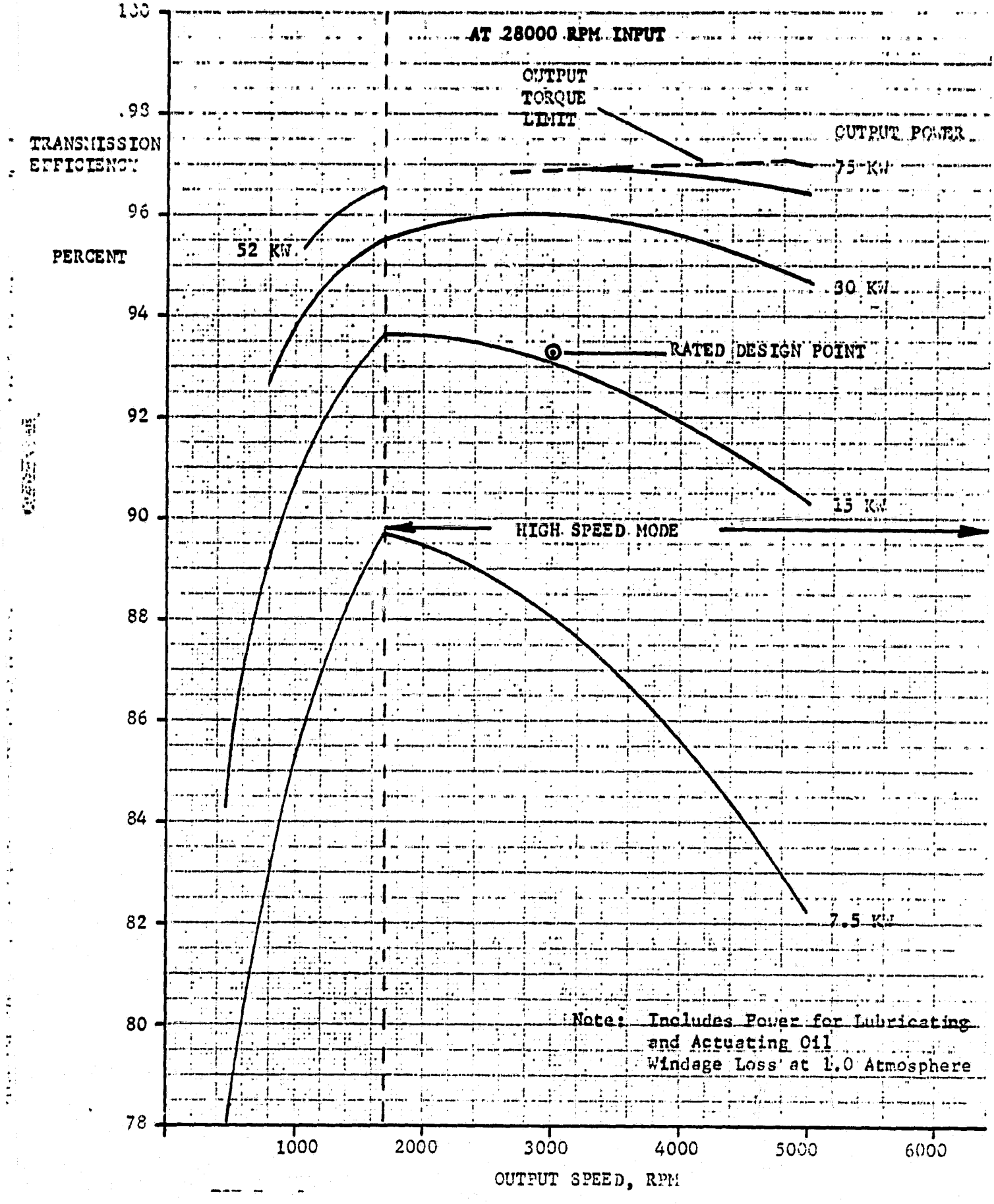

Figure I-10 — TRANSMISSION EFFICIENCY AT 28000 RPM INPUT

The proposed flat belt CVT design is easily adapted to operation by only an electric motor input, since it merely means detaching the flywheel, with no change in controls. However, the modifications required to adapt the proposed flat belt CVT design for use in a hybrid vehicle powered by both an electric motor and internal combustion engine are shown to be more extensive and involved.

The proposed design appears to offer a very attractive solution to obtaining an efficient, compact CVT that would greatly improve the overall utility and efficiency of electrically powered vehicles.

II. INTRODUCTION

The current dependence of this country on importing over eight million barrels of oil per day not only affects significantly our overall economic well being but can force us to be unduly dependent on foreign nations. Such a dependence may be significantly reduced by the development of electrically powered vehicles for urban use. Gasoline consumption in urban travel accounts for most of the current seven million barrels of oil consumed by the 125 million automobiles and light trucks in the United States. The alternative electrical power may be produced using our own coal, uranium, waterfalls, waste product fuels, and other non-oil energy sources.

Studies of electric powered vehicles show that the performance and economy of such vehicles may be improved significantly using an energy storage flywheel for purposes of rapid acceleration and other large transient power requirements. In some cases, the flywheel may also be used to absorb power, conserving energy from vehicle deceleration. However, the major essential element needed to couple the high-speed output shaft of an energy storage flywheel to the wheels of an electrically powered vehicle is an efficient, compact, reliable continuously variable transmission (CVT) of reasonable cost. Recognition of this need led the U.S. Department of Energy, through NASA, to request proposals for design studies of continuously variable transmissions (CVT) for electrical vehicles late in 1978. The studies reported in this work started in April 1979 and continued to February 1980.

Nearly all of the previous work on CVTs has been related to coupling the output of internal combustion engines, with or without flywheels, to the wheels of automobiles. The chief stimulus for such work was the potential fuel

economy improvement that could result from an efficient CVT which would permit operating the automotive engine at its best fuel economy at all times, while obtaining the necessary acceleration power from a rapid speed change of engine rather than by increasing the inlet engine charge pressure. The types of CVTs that have been stutied in detail range from all mechanical traction drives of various types to hydraulic and electric drive systems, including hybrid hydro-mechanical and electromechanical drive arrangements. The mechanical traction drives using friction discs or toroidal elements have had a long development history at General Motors, Curtiss Wright, Tracor, Excelermatic, etc. Such elements, including a nutating variant by Vadetec, operate to load a special oil film to transfer torque, using friction coefficients up to about 0.1. Mechanical traction drives based on a pulley-belt system have been studied and developed by many concerns, including DAF (Holland)[1], Fiat (Italy),[2] and others. Perhaps the largest number of small engine-powered belt drive systems has been manufactured by Salsbury (U.S.) for snowmobiles. Many other belt drive variations have also been studied — such as Van Doorne's Transmatic (Holland)[3] — which pushes rather than pulls a belt between pulleys, and a novel hydraulic ratchet arrangement at Mechana-Power (U.S.).[4] The simple all electric or hydraulic systems have relatively large losses due to the component efficiencies. Hence, nearly all efforts on CVTs using such components have focused on hydromechanical and electromechanical systems using the higher efficiency gears to transfer much of the power. The study and development of a hydromechanical transmission by Orshansky Transmission Corporation[5] gives efficiencies of about 85-89 percent at 26 KW. Some previous studies by Sundstrand[6] indicate lower efficiencies for a flywheel-internal combustion engine drive using a hydromechanical transmission. A development by Renault (France)[7] shows higher efficiencies to

(1), (2), etc. — See Table of References - Section VIII

lower powers using the "Transmatic" transmission of Van Doorne. Garrett Corporation (AiResearch) is studying an electric motor and generator in an electromechanical system. Many other companies are known to be studying and developing drives for their own specific products.

While many CVTs can be engineered to give good operating efficiency at higher powers, it is difficult to achieve very high transmission efficiency (over 90%) at low output powers while maintaining other desirable features. However, low output powers are typical in operating small vehicles in urban travel.

The unique flat belt CVT of the studies reported herein appears to offer efficient operation to very low powers in a compact and low weight configuration involving very little new technology. A complete transmission preliminary design is given by this report that should permit an accurate evaluation to be made of its overall desirability and potential application in electrically powered vehicles.

This work was part of the Electric and Hybrid Vehicle Program of the U. S. Department of Energy. It was performed under contract DEN 3-114 and managed by the Bearing, Gearing, and Transmission Section of the NASA, Lewis Research Center.

III. DESCRIPTION OF THE SELECTED FLAT BELT CVT

A. The Transmission Arrangement and Operation

The gearing for the flat belt CVT is given schematically in Figures I-2 and III-1 and detailed in the reduced drawings shown on Figures I-3, I-4, and I-5. A differential planetary gear assembly is positioned between the pulley shafts to give a compact configuration. The power from the electric motor and also from the flywheel, when engaged by its clutch, passes directly from gear (1) to gear (2) to gear (3) to gear (4), reducing in speed by a factor of about 10.5 to 1.0. Gear (4) is located on the planetary carrier in the differential planetary gear assembly and is geared directly to gear (B) on the shaft of pulley B of the flat belt pulley arrangement. Gear (A) of pulley A is geared directly to gear (F) located on the shaft of the sun gear (S) of the differential planetary. The ring gear (R) of the differential planetary is connected by a shaft to a low speed mode gear (L), while the high speed mode gear (H) is mounted on the sun gear shaft. The output shaft may be connected to either the low output gear (LO) or the high output gear (HO) by means of a synchronizer, as shown, to obtain power at the output shaft. Connection by the synchronizer to the low output gear (LO), geared to the low speed mode gear (L), permits output operation from zero to about 6% of the input speed at gear (1). Connection by the synchronizer to the high output gear (HO) geared to the high speed mode gear (H) gives an output operation from about 6% to about 24% of the input speed at gear (1). Thus, an input speed of 21,000 RPM at gear (1) gives a maximum output speed of 5,000 RPM. Pulley A is designed to operate over a speed range of 0.5 to 2.0 times the speed of pulley B, resulting in the pulley and output speeds, as shown in Figure I-6.

In the low speed operating mode, power is transferred through the planetary

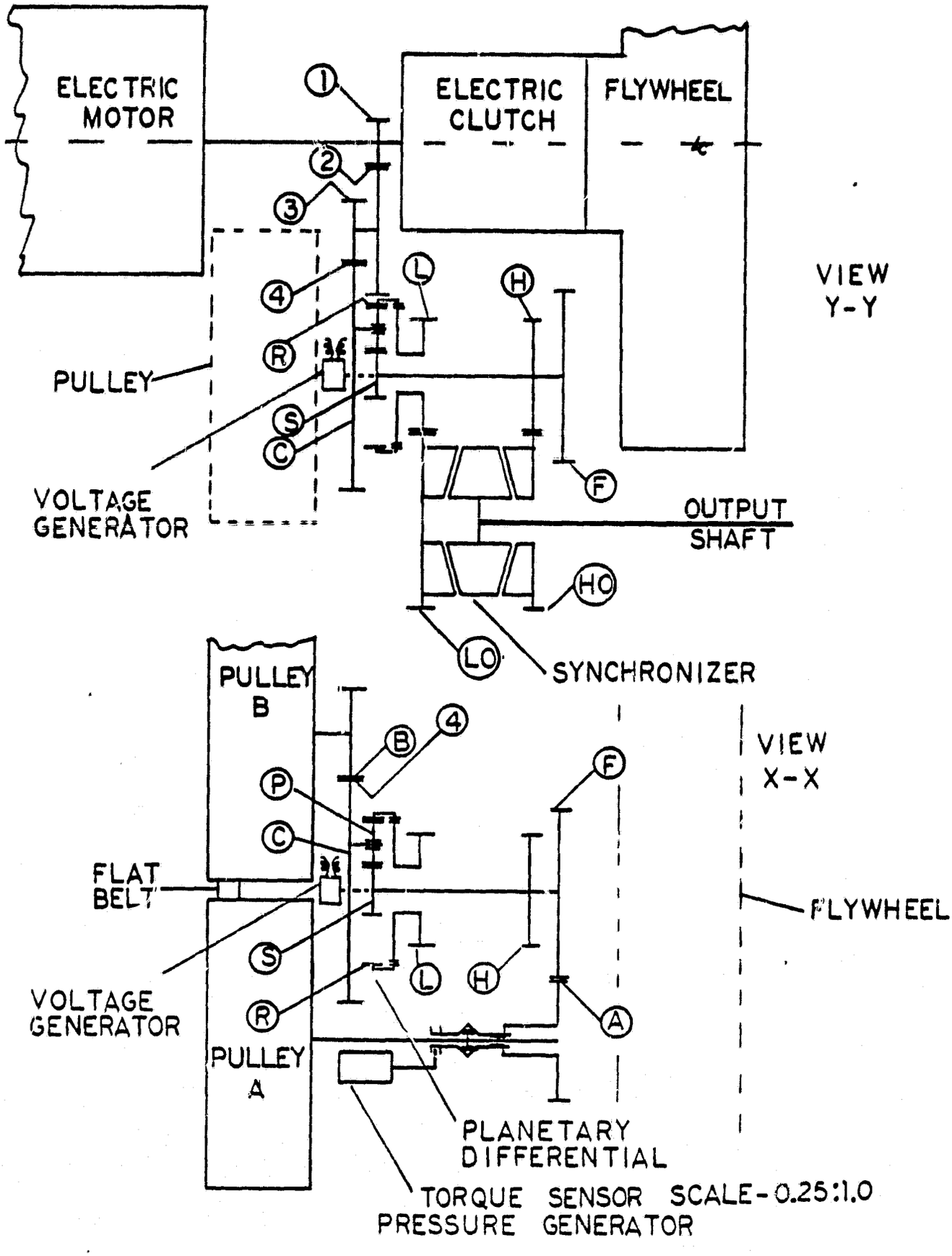

Figure III-1 — SECTIONAL VIEWS - TRANSMISSION GEARS

differential gearing from the carrier, both to the ring gear (R) and low speed gear (L), and to the sun gear (S), and gear (F) to gear (A), resulting in a transfer of power from pulley A to pulley B and to gear (4) through gear (B), increasing the torque on the carrier in a regenerative fashion. Thus, at very low transmission output speeds, small input torques from the electric motor can generate very high output torques with such regenerative power flow. Pulley A operates at its maximum speed related to the input speed at zero output speed and decreases in speed as the output speed increases, as shown on Figure I-6. The gear ratios are chosen so that when pulley A is operated at its minimum speed relative to pulley B, the speed of gear (L) is identical to the speed of gear (H), the planetary differential then turning without any relative motion of carrier, sun, and ring gears. The synchronizer is then operated to switch the drive from the low output gear (LO) to the high output gear (HO) and the controls are simultaneously changed with reversal of the power flow through the pulleys. The transmission operates in the high speed mode without power transfer in the planetary differential gear section. In the high speed mode, power is transferred from gear (4) through pulley gear (B), from pulley B to pulley A, from gear (A) to gear (F) on the sun gear shaft, and hence from gear (H) to gear (HO) on the output shaft. Increase in speed of pulley A in the direct drive high speed mode then causes a corresponding output speed change, pulley A varying in speed from 0.5 to 2.0 times the speed of pulley B. Thus, with the use of the synchronizer, the complete pulley speed variation is used twice in encompassing the desired speed range from zero to maximum rated speed.

Other basic design features of the flat belt CVT include automatic operation from zero to maximum output speed, using a single lever control by the operator that demands more or less output speed. The operator selects forward or reverse speed by reversing the battery input to the D.C. drive motor. The

electric motor will deliver ample power for reverse operation at conventional low output speeds and give the maximum design stall torque, due to the regenerative power transfer in the pulleys and planetary differential gears. However, the flywheel would be disengaged from the transmission during the reverse operation, since it rotates only in one direction. The flywheel may be accelerated to operating speed by the D.C, motor before operation of the vehicle by positioning the synchronizer element in the neutral disengaged position, disconnecting the CVT output to the wheels. Also, the power flow through the flat belt CVT is bi-directional — the torque sensor on pulley A operating in either direction. Hence, the CVT can be used for regenerative braking of the vehicle, using either the electric motor as a generator or the flywheel to absorb energy, or both simultaneously.

B. The Flat Belt Pulley Drive

The transmission uses a novel compact flat belt pulley drive with rotary actuator and integrated control system, for which a patent has been applied. An initial conceptual arrangement is described in this section, which was then modified and refined, as discussed in the following section of this report.

All previous continuously variable speed belt drives obtain changes in their operating speed ratio by an axial movement of one sheave of each pulley. This feature is in marked contrast to the rotary movement utilized with the unit to be described here, which gives reduced size, higher efficiency, greater economy of manufacture and use, simplified belt replacement and permits incorporation of an integrated control to achieve more optimum overall drive performance, such as when applied to automobiles, driven for either internal combustion engines or electric motors and/or flywheels.

Present variable speed pulley drives, except Kumm U.S. Patent No. 4,024,772,

are of the type using Vee-belts, which are composed of a rubber composition and have a trapezoidal cross section. The belt transmits rotary motion at one speed from a source of power, such as an engine or motor, to an output power shaft at another speed. The speed ratio is varied in a continuous fashion from a minimum to a maximum, as dependent on the geometry of the belt and pulley system. The Vee-belt is compressed between smooth conical sheave sections in each of two pulleys by external axial forces on the sections to apply tension to the belt and friction between the sides of the Vee-belt and sheave sections to prevent slippage. In operation, a force unbalance caused by changes in the axial loading of the sheave sections causes the Vee-belt to change its radial positions in the two pulleys until a force balance is achieved or a limit range stop is reached. For a large transmitted torque the required axial force exerted on the sheaves results in a large compressive load on the Vee-belt, which requires the belt to have a substantial thickness to prevent axial collapse or failure of the belt. The increase in thickness increases its centrifugal force and causes higher belt tension loads. Also, as the belt thickness increases, pulley size must be increased, due to higher stress loads at a given design minimum pulley radius. Further, the typical Vee-belt must continuously pull out from the compressive sheave load on leaving the pulley, which results in significant friction losses and belt fatigue, affecting overall efficiency and operating life. Consequently, although variable speed pulley drives have successfully used Vee-belts in a wide range of applications (industrial drives to snowmobiles and even automobiles) they have been severely limited in their power capabilities for more competitive smaller size equipment.

The flat belt transmission utilizes a thin flexible flat belt supported on drive elements similar to that of patent No. 4,024,772, but with totally different more compact sheaves and actuator, which reduces the transmission size and volume

by eliminating the axial movement of the usual actuators. Also, the efficiency of this transmission is improved by reducing the number of bearings and pulley diameter and gives a design which permits a more simple belt replacement and maintenance as compared to patent No. 4,024,772. Further, this arrangement permits the use of smaller actuator forces to give the same belt tension, thus reducing the required fluid pressure and pump work. The fluid pressures required for rotary actuator may be controlled to automatically give the minimum required belt tension, preventing slip over the complete load range, thus improving the transmission efficiency by reducing bearing losses. Also, this arrangement permits a simple practical control for changing the output power and/or speed that may be applied directly to operating internal combustion engines or electric motors on or near their optimum overall efficiency schedules for torque and speed.

The problems associated with the prior art use of axially positioned actuators which change the radial position of the belt by moving one pulley sheave axially with respect to the other are overcome by using two axially fixed discs in place of each sheave of the pulley. These discs use oppositely angled guideways for containing and supporting the ends of the drive elements, with the inner discs connected but separated from the outer connected discs, as shown on Figures I-1, III-2, and III-3. The inner discs of each pulley are connected to one side of pressurized annular volume sectors in the rotary actuator and the outer discs are connected to the other side of the pressurized annular volume sectors in the rotary actuator so that fluid pressure between the radial sides of the sectors comprising the actuator urges the inner and outer discs to rotate in the opposite direction in each pulley, as shown in Figures III-3 and III-4. The oppositely angled guideways, which contain the ends of the belt drive elements at the intersection of such guideways, then position the drive elements to a larger or smaller radius about the pulley axis (see Figure III-2), dependent on

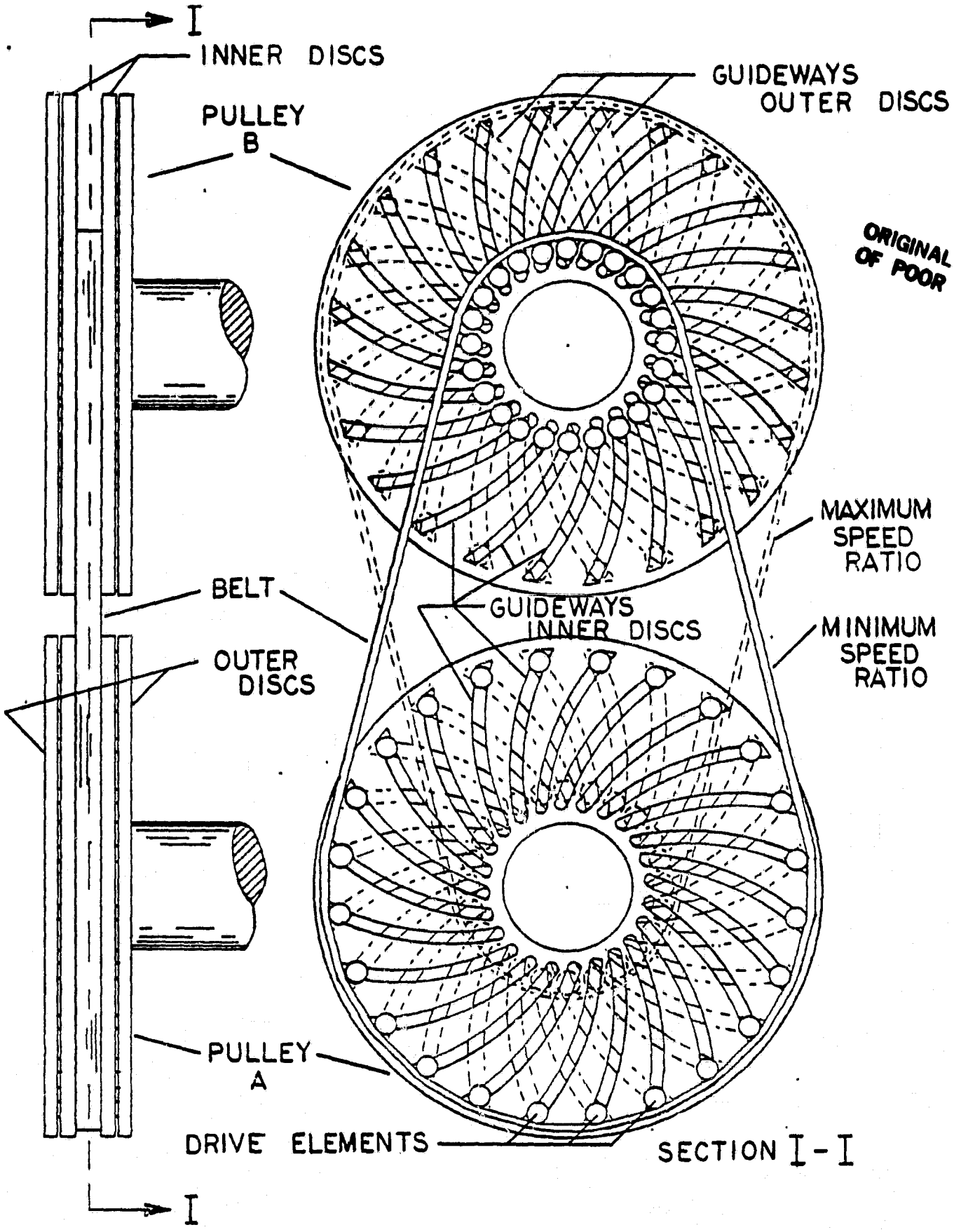

Figure III-2 — FLAT BELT RADIUS RATIO RANGE

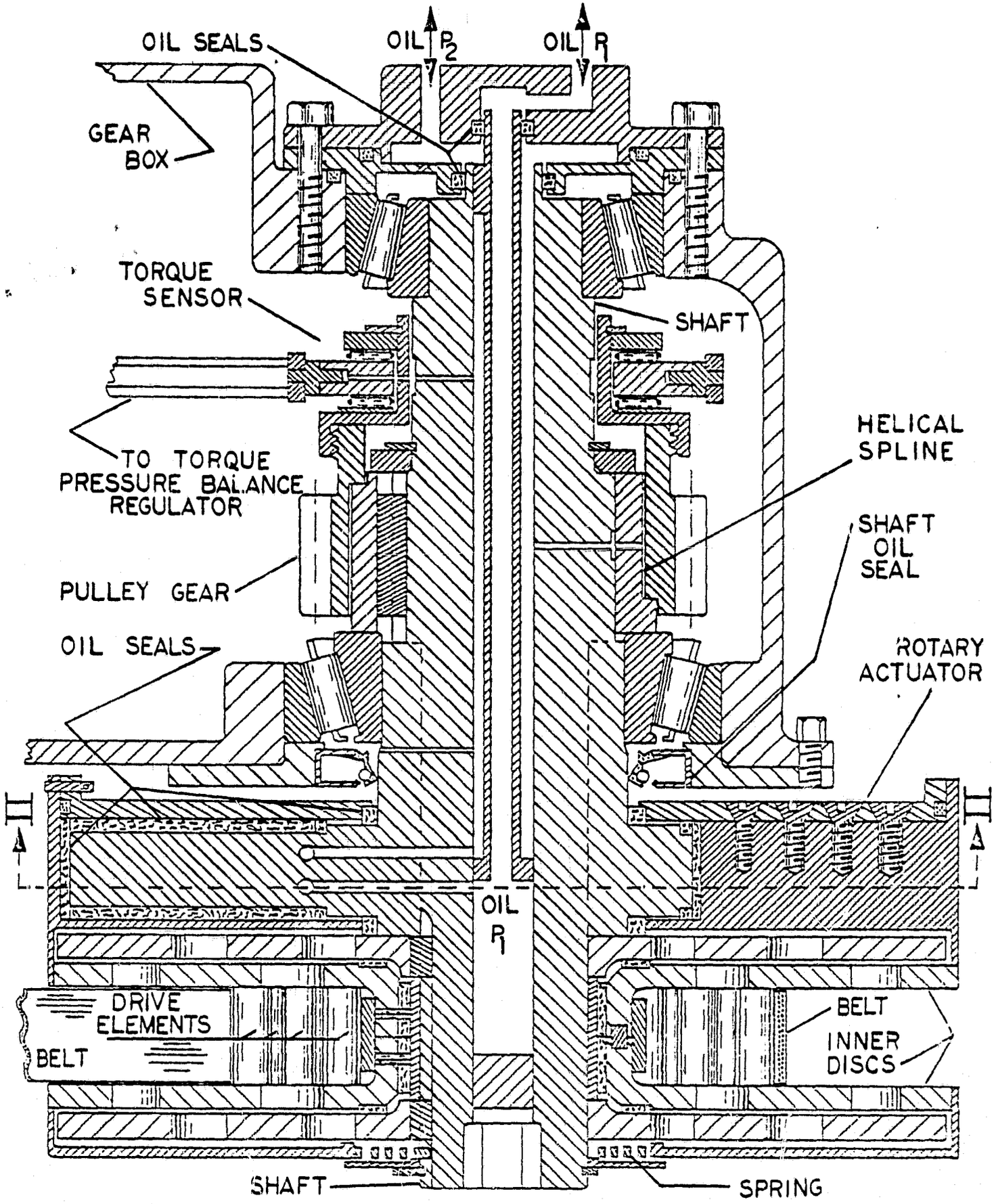

Figure III-3 — PULLEY DESIGN

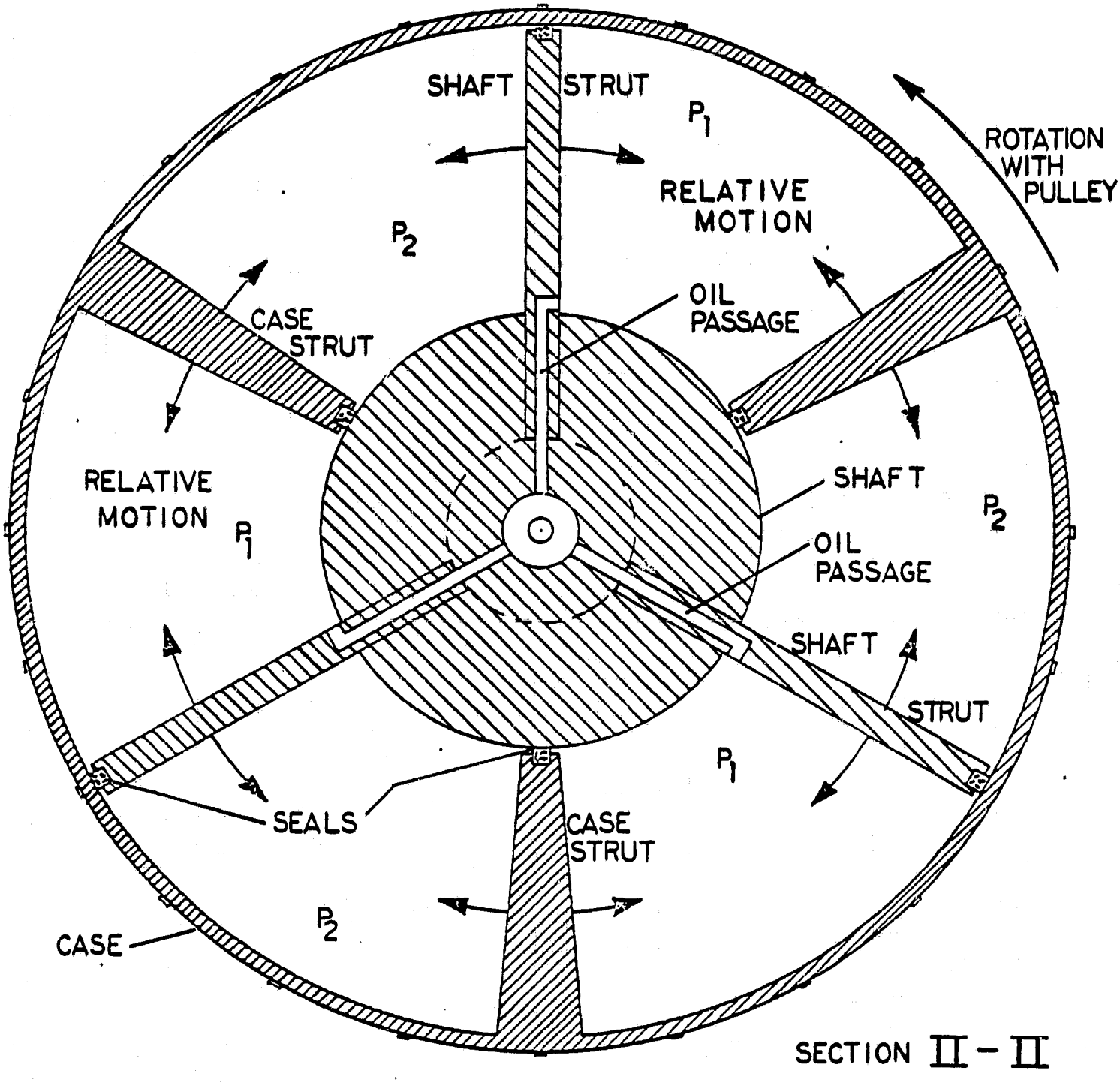

DRIVE ELEMENT WITH BELT

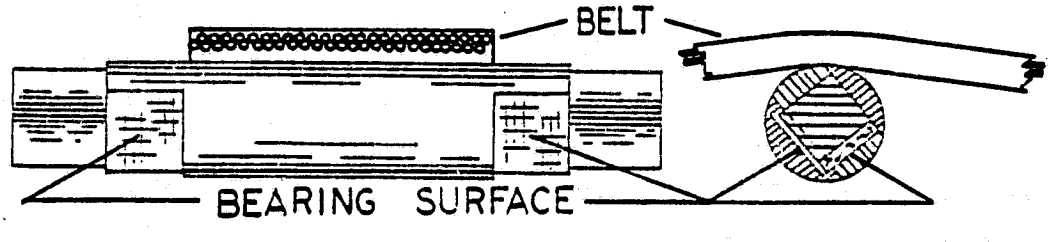

Figure III-4 — HYDRAULIC ROTARY ACTUATOR

the direction of the relative rotation of the inner and outer discs. The torque developed by the annular actuator, which rotates with the pulley, results in urging the drive elements toward a larger radius on each pulley, thus tensioning the belt as desired to prevent slippage on the drive elements. A 2X scale drawing of the drive element (Figure III-4) shows them to be cylinders with bearing surfaces on the bottom sections of both ends. A more efficient shape is described in a subsequent section of this report.

A larger pressure differential supplied to one annular actuator of the two pulleys will then cause the drive elements to be positioned to a larger radius in that pulley having the larger pressure differential, and results in the drive elements moving to a smaller radius in the other pulley, due to the resulting belt tensions and fixed belt length. Hence, by controlling the pressures to the actuators, the speed ratio of the transmission may be varied over the limits of the pulley geometry while transmitting power at various speeds. Thus, the axial movement of conventional continuously variable belt drive pulleys with its larger fluid volume is avoided, together with the necessary pulley sheave displacement volume, as well as the bearing required to prevent rotation of the axial moving actuator.

A highly efficient flat belt, that does not have the Vee-belt frictional losses and fatigue due to the compressive sheave load on leaving the conventional pulley, is used. The flat belt also is able to operate at smaller effective pulley radius to higher speed because of its flexibility and thinner sectional thickness. Further, the axially fixed position of the pulleys does not require the belt to move axially to keep the belt aligned when changing speed ratio as required in other continuously variable belt drives employing axial sheave movement. This axial movement significantly complicates any design which would place

the two actuators on the same side of the pulleys. However, with the present arrangement, both actuators may be easily placed on the same side of the pulleys connected to the input and output shafts, permitting belt replacement to be made directly without removing rotating equipment, i.e., bearings and shafting. Also, both actuators on the same side of the pulleys permits an overhung bearing arrangement, so that only two bearings and one shaft seal are required per shaft, as compared to three bearings and several shaft seals normally required in previous design arrangements. This reduction in bearings and seals improves the efficiency of the drive.

Lower pressures in the rotary actuators may be used to give the belt tension needed to prevent slippage. This is accomplished in part by the increase in the cross sectional area obtained in the rotary actuator of a given width by dividing the total annular fluid space into multiple pressurized volume sectors to permit generating a multiple torque compared to that obtained using a single volume. This is permitted in this arrangement, since the actuator counter-rotational total movement angle is relatively small, i.e. about 80 degrees for a design total angle between guideways of 90° corresponding to the conventional pulley sheave total angle of 90°, to give a drive element radius change of 2.0 to 1.0. Allowing for the necessary structure in the actuator, three pressurized volume sectors in the actuators with the 90° total angle guideways are possible. Such large total angles are not practical with conventional pulley sheaves in continuously variable Vee-belt drives due to the required belt angle for compression loading and also results in excessive volume and space requirement for the actuator movement, using axially positioned sheaves to change speed ratio. However, the required actuator torque load is reduced as the guideway design total angle is increased — inversely proportional to the tangent of one half of

the total angle between the oppositely inclined guideways, thus reducing the required actuator pressure to obtain the necessary belt tension.

A gearing arrangement is used with one gear supported on a shaft helical spline and attached to a collar which through thrust bearings applies to a non-rotating yoke a force proportional to the torque transmitted by the gear, as shown on Figure III-3. The yoke is connected to a lever to apply force to a spool in the torque pressure balance regulator to generate one pressure of the actuator differential pressures substantially proportional to the gear torque, as shown more completely on the hydraulic speed control, Figure I-7. The complete actuator pressure differential then becomes substantially proportional to the gear torque since the other lower pressure is held fixed by a pressure regulator. Thus, the belt tension is increased for large loads to prevent belt slippage and decreased as loads are reduced to give lower bearing losses. The hydraulic speed control system then permits changing the output power and/or speed by operating a speed servo control valve in the lower pressure supplied to the actuators.

The hydraulic connections to the rotary actuators on the input and output pulleys would be reversed for driving by a flywheel, as compared to an internal combustion engine or electric motor for identical operation of the speed servo control valve. The engine will accelerate to a higher speed and power by moving the speed servo control valve spool to initially reduce the load on the engine -- i.e. allow the engine to go to a higher speed for the same initial output speed-- which then permits reapplying the load with a higher engine to wheel speed ratio, giving more output torque to the wheels. In the case of transmitting power from a flywheel, the speed servo control valve spool is moved to increase the load on the flywheel by changing the pulley speed ratio to give more output speed, not

less, as given in the initial transient for the engine or electric motor. The hydraulic pressures generated for the rotary actuator may be used together with a flow from a positive displacement pump driven at a speed proportional to engine or electric motor speed to operate the engine or electric motor on a torque-speed schedule giving best operating efficiency, as shown on Figure III-5. The schedule control operates a servo to change either the carburetor throttle position for an Otto cycle internal combustion engine or the fuel flow in fuel injected engines or the voltage applied to an electric motor. Operation on a desired engine or motor torque versus speed schedule results from using a positive displacement pump together with a contoured pintle in the schedule control regulator as located within a flow orifice to give an engine speed related hydraulic pressure, P_s, to balance the torque related pressure, P_1. The servo valve portion of the control then holds the butterfly throttle in fixed position only when the predetermined engine torque versus speed characteristic is obtained.

C. Transmission Controls

The transmission speed control is shown on Figure I-7. A speed mode selector is used to change the direction of the hydraulic flows between the speed servo valve and the rotary actuators, and a follow-up regulator on the discharge from the torque sensor gives a wider operating range. The speed mode selector causes the rotary actuators to operate in the proper direction, with the same operator input direction, irrespective of the transmission speed mode. The follow-up regulator permits obtaining P_1 pressures smaller than P_2, so that the rotary actuators will then operate to reduce belt tension caused by the centrifugal loads of the belt drive elements at higher pulley speeds. At normal speeds and torques, P_1 is larger than P_2, as needed to prevent slippage of the belt. Hence, the belt loads are minimized at all speeds and torques to reduce the associated pulley shaft bearing loads and energy losses. A voltage generator

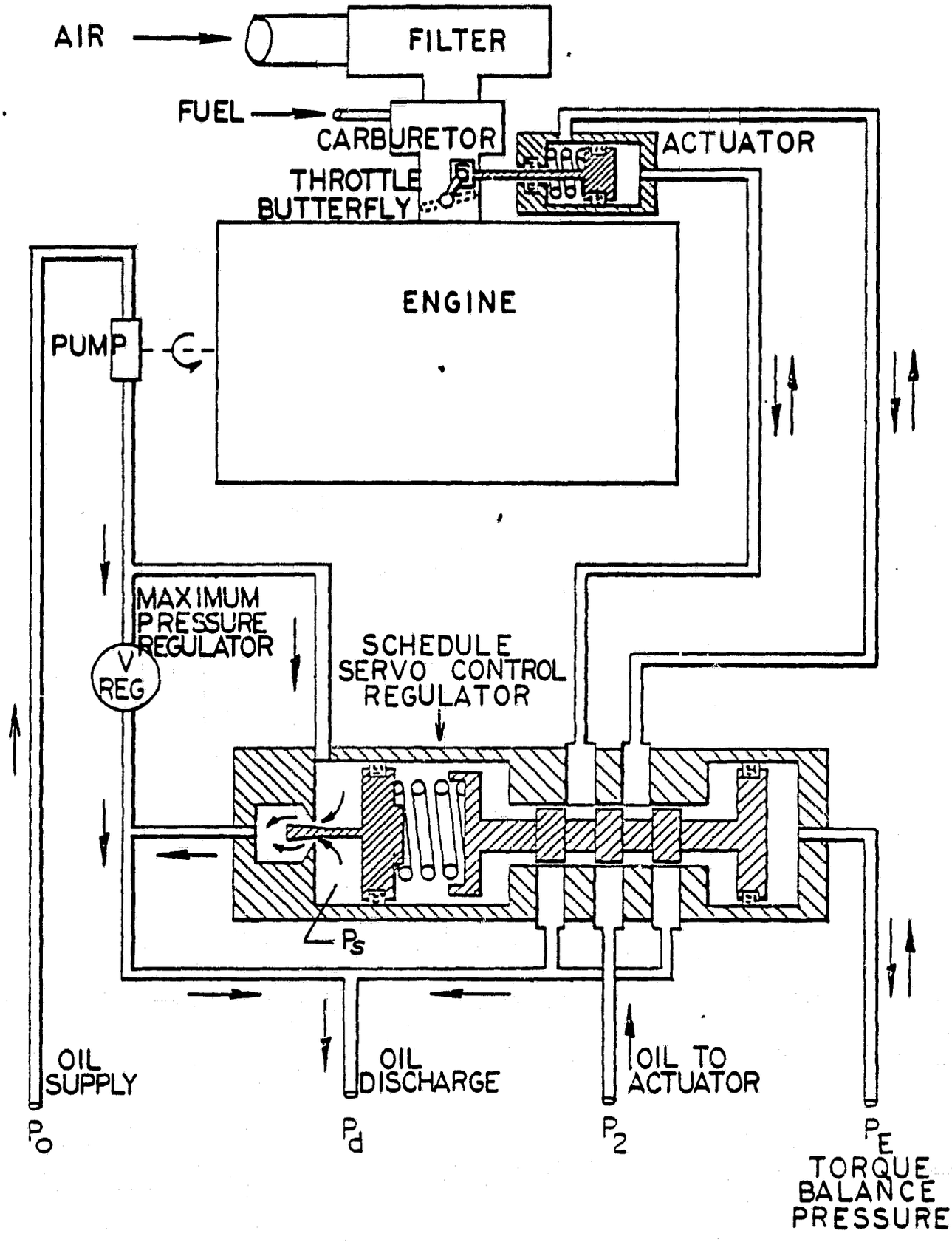

Figure III-5 — ENGINE SCHEDULE CONTROL

output is used with P_1 and P_3 to generate the desired control pressure P_c for the follow-up regulator in another control not shown on Figure I-7, but discussed in Section IV-H of this report. The transmission may use solenoids to operate the synchronizer to switch from neutral to low or high speed modes. This is discussed in Section IV-H.

The transmission arrangement of Figures I-3, I-4, I-5, and III-1 shows a D.C. motor located at the input to the CVT rather than between the CVT and the wheels. This was done partly to avoid using the D.C. motor at low speeds where its efficiency is poor, as shown on Figure III-6, and partly because of the major reduction in the size and weight of the D.C. motor, which is achieved by operating it at high speed. Also, an improvement in the D.C. motor maximum operating efficiency is usually obtained by designing to higher speed. The flat belt CVT permits operating the D.C. motor at relatively higher speeds at all times for high motor efficiency, although, as will be discussed later, the transmission efficiency decreases with increasing D.C. motor input speed. Hence, it is desirable to operate the D.C. motor input at its minimum speed capable of producing the desired output power and output speed. In this regard, as shown on Figure III-6, the better speed regulation of the simple shunt wound motor as compared to the compound or series wound motors is very attractive. However, both the shunt and compound wound motors can be operated efficiently at higher than full field speed in increasing the full field resistance (usually up to 1.7 times without commutation becoming bad). Also, the arrangement of Figure III-7 may then be used to step change the battery voltage to the D.C. motor, making possible a significant power and speed variation. Solid state power switching transistors are now available to handle up to 500 amperes on a continuous basis, with very low voltage losses (0.5-1.0 volts) at the transistor switch. In addition, the use of ripple free voltage improves the D.C. motor efficiency

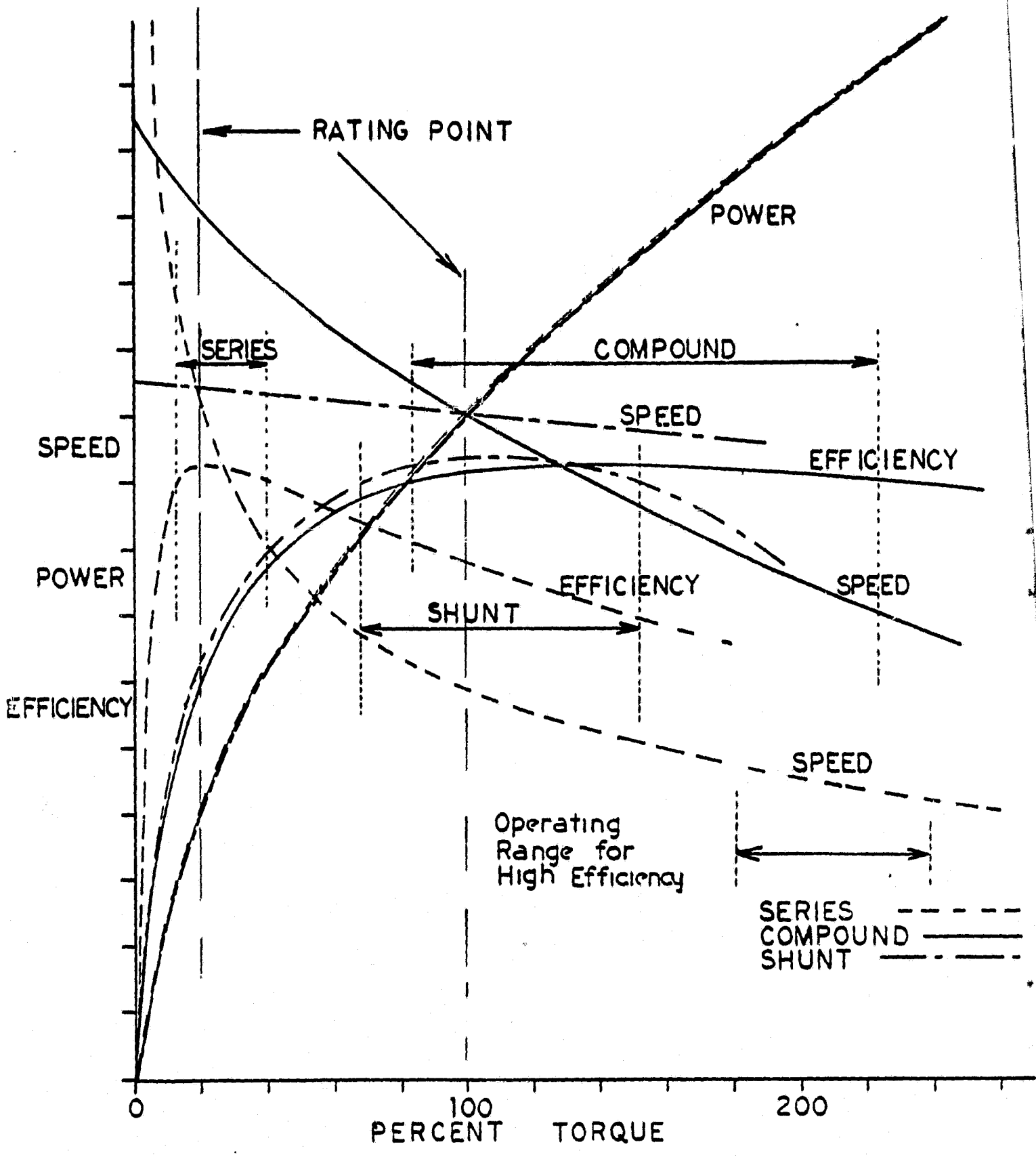

Figure III-6 — D.C. MOTOR CHARACTERISTICS

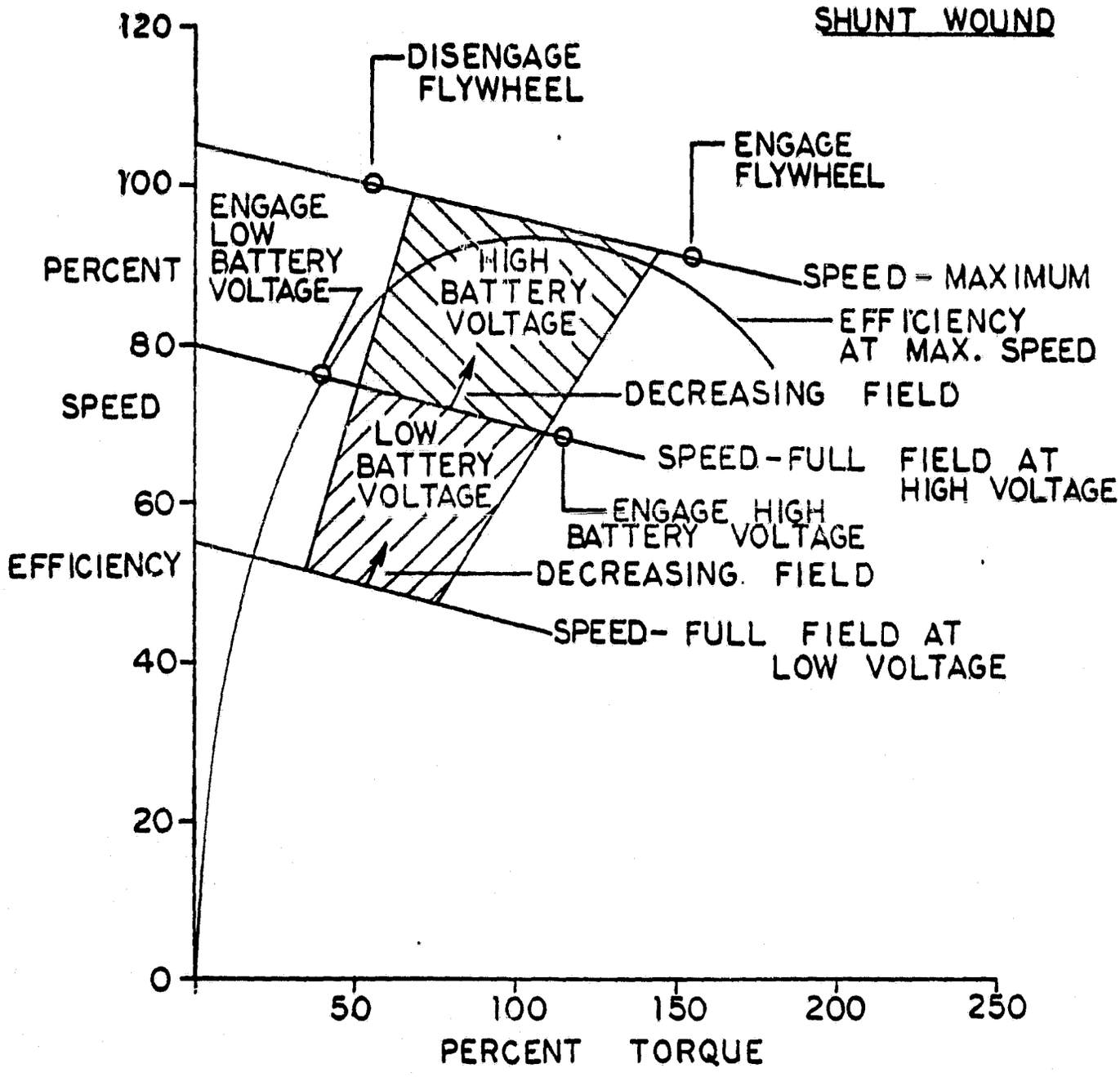

Figure III-7 — D.C. ELECTRIC MOTOR OPERATION WITH FLAT BELT CVT

somewhat. An optimum D.C. motor control would then incorporate a means for varying the D.C. motor field current (increasing the field resistance with increase in the demand by the driver for increased vehicle speed) integrated with the flat belt variable speed drive. The hydraulic control pressure, which is a function of the output torque and the pulley A speed, may then be used to vary the field current to the motor. The motor torque variations can then be minimized on an appropriate control arrangement. However, the complete analysis of a suitable integrated electric motor and CVT control must await specific operating characteristics of a motor. The above cursory comments indicate that using a simple D.C. field current control may make it possible to nearly always operate on the CVT in the high efficiency operating regime of the D.C. motor.

D. Performance

The flat belt CVT is designed principally for an electrically powered urban vehicle to give good economy of operation by using a flywheel to obtain adequate acceleration for starting, entering high speed traffic, and performing pass maneuvers. The transmission is designed to be continuously controllable from zero to 5,000 RPM output speed, with an input speed of 21,000 to 28,000 RPM. The output speed range decreases to zero to 3,333 RPM as the high speed input is decreased to 14,000 RPM. The design uses a torque sensor on the belt drive that limits the maximum output torque at stall or zero vehicle speed to 450 N-m (330 lb-ft), which then gives the design maximum tension in the flat belt. A maximum output torque of 150 N-m (110 lb-ft) corresponding to the same maximum flat belt tension is obtained in the high speed operating mode. This results in the output power exceeding 75 KW (100 HP) only at output speeds close to 5,000 RPM. While this meets the specified requirements of the transmission, an additional "high speed accelerator" modification is also described that can achieve higher output powers without increasing the masimum belt tension with some additional power losses in the acceleration transient operation. A conservative

approach was used in applying a belt tension limit that uses the best present "state of the art" in the design of flat belts. However, the potential of new materials and designs indicate that much higher belt tension limits may be practical in the near future, permitting perhaps twice the current amount of power to be transmitted efficiently on a transient basis in the same size CVT. The future transmission design must then depend on what power can be actually transmitted by new improved belts.

Examination of the potential operation of the electric vehicle in an urban environment resulted in the compilation of a duty cycle given in Table III-1. This was then used to determine the gear and bearing loads, which resulted in the selection of appropriate components to give the necessary life. This CVT is particularly capable of withstanding all sudden shock loads and torque conditions that can be expected in typical automotive application, simply by a transient slippage of the belt. Also, all components exceed ninety percent reliability to operate 2,600 hours with an input speed of 21,000 RPM, output speed of 3,000 RPM, and power output of 16 KW (22 HP) — a general duty cycle specification.

The transmission speed ratio may be varied over its complete range in less than 2.0 seconds, as shown later in this report, by operation of the rotary actuators. However, speed changes possible with the vehicle would normally cause the transmission speed ratio change to be slower.

The CVT efficiency was determined by computing the losses in the gears, bearings, pulleys, seals, pumps, and clutch elements over the output speed range for various output powers at input speeds of 14,000, 21,000 and 28,000 RPM, as shown on Figures I-8 I-9, and I-10. These curves show that it is desirable to

TABLE III-1

ELECTRIC VEHICLE TRANSMISSION REQUIREMENTS

Operating Mode	% of Life	Output Speed RPM	Vehicle Speed KMPH	Output Torque N-m(ft-lb)	Output Power KW	Hours
Starting Flywheel	5	0	0	0	0	130
Starting Vehicle	2.5	0	0	124.12(91.54)	0	65
Normal Acceleration	2.5	1250	26.15	60.38(44.53)	7.90	65
Normal Deceleration	2.5	1250	26.15	-60.38(-44.53)	-7.90	65
Stopping Vehicle	2.5	0	0	-124.12(91.54)	0	65
Low Speed Cruise	50.0	2500	52.3	19.10(14.09)	5.0	1300
High Speed Cruise	32.7	4500	94.14	30.0(22.13)	14.14	850
Max. Power, Speed	0.11	5000	104.6	143.26(105.66)	75.0	3
Max. Torque, Grade	1.0	1000	29.2	450.0(327.40)	47.12	26
Max. Torque, Stall	0.19	0	0	450.0(327.40)	0	5
Reverse	1.0	1250	26.15	-60.38(-44.53)	7.90	26
Requirement (Alternate) Exhibit A	100	3000	62.76	52.22(38.52)	16.41	2600

Note: Based on 0-5000 RPM output shaft speed

operate the transmission at the lowest input speeds at which the desired power is available from the electric motor. The electric motor must be sized to sustain the vehicle at its maximum level ground cruise speed. Selecting a maximum cruise speed of 105 KMPH (65 MPH) for the urban vehicle and computing the wheel power requirement of a 1700 KG (3750 pound) vehicle gives the curves of Figure III-8. This shows that the electric motor should be capable of delivering at least 18 KW (24 HP) at perhaps 24,000 RPM on a steady state basis when used as shown with the flat belt CVT. It is assumed that the D.C. electric motor variations in speed from 14,000 to 24,000 RPM are proportional to a power change of zero to 18 KW. This gives the flat belt transmission efficiency as shown in Figure III-9 Figure III-9 also gives the flat belt CVT efficiency for maximum torque and power output as detailed on Figure III-10 The very low cruise vehicle power requirement reduces the possible transmission efficiency at low speeds, but the operating efficiency is still 90% and above in the usual vehicle speed range. (Input speeds lower than 14,000 RPM would significantly improve the transmission efficiency in the low vehicle speed cruise power range.) The transmission efficiency improves significantly with increase in output power, particularly at the lower output speeds, which is characteristic of the acceleration operation from lower speed to higher speed. Hence, this transmission should demonstrate overall integrated efficiencies in excess of 90% when used in an electric vehicle with a high speed flywheel and D.C. motor.

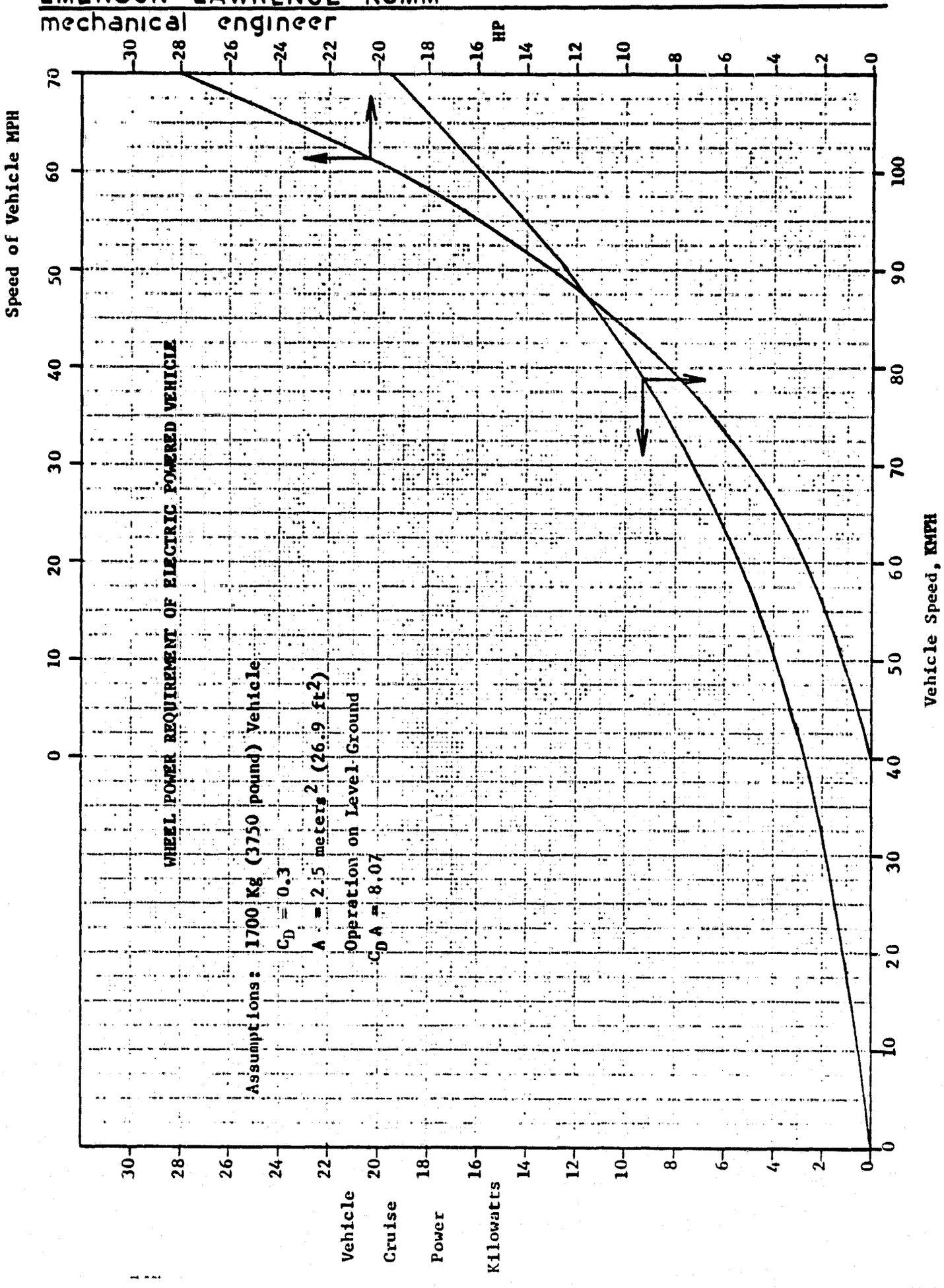

38 Figure III-8 — WHEEL POWER REQUIREMENT OF ELECTRIC POWERED VEHICLE

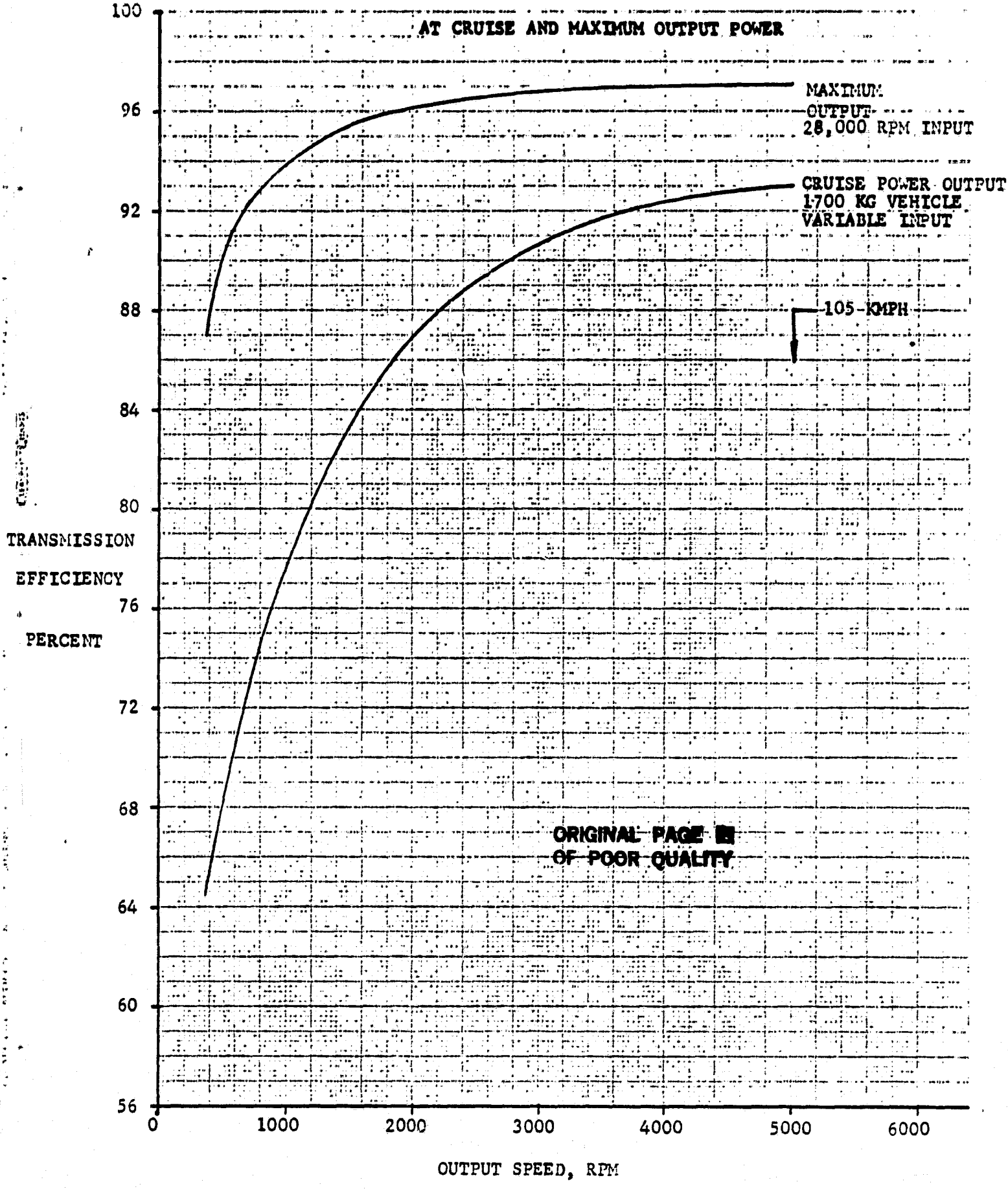

Figure III-9 — TRANSMISSION EFFICIENCY AT CRUISE & MAXIMUM OUTPUT POWER

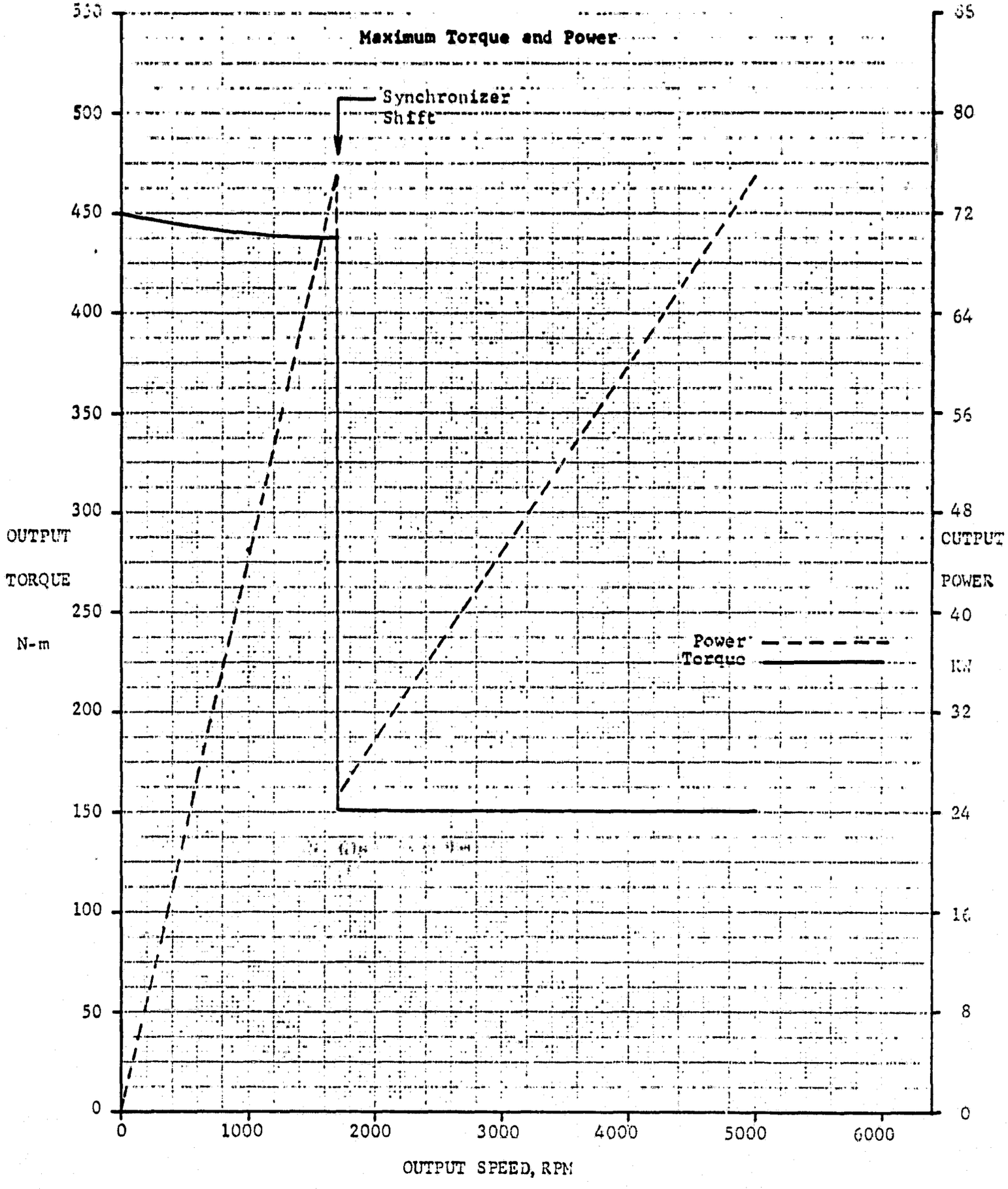

Figure III-10 — FLAT BELT TRANSMISSION TORQUE & POWER AT 28000 RPM INPUT

IV. DESIGN OF THE FLAT BELT CVT

A. Optimization of Transmission Arrangement

The basic assumption for optimizing the flat belt CVT is that its overall size is directly dependent on the maximum amount of torque and power that is transferred through the belt. Both a direct drive and differential drive gearing configurations were examined initially, as shown in Figure IV-1. While the direct drive configuration has less gearing, a slipping clutch is required for output at stall and low vehicle speeds. Also, the differential geared system has a major advantage in reducing the belt loads, due to the power transfer through the planetary differential gearing. Six different differential configuations were then analyzed as to their suitability for the proposed transmission as shown in Figure IV-2. The six differential configurations assume that the flywheel is always geared to pulley B as shown in Table IV-1.

TABLE IV-1

DIFFERENTIAL GEARED CONFIGURATIONS

DIFFERENTIAL VERSION	FLYWHEEL CONNECTION	PULLEY A CONNECTION	OUTPUT CONNECTION
A	Carrier	Sun	Ring
B	Carrier	Ring	Sun
C	Sun	Carrier	Ring
D	Sun	Ring	Carrier
E	Ring	Carrier	Sun
F	Ring	Sun	Carrier

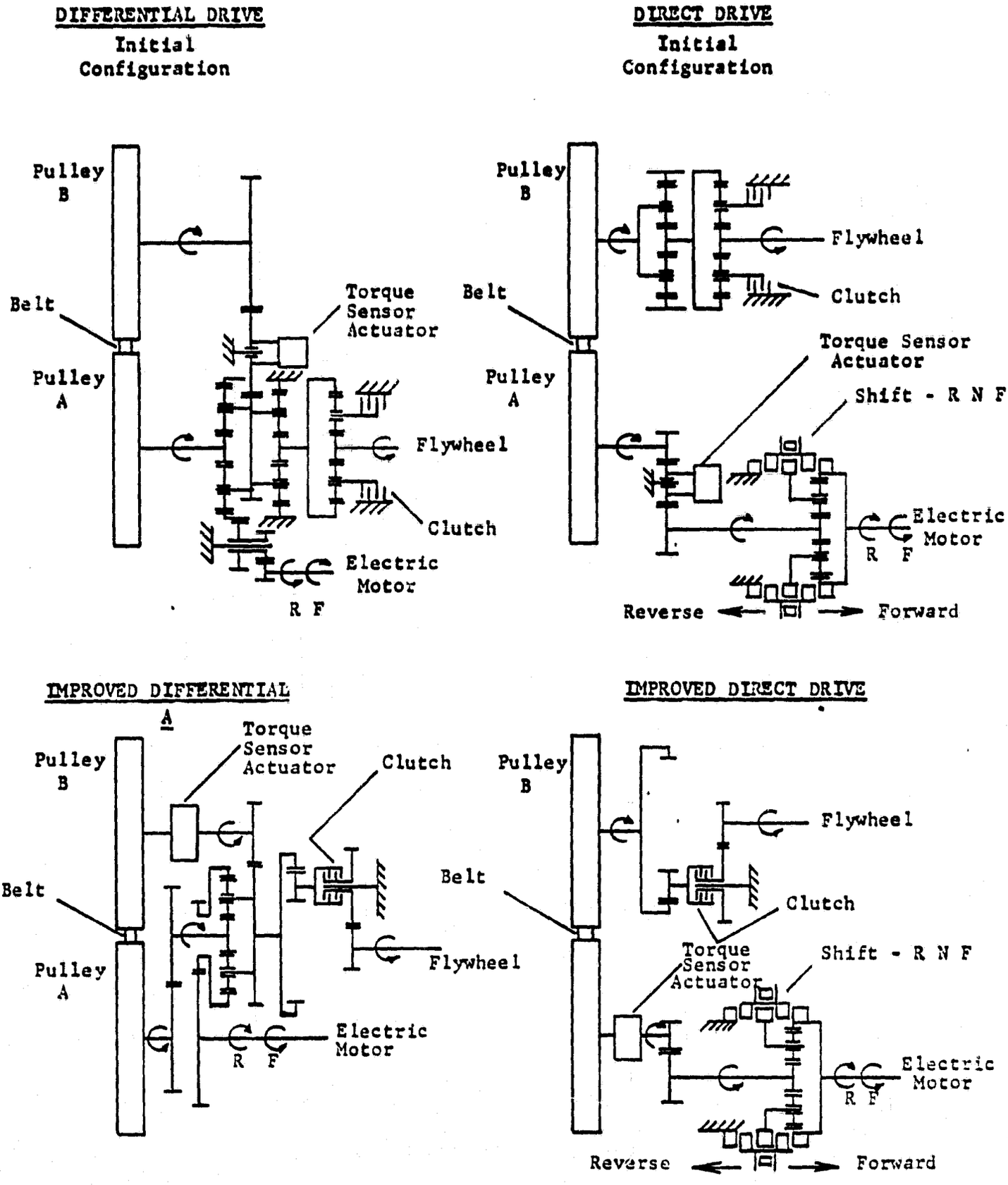

Figure IV-1 — TRANSMISSION CONFIGURATIONS

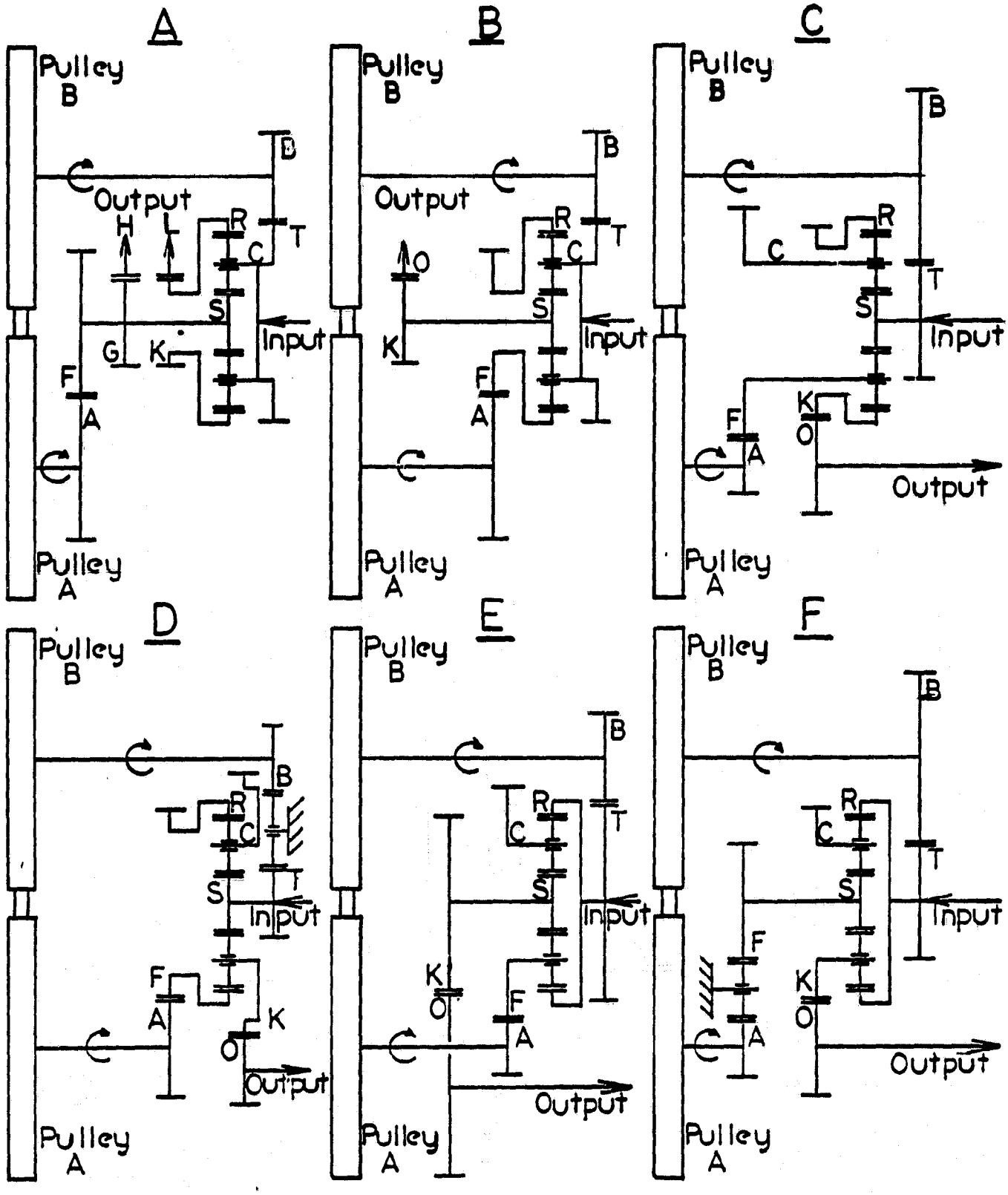

Figure IV-2 — PULLEY DIFFERENTIAL DRIVE ARRANGEMENTS

The speed and power data for the various configurations may be computed using the planetary differential relationships as shown in Table IV-2.

TABLE IV-2

PLANETARY DIFFERENTIAL SPEED, TORQUE, POWER RELATIONSHIP

Speed Relationship

$$(D_s/D_r)\ N_s + N_r = (1 + D_s/D_r)\ N_c$$

Note: Same rotational direction

Torque Relationship

$$T_s/T_r = D_s/D_r$$

$$T_c/T_r = 1 + D_s/D_r$$

$$T_c/T_s = 1 + D_r/D_s$$

Power Relationship

$$P_s/P_r = (1 + D_s/D_r)\ N_c/N_r - 1$$

$$P_c/P_r = 1 + (D_s/D_r)\ N_s/N_r$$

$$P_c/P_s = 1 + (D_r/D_s)\ N_r/N_s$$

Symbols: N - - - Speed, RPM
T - - - Torque, N-m
P - - - Power, KW
D - - - Diameter of gear, mm

Subscripts:

s - sun
c - planet carrier
r - ring

The output speed is required to vary over the range of zero to 5,000 RPM and the flywheel at 21,000 RPM is assumed to be geared as needed to supply the desired input speed to the differential gears. With exception of Configuration A, all configurations were designed to use a pulley speed ratio range of 4:1 only. Hence, using the differential gear speed and torque relationships, the speed and power data on the various configurations is presented in Table IV-3.

CHARACTERISTICS OF PULLEY DRIVE CONFIGURATIONS

CONFIGURATION	RATIO r_R/r_S	GEAR SPEEDS - RPM N_O	N_C	N_R	N_S	N_A	N_P	T_A/T_O	P_A/P_O	(KW) MAX			NOTES
A-DIFF	2.5	0	2000	0	7000	10000		0.200		94.3			
A-DIFF	2.5	1430	2000	2000	2000	2857		0.200	0.400				SHIFT POSITION
A-DIRECT	2.5	5000	2000	-	8000	10000		0.500	1.000	75.0			3.5:1 SPEED RATIO
A-DIFF	3.0	0	2000	0	8000	10000		0.167		78.6			
A-DIFF	3.0	1250	2000	2000	2000	2500		0.167	0.333				SHIFT POSITION
A-DIRECT	3.0	5000	2000	-	8000	10000		0.500	1.000	75.0			4:1 SPEED RATIO
A-DIFF	4.0	0	2000	0	10000	10000		0.125		58.9			5:1 SPEED RATIO
A-DIFF	4.0	1000	2000	2000	2000	2000		0.125					SHIFT POSITION
B	2.5	0	2000	2800	0	10000		0.667		314.3			EXCESSIVE BELT
B	2.5	5000	2000	700	5250	2500		0.667	.333	25.0			POWER AT MAX
B	3.0	0	2000	2667	0	10000		0.667		314.3			TORQUE STALL,
B	3.0	5000	2000	667	6000	2500		0.667	.333	25.0			NO ADVANTAGE
B	4.0	0	2000	2500	0	10000		0.667		314.3			USING SHIFT,
B	4.0	1333	2000	2000	2000	8000		0.667	4.000				HIGH POWER THRU
B	4.0	5000	2000	625	7500	2500		0.667	.333	25.0			BELT-LOW SPEEDS
C	2.5	0	2000	0	7000	10000		0.667		314.3			EXCESSIVE BELT
C	2.5	5000	500	-2100	7000	2500		0.667	.333	25.0			POWER AT MAX
C	3.0	0	2000	0	8000	10000		0.667		314.3			TORQUE STALL,
C	3.0	5000	500	-2000	8000	2500		0.667	.333	25.0			HIGH POWER THRU
C	4.0	0	2000	0	10000	10000		0.667		314.3			BELT-LOW SPEEDS
C	4.0	5000	500	-1875	10000	2500		0.667	.333	25.0			
D	2.5	0	0	-1240	3100	-2493		0.667		78.6			POWER THROUGH
D	2.5	3000	-1600	-3480	3100	-7000		0.667	1.556	116.7			BELT LARGER
D	2.5	5000	-2667	-4973	3100	-10000		0.667	1.333	100.0			THAN OUTPUT POWER
D	3.0	0	0	-1185	3555	-2500		0.667		78.6			THROUGHOUT
D	3.0	3000	-1600	-3319	3555	-7000		0.667	1.556	116.7			OPERATING RANGE
D	3.0	5000	-2667	-4740	3555	-10000		0.667	1.333	100.0			
E	2.5	0	2000	2800	0	10000		0.667		314.3			COMMENTS —
F	2.5	-5000	500	2800	-5250	2500		0.667	.333	25.0			SAME AS
E	3.0	0	2000	2500	0	10000		0.667		314.3			CONFIGURATION C
E	3.0	-5000	500	2500	-5625	2500		0.167	.333	25.0			
F	2.5	0	0	5000	-12500	10000		0.667		314.3			COMMENTS —
F	2.5	5000	2667	5000	-3165	2500		0.667	.333	25.0			SAME AS
F	3.0	0	0	4750	-14250	10000		0.667		314.3			CONFIGURATION C
F	3.0	5000	2667	4750	-3585	2500		0.667	.333	25.0			

TABLE - IV-3

Table IV-3 — CHARACTERISTICS OF PULLEY DRIVE CONFIGURATIONS

It is desired to minimize the belt power and torque through the operating range but it is critical that the belt power or torque not be excessive at any point in the operating range. Examination of the results of Table IV-3 shows the "Configuration A" to have an advantage over the other configurations in that (1) in the differential mode of operation, the belt torque is much less than the belt torque of the other drives and (2) the required belt power in the direct drive mode is less at lower speeds and 60% rated speed.

Only one differential geared transmission, Configuration A, can use a synchronizer shift to advantage to change operation from the differential mode to a direct drive mode. A "Combined Configuration A" is shown as initially conceived in Figure IV-3. The electric motor is also shown for the first time as being located on the input side rather than the output side of the transmission to improve its operating efficiency.

Simultaneous design calculations on the size requirements of the flat belt pulleys then was used to specify the center distance of the pulley shafts and their gears. The high efficiency and relatively low cost of spur gears made them a logical initial choice. The transmission gear arrangement was then studied, considering all elements, the envelope of the elements, and their possible location in a vehicle. It was decided to use an electric clutch to isolate the flywheel and arrange the flywheel input to allow a direct-in-line coupling to an electric motor, maintaining direct access to uncovering the pulley section. This minimizes the motor size and weight, as well as losses in driving the flywheel up to speed. Further investigation showed that the planetary differential gearing should be positioned close to the pulleys so that the same transmission width required for the synchronizer can also be used for the electric clutch. Now, as shown in Figures I-2., I-3, I-4, I-5 and II-1,

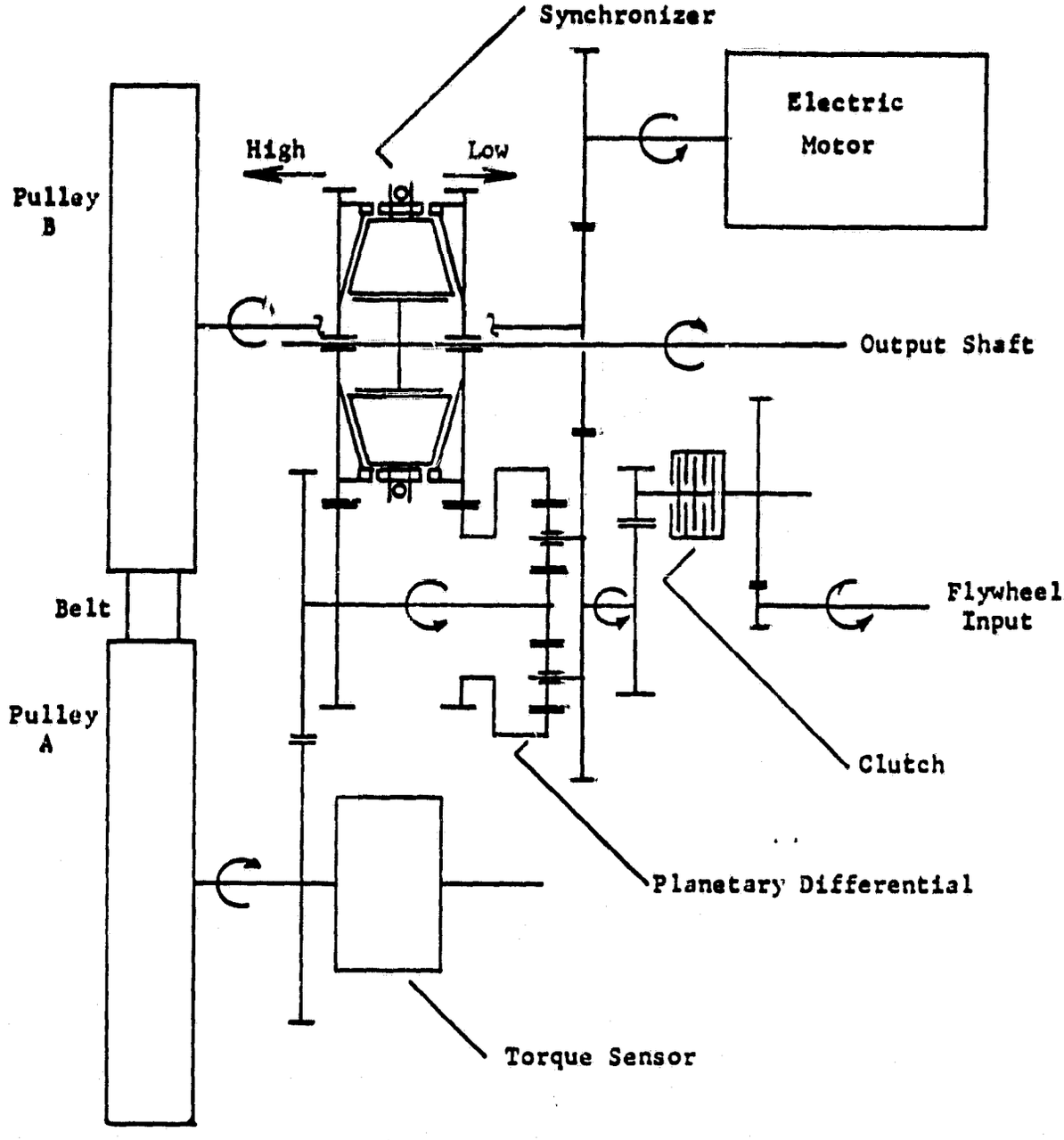

Figure IV-3 — DIFFERENTIAL BELT TRANSMISSION COMBINED CONFIGURATION A

it should be possible to drive directly from the transmission to the differential on the axle to the wheels, with clearance for the close coupled flywheel.

B. Flat Belt Drive Components

1. Pulley Design

As described previously, an angular movement between the inner and outer support plates in the pulleys causes the belt drive elements to change position radially. The guideways for the belt drive elements should be logarithmic spirals of the radius to balance forces and torques irrespective of the belt radial position, as shown in Figure IV-4 and associated analysis.

$$\tan \alpha = r\Delta\theta/\Delta r$$

$$\int dr/r = \int d\theta/\tan \alpha$$

$$\ln r/r_1 = \theta/\tan \alpha$$

$$r = r_1 e^{\theta/\tan \alpha}$$

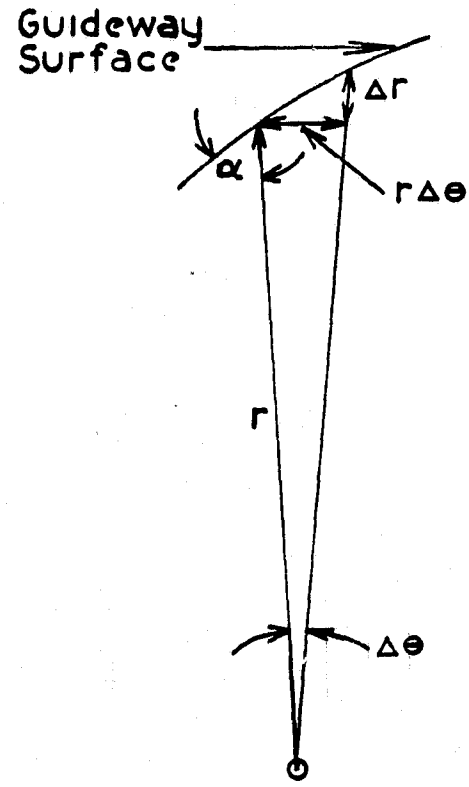

Figure IV-4 - GUIDEWAY GEOMETRY

Detailed layouts showed that the ideal logarithmic spiral guideway geometry may be accurately approximated by a circular arc which makes possible a simple accurate machining of the guideways. Using $\alpha = 45^{\circ}$, the resulting proposed geometry of the guideways in the pulley plates is shown in Figure IV-5. The pulley side plates containing the guideway grooves for the ends of the drive elements must be designed to absorb the maximum possible centrifugal loads without rupture or significant creep. The outer ring acts in hoop tension to hold the guideway section together under the centrifugal loading due to rotational speed. Initial calculations indicate that it will be necessary to minimize the weight of the guideway plates by using lightening holes and use a high strength outer ring, such as 7075-T6, as shown in Figure IV-5. Using a possible control failure mode that would rotate pulley A at a speed of 13817.5 rpm (normal maximum speed is 9899 RPM) would stress the outer aluminum ring as given to about 50000 PSI. However, an additional safety factor is involved in that the drive attachment to the inner plates is stronger and fits around the outer plates. With 7075-T6 having a yield tensile of 73000 PSI, this should be an adequate safety factor in the design for this exceptional control failure mode condition.

2. Belt Drive Element Design

Considering recommendations by the manufacturers of belts, it was decided to design to a 37.50 mm wide belt, which then resulted in the design of the belt drive element, as shown in Figure IV-6. Using maximum torque at stalled output gives the maximum load of the belt on the drive element. The conservative assumption was made to neglect the centrifugal force of the drive element to compute the stress on the drive element. The computations resulted in a maximum radial load of 689.4 N on the drive element

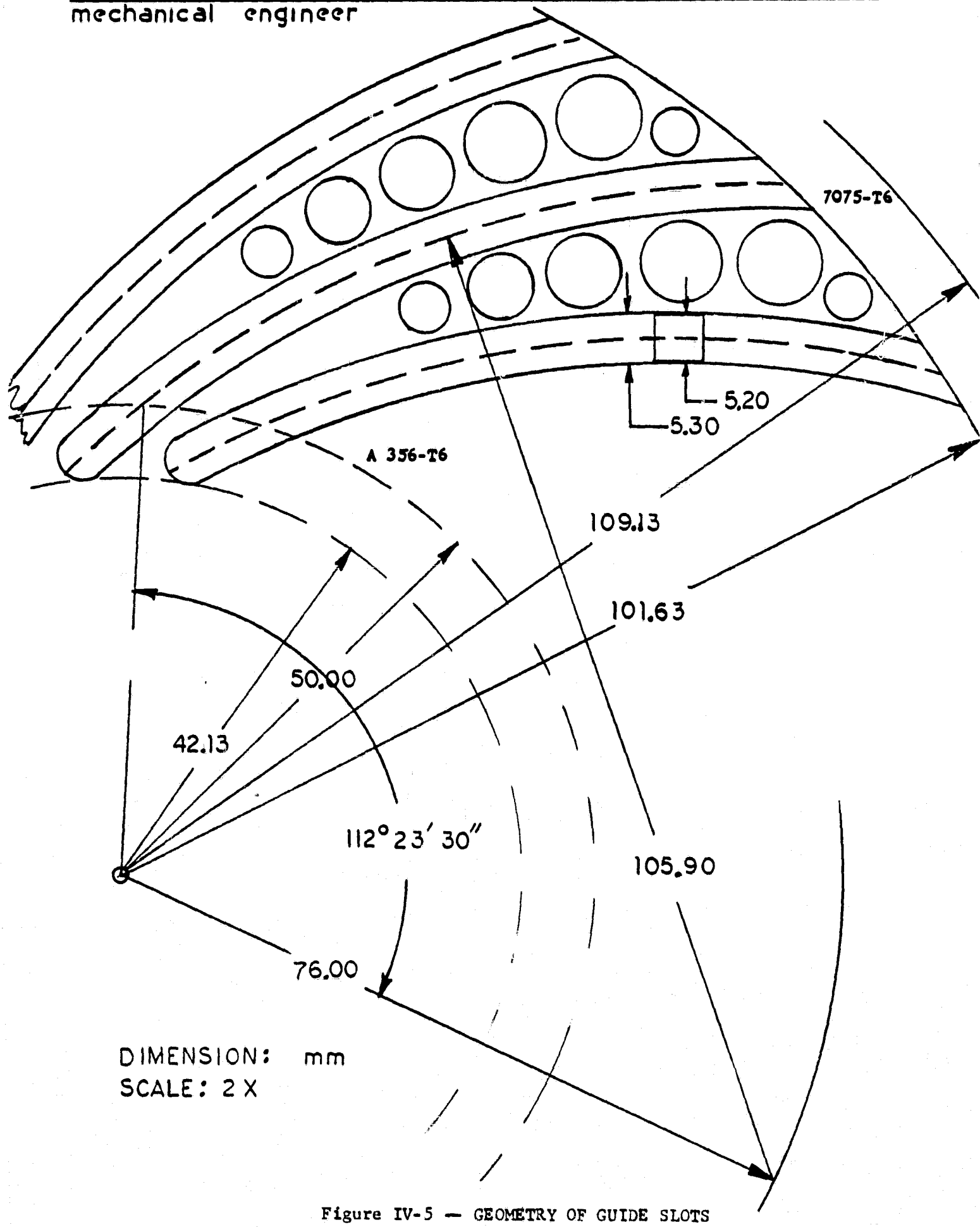

Figure IV-5 — GEOMETRY OF GUIDE SLOTS

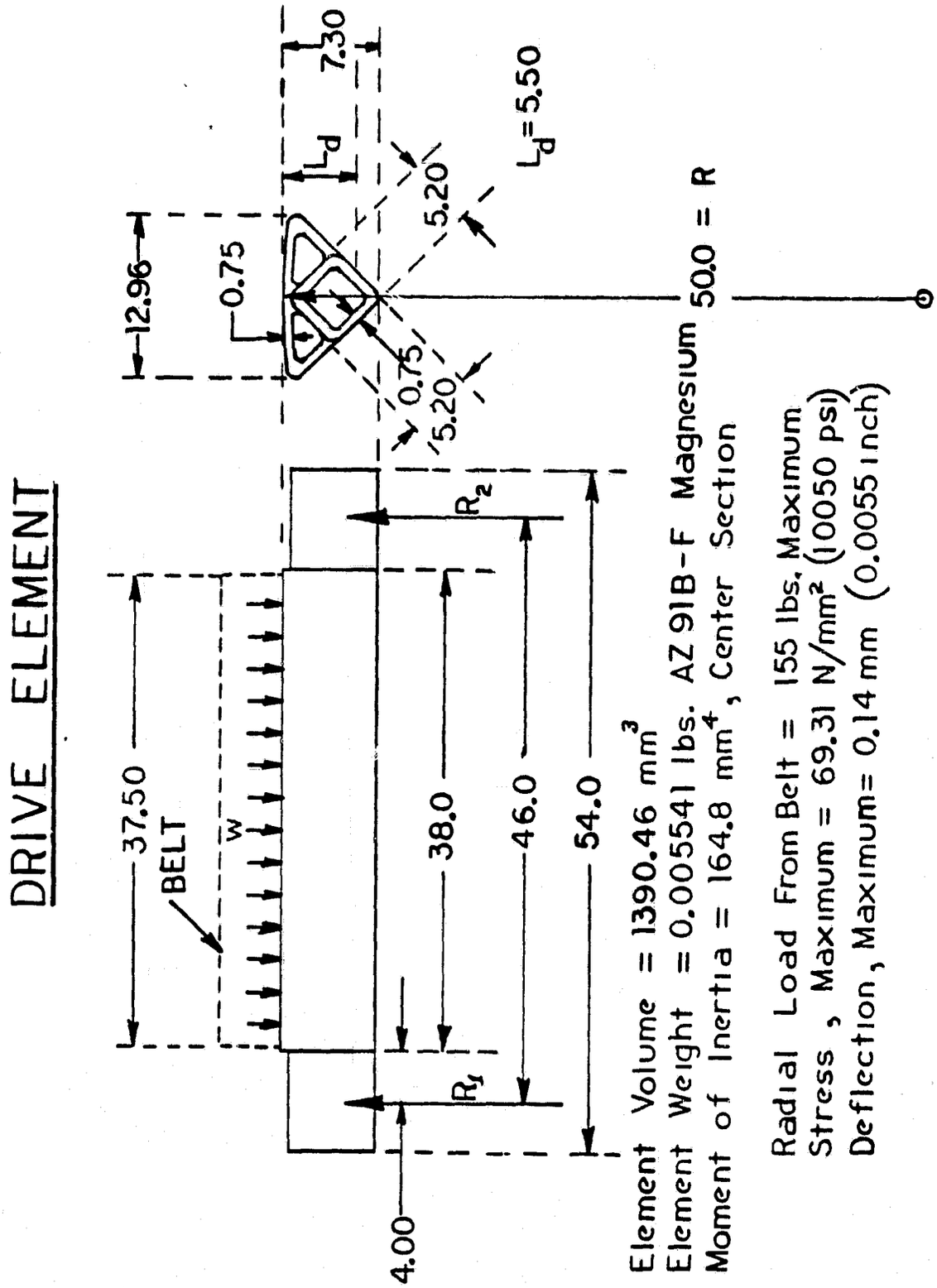

Figure IV-6 — DRIVE ELEMENT

as a result of a belt tension of 2764.4N. The moment of inertia of the drive element cross section was computed and the stress and deflection then calculated using appropriate stress formulae. The maximum stress was 69.31 N/mm^2 (10050 PSI) and deflection was 0.14 mm (0.0055 inch). It is proposed to use a cast magnesium alloy such as AZ 91B-F (yield strength = 23000 PSI). The drive element could also be extruded (ZK60A-75 with yield strength of 40,000 PSI), with the ends machined to leave the bottom box structure to fit the guideways of the pulley side plates. The low density of the magnesium alloys (.065 lbs/in^3) is attractive in reducing the centrifugal force of the drive elements in the pulley assembly. In addition, its thermal conductivity is much higher than high strength plastic composites, thus reducing any temperature gradients, and its high damping capacity should help to reduce vibratory loads and stresses.

3. Drive Element Counter Balance and Pressure Balance Chamber Design

The centrifugal force of the drive elements is significant, even though the total weight of 24 elements is only 0.5915 N (0.1330 lbs). At maximum pulley A speed of 9899 RPM, this gives a centrifugal force of 3191.9 N (717.6 lbs), which corresponds to a torque equivalent from the rotary actuator of 78.14 N-m (691.5 in.lbs). The counter balance for the centrifugal force of the drive elements reduces the rotary actuator pressure, P_1, as the speed of pulley A increases to give a net belt tension desired for the assumed operating friction coefficient. The design of the drive element counter balance is given in Figure IV-7 and consists of two sets of circumferentially located balls in radial slots, which operate to give an axially thrust opposing the thrust resulting from the helical spline between gear (A) and pulley A shaft. The two sets of balls permit balancing for either direction of torque through gear A. Displacement of the

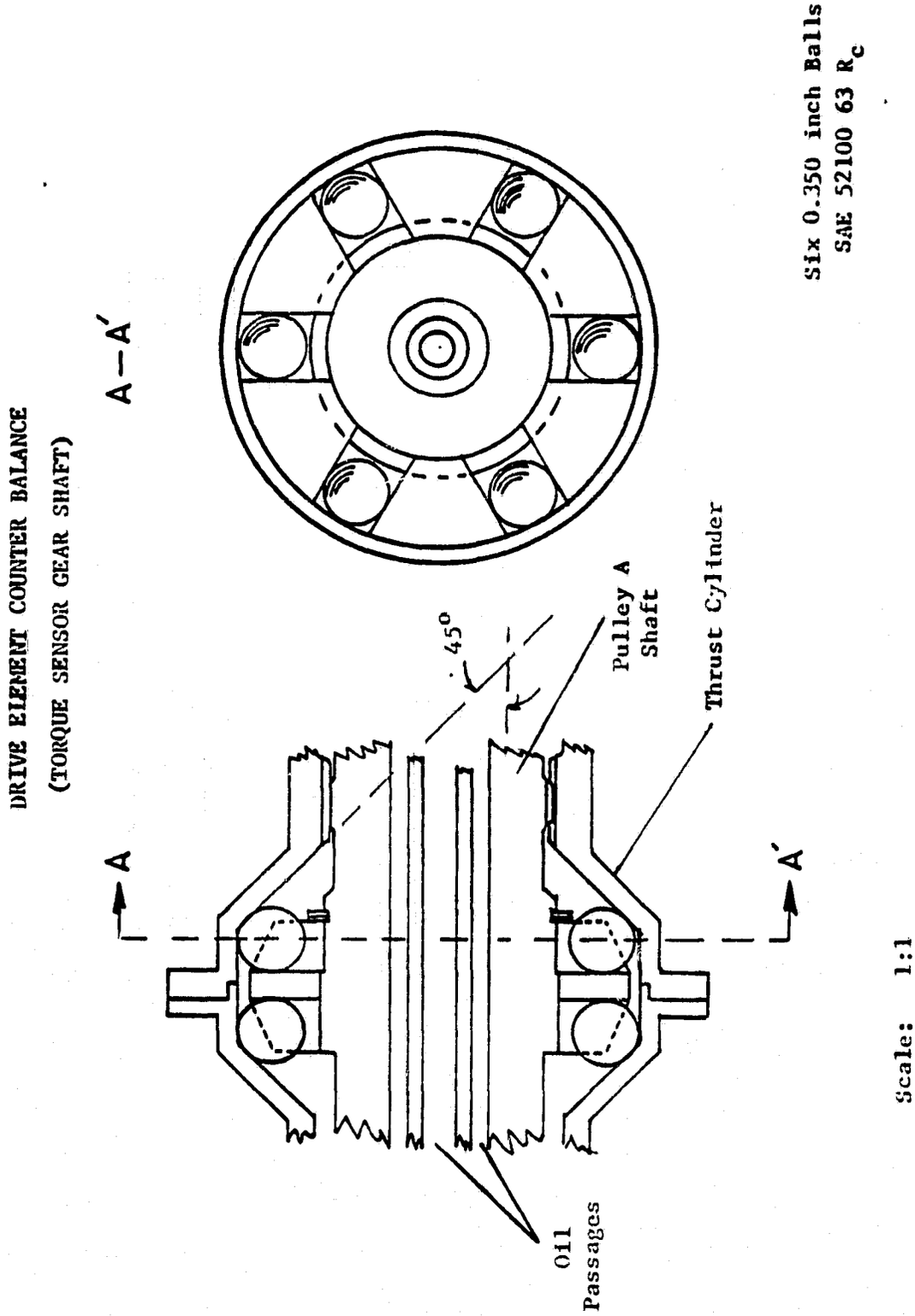

Figure IV-7 — DRIVE ELEMENT COUNTER BALANCE

thrust cylinder is necessary to give pressure balancing in the torque balance pressure chamber, which then moves one or the other set of balls from their rest position at the maximum inner circumference of said thrust cylinder. It now is possible to balance the drive element centrifugal loads over the complete speed range by changes in the actuator pressure, P_1. The actuator pressure, P_2, is normally regulated to a constant value that is changed, one pulley relative to the other, only when the operator demands speed change. Hence, the actuator pressure, P_1, will be varied both larger than and smaller than P_2, depending on pulley A's speed. The pressure range depends on the rotary actuator sizing and the desired torque and speed of the pulleys. The centrifugal force of the drive elements is compensated by the same pressure, P_1, in both the driving and driven pulleys. This occurs because with the same belt or drive element velocity, an equivalent torque is involved, irrespective of the different pulley speeds. With a continuous oil flow through the spline section from the filled ball chamber, the spline friction coefficient is estimated to be less than 0.02. This affects the torque sensor by less than 16%, using 7.5 degree helix angle splines.

Chose a 16/32 spline with 7.5 degrees helix angle. This gives a pitch diameter of 33.625 mm (1.3238 inch) with 21 teeth. The maximum torque of 72.36 N-m (640.37 in.lb.) on gear (A) at 9899 RPM gives 75.0 KW (100.58 hp). This gives a tangential load of 4303.2 N (967.45 lbs) at the spline. The resulting maximum thrust on the thrust cylinder is

$$F_A = F_T \tan \gamma = 4303.2 \tan 7.5^\circ = 566.5 \text{ N } (127.37 \text{ lbs}) \quad \text{(IV-1)}$$

Assuming a torque balance pressure differential of 100 PSIG then gives a hydraulic balance area of

$$A_{HYD} = F_A / \Delta P = 127.37/100 = 1.2737 \text{ in}^2 \quad \text{(IV-2)}$$

Choosing an inlet tube diameter of d_i = 0.375 inches (9.53mm), the required outer pressure chamber diameter may be calculated

$$d_o = \left[4(1.2737) / \pi + (0.375)^2\right]^{\frac{1}{2}} = 1.3275 \text{ in. } (33.72\text{mm}) \qquad \text{(IV-3)}$$

It is shown in the next section on the design of the rotary actuator that the maximum pulley torque of 75 N-m gives a required actuator torque of 95.67 N-m to operate at a belt friction coefficient of 0.35. Hence, the actuator torque of 78.14 N-m, which is required to offset the maximum centrifugal force of the belt drive elements, then requires balancing 78.14/95.67 of the 100 PSI differential, or the equivalent axial force of F_A = 133.17 lbs. Therefore, the required maximum axial thrust due to the balls is

$$(78.14/95.67)133.17 = 108.77 \text{ lbs.}$$

Using a 45° conical enclosure for the counter balance balls results in the centrifugal force of the balls being equal to their axial force.

$$F_a = F_c \tan \beta = 108.77 \text{ lbs.} \qquad \text{(IV-4)}$$

$$\beta = 45^\circ$$

$$F_a = F_c$$

The centrifugal force of the balls is given:

$$F_c = mV^2/r \qquad \text{(IV-5)}$$

$$m = W/g \qquad \text{(IV-6)}$$

$$W = N_b W_b \qquad \text{(IV-7)}$$

$$W_b = \rho \pi D_b^3/6 \qquad \text{(IV-8)}$$

for SAE 52100 steel, $\rho = 0.281 \text{ lbs/in}^3$

Using $N_b = 6$

D_b = 0.350 inches (8.890mm)

$$r = 6 (894981) F_a / N^2 N_b \rho \pi D_b^3 \qquad \text{(IV-9)}$$

$$r = 6 (894981) 108.77 / 10^8 (6) (0.281)\pi(.350)^3$$

$$r = 25.72 \text{ mm}$$

Therefore, operate at

$r = 25.60$ mm

Housing Radius = 25.60 + 8.890/2 = 30.6 mm

4. Rotary Actuator Design

The rotary actuator on each pulley supplies the torque for tensioning the belt by means of a pressure differential, $P_1 - P_2$. The shaft which is connected to the outer plates containing the guideways for the ends of the drive elements is also connected to three shaft struts, which may rotate about 90° in three chambers comprised of the case struts and outer case, as shown in Figure IV-8. The case and case struts are connected to the inner plates containing the guideways for the ends of the drive elements so that rotation of the case relative to the shaft then changes the radial position of the drive elements, as has been described in previous sections. Oil at pressure P_1 and P_2 is supplied through appropriate passages in the shaft to the actuator cavities where the differential pressure, $P_1 - P_2$, acts on the exposed case strut and shaft strut areas to supply a torque between the inner and outer guideway plates. The vector diagram of loads on the belt and drive elements as given in Figure IV-9 show the actuator torque to be

$$T_{ACT} = \sum F_n \, (R - L_d) \, / \, 2 \tan \alpha \qquad \text{(IV-10)}$$

Using a friction coefficient of $\mu = 0.35$ at maximum speed with eleven drive elements in contact with belt gives

$$\sum F_n = 2.855 \, (F_1 - F_2) \qquad \text{(IV-11)}$$

Using $\alpha = 45^\circ$

$L_d = 5.5$ mm

$R = 51.7$ mm (Maximum speed)

$$T_{ACT} = 0.06595 \, (F_1 - F_2) \text{ N-m} \qquad \text{(IV-12)}$$

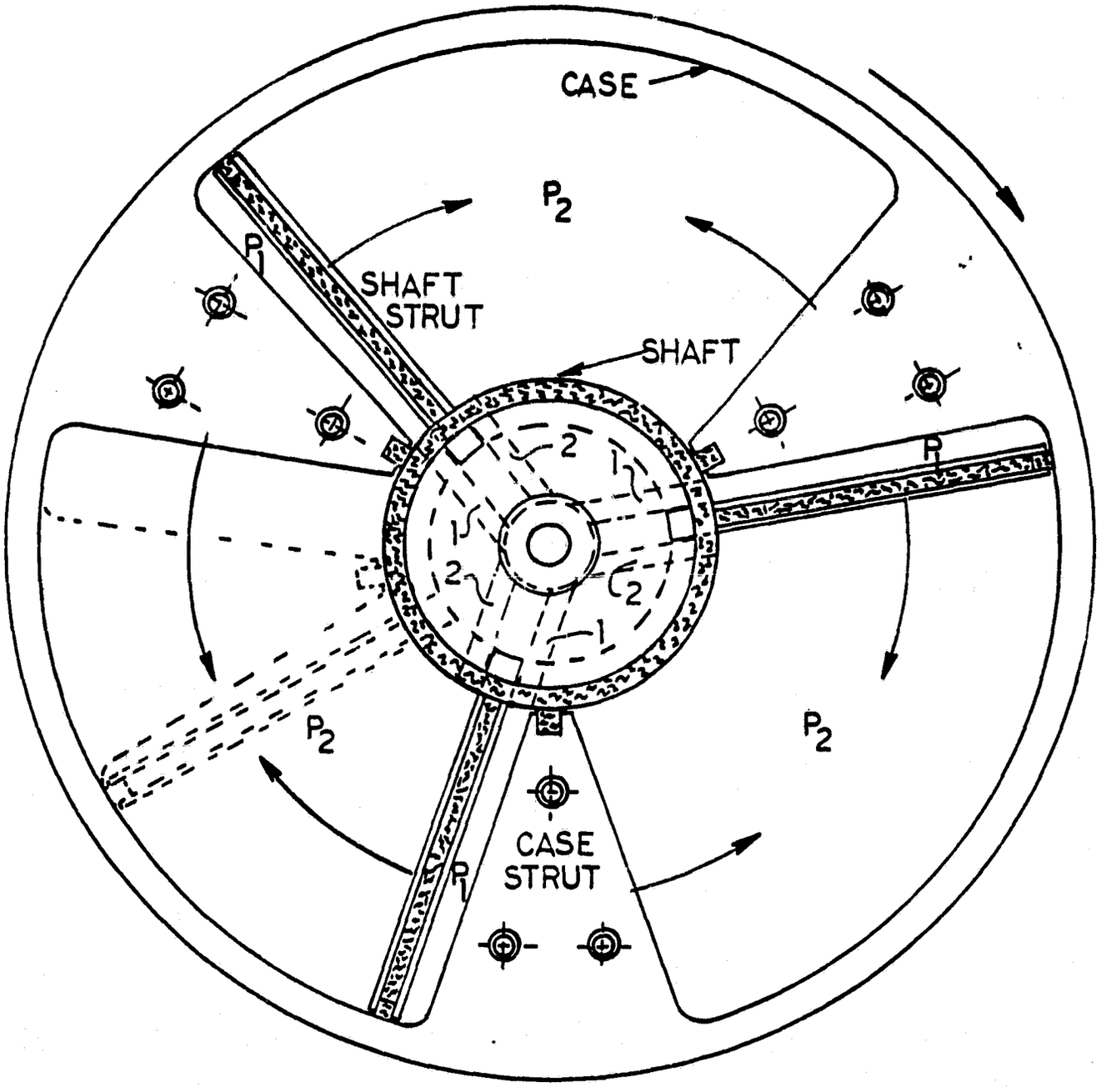

Scale: 1:1

Figure IV-8 — ROTARY ACTUATOR

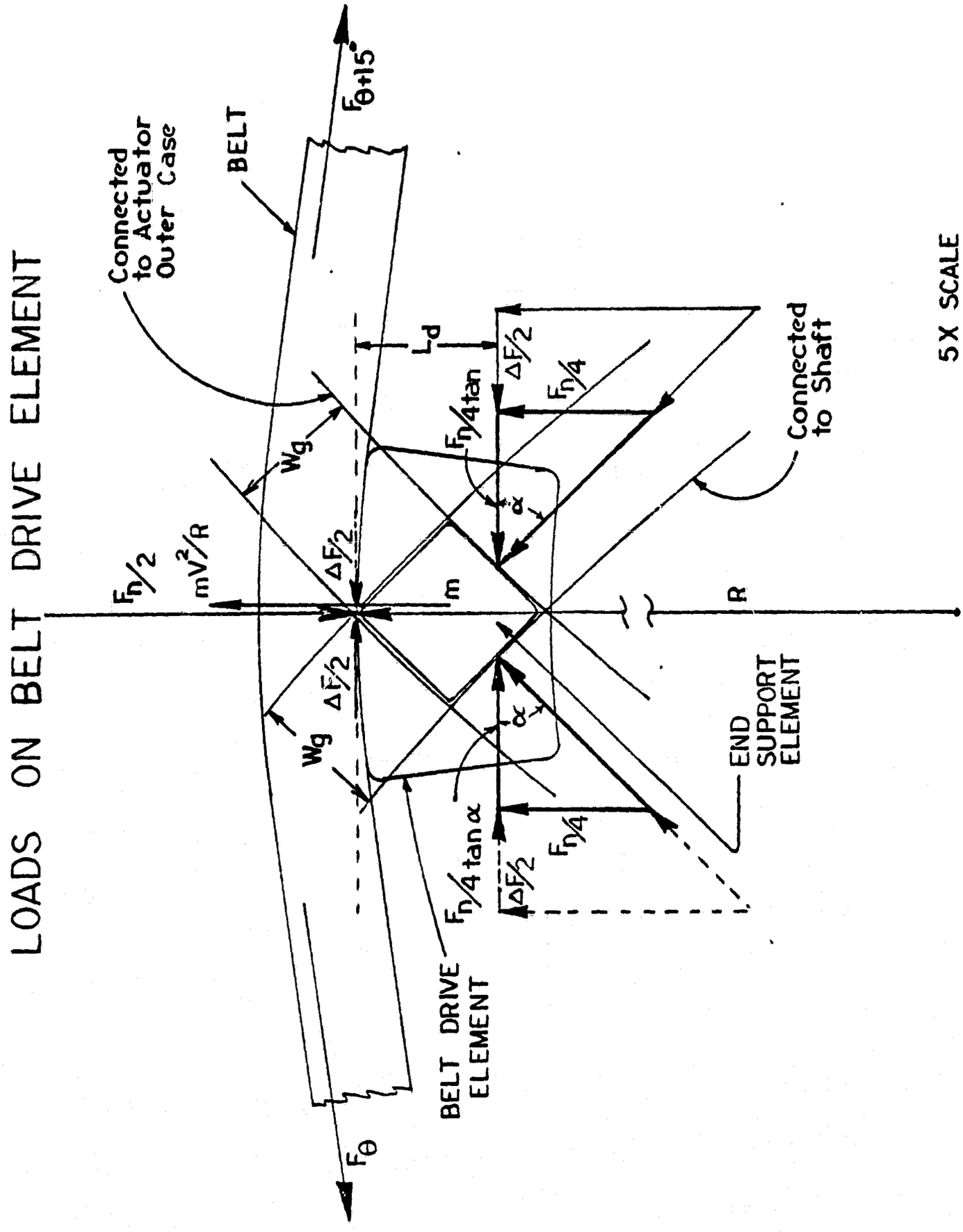

Figure IV-9 — LOADS ON BELT DRIVE ELEMENT

Assuming a pulley A torque of 75 N-m

$$F_1 - F_2 = 75000 / 51.7 = 1450.68 \text{ N (326.14 lbs)} \qquad \text{(IV-13)}$$

Thus, the required T_{ACT} is from Eq. (IV-12)

$$T_{ACT} = 0.06595\ (1450.68) = 95.67 \text{ N-m (846.71 in-lb)}$$

The total actuator torque may be shown to be for the three sections of the rotary actuator

$$T_{ACT} = 3\ (P_1 - P_2)\ W\ (r_o^2 - r_i^2)\ /\ 2 \qquad \text{(IV-14)}$$

W = width of actuator

Using $r_o = 79.0$ mm (3.1102 in)

$r_i = 27.0$ mm (1.063)

$P_1 - P_2 = 0.6897$ MPa (100 PSI)

$$W = T_{ACT}\ \frac{2}{3}\ \frac{1}{(P_1-P_2)}\ \frac{1}{(r_o^2 - r_i^2)} \qquad \text{(IV-15)}$$

W = 18.78 mm (0.739 inches)

Hydraulic pressure is developed in the rotary actuator cavities, due to the rotational speed of the pulley. This may be calculated as follows:

$$F_{c_{HYD}} = m\omega^2 r = \rho\omega^2\ W2\pi(r_o^3 - r_i^3)\ /\ 3\ g \qquad \text{(IV-16)}$$

Using $\rho = .0289 \text{ lbs/in}^3 = 1.762 \cdot 10^{-6} \text{ lb/mm}^3$

$\rho = 7.839 \cdot 10^{-6} \text{ N/mm}^3$

Max speed, $\omega = 9899\ (2\pi)\ /\ 60 = 1036.62$ radians/sec. and using Eq. (IV-16)

$$F_{c_{HYD}} = 1.762 \cdot 10^{-6}\ (1036.62)^2\ 18.78(2\pi)(79^3-27^3)/32.2(25.4)(12)3$$

$$= 3591.8 \text{ lbs} = 15976.5 \text{ N}$$

Equivalent internal pressure, P_i

$$P_i = F_c\ /\ 2\pi r_o\ W = 15976.5\ /\ 2\pi(79)(18.78) \qquad \text{(IV-17)}$$

$$P_i = 1.71 \text{ N/mm}^2 \text{ (248.5 PSI)}$$

The operating pressure, P_1 or P_2, are in addition to P_i. Assuming a maximum P_1 of 145 PSI or 1.0 N/mm^2 gives a total maximum internal pressure of 2.71 N/mm^2 (this high value would occur only in a failure mode where the ball

counter balance did not function). However, using a case thickness of 5.0 mm (.20 inch) the case stress would be

$$\sigma = pr/t = 2.71(79)/5 = 42.82 \text{ N/mm}^2 \qquad \text{(IV-18)}$$

$$\sigma = 42.82 \text{ MPa (6208.6 PSI)}$$

The cover to the rotary actuator case is held by a threaded ring at its outer circumference (whose thickness gives essentially a clamped side) and by screws to the three case struts. The inner circumference of the case cover is not supported directly and yet must not leak through its sealing ring. It is very difficult to compute the deflection of such a diaphragm but a conservative estimate may be made using Roark.[8]

Let $a/b = 56/40 = 1.4$

$a = 56$ mm (2.21 inches)

$b = 40$ mm (1.575 inches)

Let $P = 200$ PSIG $= w$

$t = 4.0$ mm (0.1575 in)

$E = 10 \cdot 10^6$ (aluminum)

$$S = \beta wb^2 / t^2, \; y = \alpha wb^4 / Et^3 \qquad \text{(IV-19)}$$

Substituting in Eqn.s (IV-19),

$S = 15200$ PSI $= 104.8$ MPa

$y = 0.005$ inch $= 0.13$ mm

This calculation is believed to be very conservative.

The stress on the 5 mm thick steel shaft strut is estimated using beam loading formulae. Assuming a maximum differential of 100 PSI a uniform load of the beam is equivalent to 2.9 lbs/mm at 100 PSI differential pressure. Basing the beam on the bending of a 5.0 x 13.10 mm section (due to seals of 2.75 mm square in sides and end of strut) then gives

$$I = 1/12\ bd^3 = \tfrac{1}{2}(13.10)\ 5^3 = 818.75\ mm^4 \qquad \text{(IV-20)}$$

$$E = 30 \cdot 10^6\ PSI = 19.35 \cdot 10^8\ pounds/mm^2$$

$$w = \Delta P\ (A) / 1$$

$$w = 100\ (2.047)(.739) / (79-27) = 2.9\ lbs/mm \qquad \text{(IV-21)}$$

maximum $$y = -\ Wl^3 / 8EI \qquad \text{(IV-22)}$$

$$y = -\ 2\ (2.9)(79-27)(52)^3 / 8(19.35)\ 10^8\ (818.75)$$

$$y = 0.335 \cdot 10^{-6}\ mm$$

$$\sigma = M / I = (2.9)(52)^2\ (2.5) / 2(818.75) \qquad \text{(IV-23)}$$

$$\sigma = 12\ lbs/mm^2 = 53.38\ MPa\ (7740\ PSI)$$

5. Belt Tension Analyses

The belt radius ratio as a function of the pulley A radius was computed for the current configuration, as shown in Figure IV-10. The pulley speed ratio, N_B/N_A, is the same as the belt radius ratio, r_A/r_B if no slippage occurs.

The actuator torque, T_{ACT}, due to the pressure differential in the rotary actuator plus the torque due to the centrifugal force of the drive elements T_{DE_c}, combine to give actuator torque, T_{ACT_A}.

$$T_{ACT_A} = T_{DE_c} + T_{ACT} \qquad \text{(IV-24)}$$

using $\mu = 0.35$ with eleven drive elements in contact

$$\sum F_N = 2.855\ (F_1 - F_2) \qquad \text{(IV-25)}$$

From the vector diagram, Figure IV-9

$$T_{ACT_A} = 2.855\ (F_1 - F_2)\ (R_A - L_d) / 2 \tan \alpha \qquad \text{(IV-26)}$$

Let $L_d = 5.5$ mm

$\alpha = 45^\circ$

$$T_A = (F_1 - F_2)\ R_A \qquad \text{(IV-27)}$$

Substitute into Eqn. IV-24 from Eqn. (IV-26) with values of L_d and α

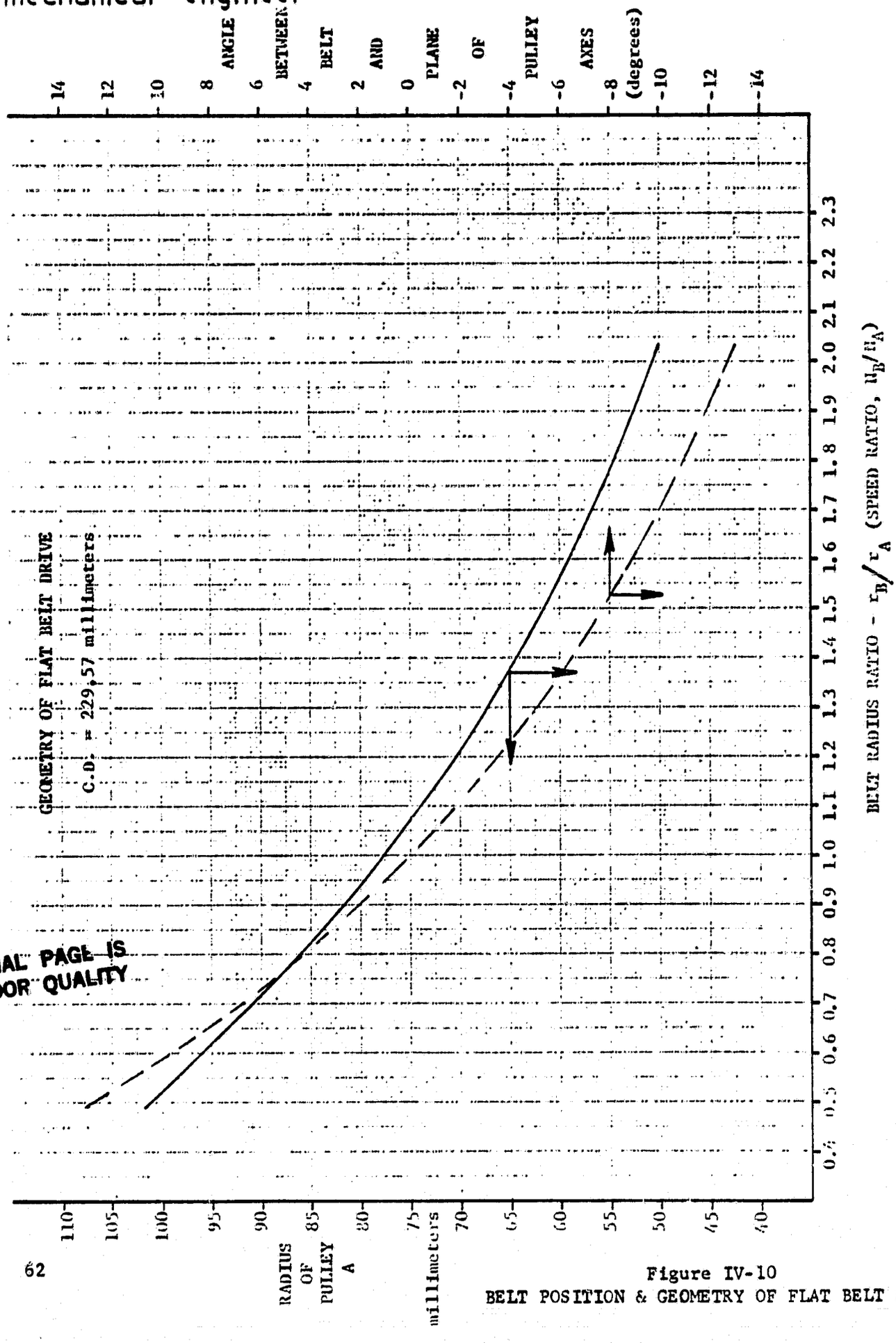

Figure IV-10
BELT POSITION & GEOMETRY OF FLAT BELT DRIVE

$$T_{ACT} + T_{DE_c} = 1.4275\ (1\text{-}5.5/R_A)\ T_A \qquad \text{(IV-28)}$$

Since $$T_{DE_c} = F_{DE_c}\ (R_A\text{-}L_d/2)\ /\ 2 \tan \alpha \qquad \text{(IV-29)}$$

and $$F_{DE_c} = 24\ m\ V^2\ /\ R_{DE} \qquad \text{(IV-30)}$$

$$R_{DE} = (R_A - 7.3/3) \qquad \text{(IV-31)}$$

The torque desired from the actuator can thus be calculated for all output speeds and torques and the necessary P_1-P_2 obtained.

The belt tension forces are calculated using the flat belt formula:

$$F_1\text{-}F_2 = (F_1\text{-}F_B)\ (e^{\mu\theta}\text{-}1)\ /\ e^{\mu\theta} \qquad \text{(IV-32)}$$

Since the design of the actuator system counter balances the centrifugal force of the drive elements, the centrifugal force of the belt causing tension, F_B, may be directly calculated from the belt as assumed.

$$\rho_B = 0.048\ \text{lbs/in}^3$$

$$b_B = 37.50\ \text{mm}$$

$$t_B = 4.763\ \text{mm}\ (3/16\ \text{in})$$

$$F_B = 12 \rho\ bt\ V_B^2\ /\ g = 4.952 \cdot 10^{-3}\ V_B^2\ \text{lbs} \qquad \text{(IV-33)}$$

$$V_B = \text{ft/sec}$$

Using the wheel power requirements as given by Figure III-8 for cruise operation and maximum torque and power as given by Figure IV-11, the calculated belt tensions are given in Figure IV-12. The tension due to the belt centrifugal load is a major portion of the total belt tension cruise torques. These belt tensions are used for calculating bearing requirements. The belt tension is a minimum at the automatic synchronizer shift point — a desirable feature considering the possibility of load transients at that time. Variation in the operating belt friction coefficient, μ, results in changing the belt tension only slightly due to the large belt centrifugal force component in the calculation, as shown on

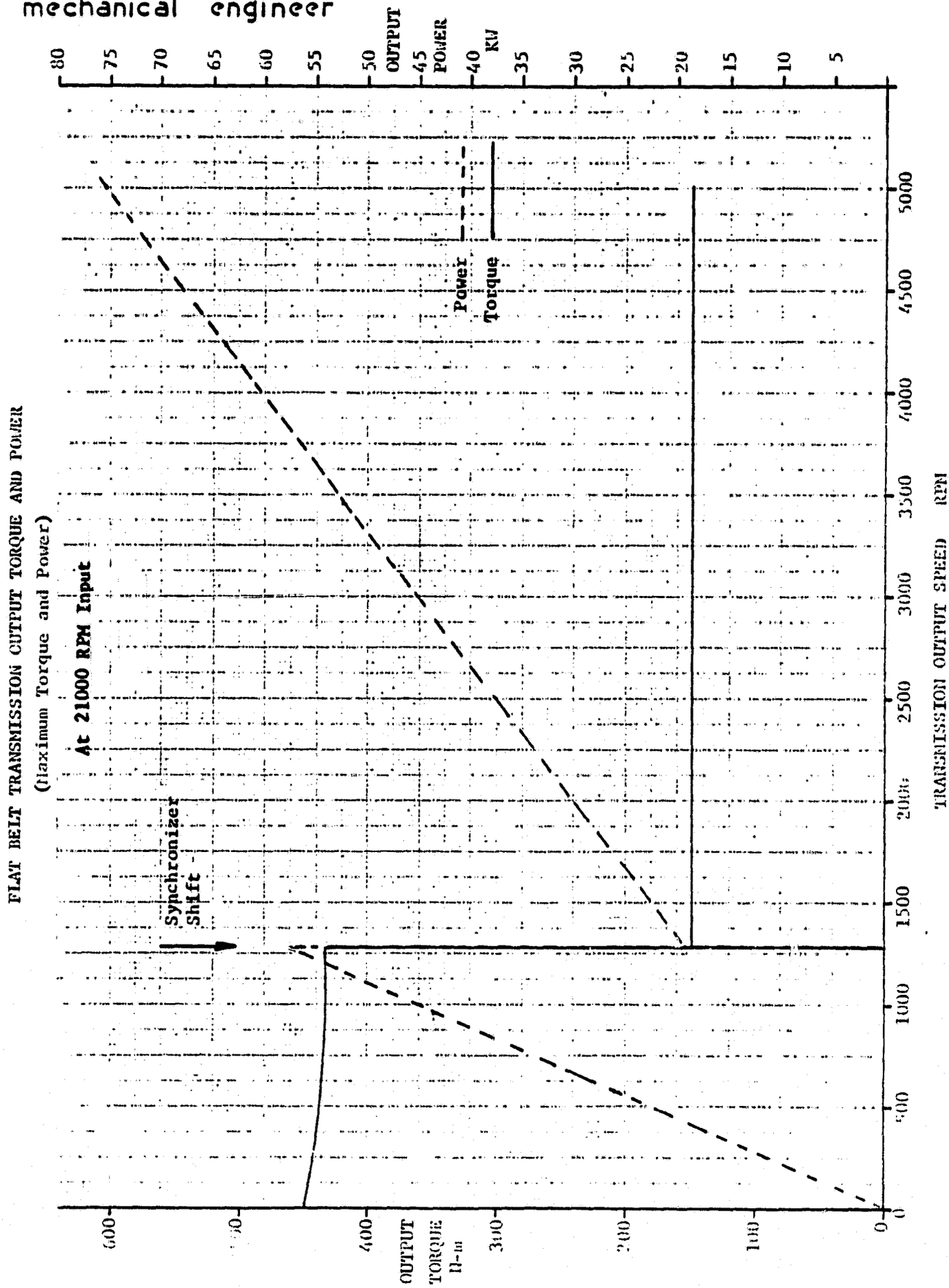

Figure IV-11 — FLAT BELT TRANSMISSION OUTPUT TORQUE & POWER AT 21000 RPM INPUT

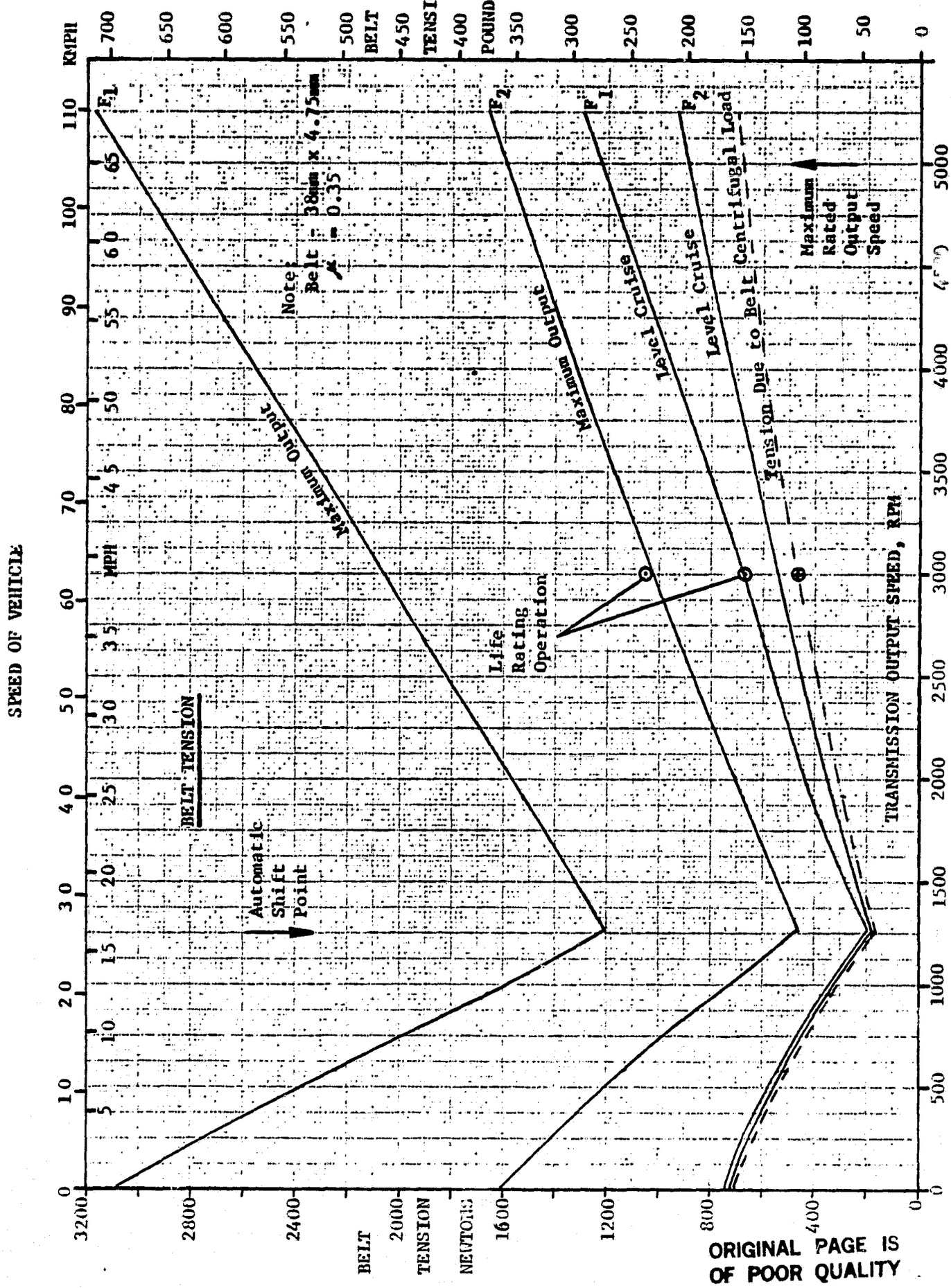

Figure IV-12 — BELT TENSION

Figure IV-13. A lighter weight belt would show a significant improvement in reducing the centrifugal tension load. This is believed probable with future belt construction improvements. However, a maximum belt load of 3042 N (684 lbs) at 9899 rpm (51.7 mm pulley A radius, 100.4 mm pulley B radius, using a 37.5 mm wide belt) is substantially consistent with the recommendation of a 2.0 inch wide belt for a 985 pound load by one belt manufacturer and the recommendation of a 1.70 inch wide belt using 720 pound load by another belt manufacturer (20 hour life estimate) for similar operating conditions.

6. Belt Stresses

Calculation of the belt stresses are required for estimation of minimum pulley size and necessary belt width. The maximum tensile load on the belt is usually only 5-10% of breaking load. Why then is the belt a critical loaded element? The most critical stress component for belt fatigue is the bending stress of the cord of the belt in passing around the minimum pulley radius. The flat belt pulley design used here has the same radius drive element for the belt, regardless of the overall operating radius. However, at the larger operating radii, only a portion of the belt is subjected to the bending fatigue stress per revolution, rather than the complete belt. Hence, on the average, the fatigue stressing of the belt due to bending decreases as the operating radius increases, with much the same effect as with a conventional pulley of larger radius.

Previous estimations of stress due to bending of belt cords around a pulley used a simple straight beam formula, which does not account for the construction of the belt initially as curved beam in the form of a circle. This becomes particularly significant with small belt length or higher

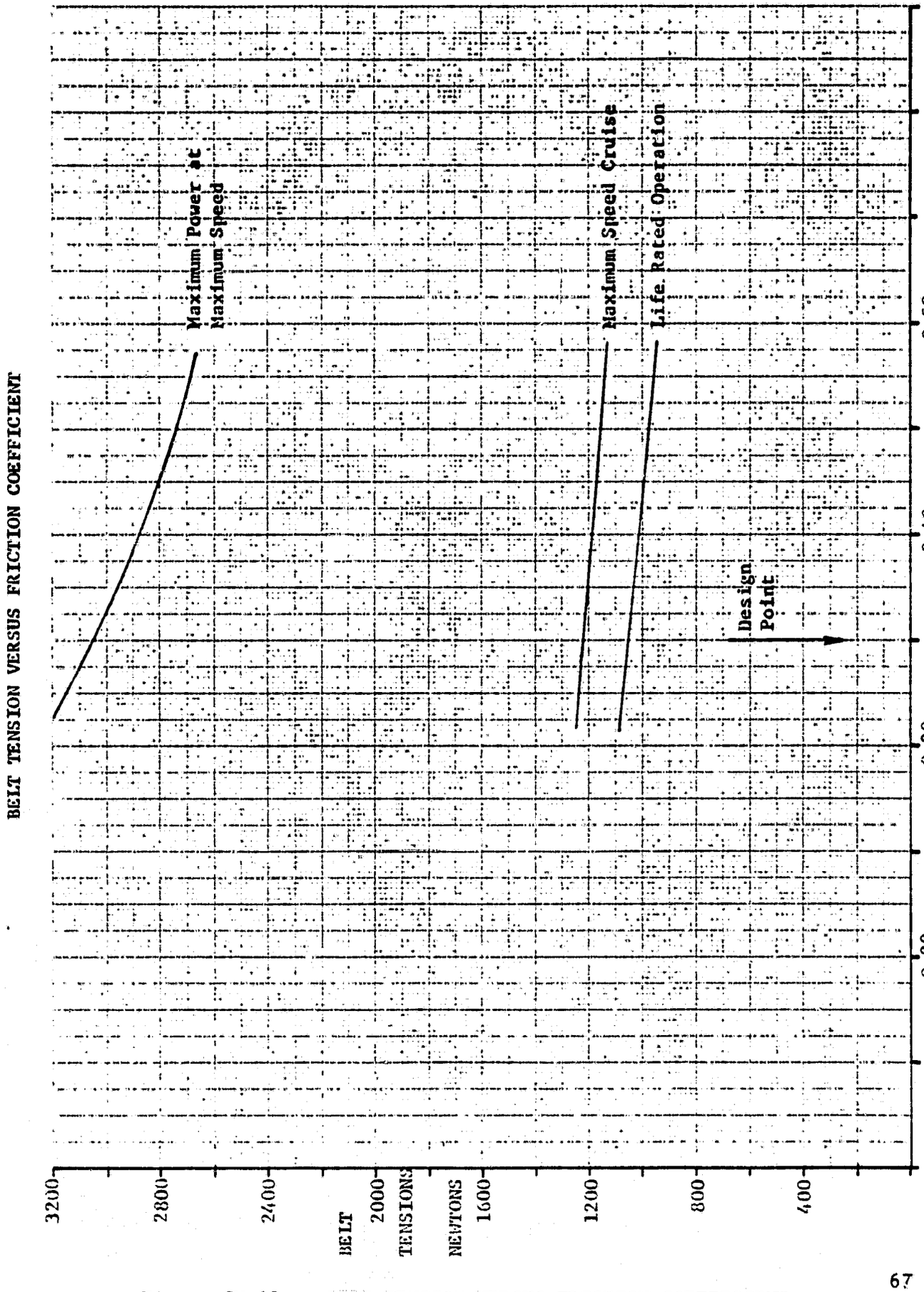

Figure IV-13 — BELT TENSION VERSUS FRICTION COEFFICIENT

initial belt curvature. The analysis for bending stress using Castigliano's theorem for strain energy is given in Appendix A. The results indicate the need for using small belt cord diameters. The overall results require additional calculation for the other stresses and their combination in the proper fashion. However, this calculation is believed to give a more accurate estimate of the bending stress of belt cords than has been previously available. For a belt length of 900 mm and pulley radius of 50 mm, the bending stress of belt cords around a pulley calculated by the new formula is 55% of the banding stress calculated using the previous formula. A question also arises as to the validity of the usual assumption that the tensile force applied to the cords in a belt do indeed prevent fiber slippage when bending the belt around a pulley and straightening it between pulleys. If there is adequate bonding material and friction, the assumption that the cord acts as a simple beam in bending appears reasonable. However, the cords are positioned in the rubber in the form of a ring, so that Castigliano's theorem for strain energy in bending of curved beams appeared more accurate for calculating bending stresses than calculations based on straight beam formula. However, the tensile cords in the belt in a rubber matrix having a tensile stress of only 0.10 the bending stress may indeed fray upon each other when bent or straightened. A belt construction as shown in Figure IV-14 would prevent the belt fibers from abrading each other during operation while passing around pulleys. The belt cords could be fabricated in a conventional fashion, but then could be passed through an epoxy resin or other liquid plastic bath in such a fashion as to thoroughly impregnate the cord. The cord would then be wrapped over a suitable diameter corresponding to the desired belt length and hardened to a thin solid ring. The thin solid ring would be bonded appropriately

FATIGUE RESISTANT BELT DESIGN

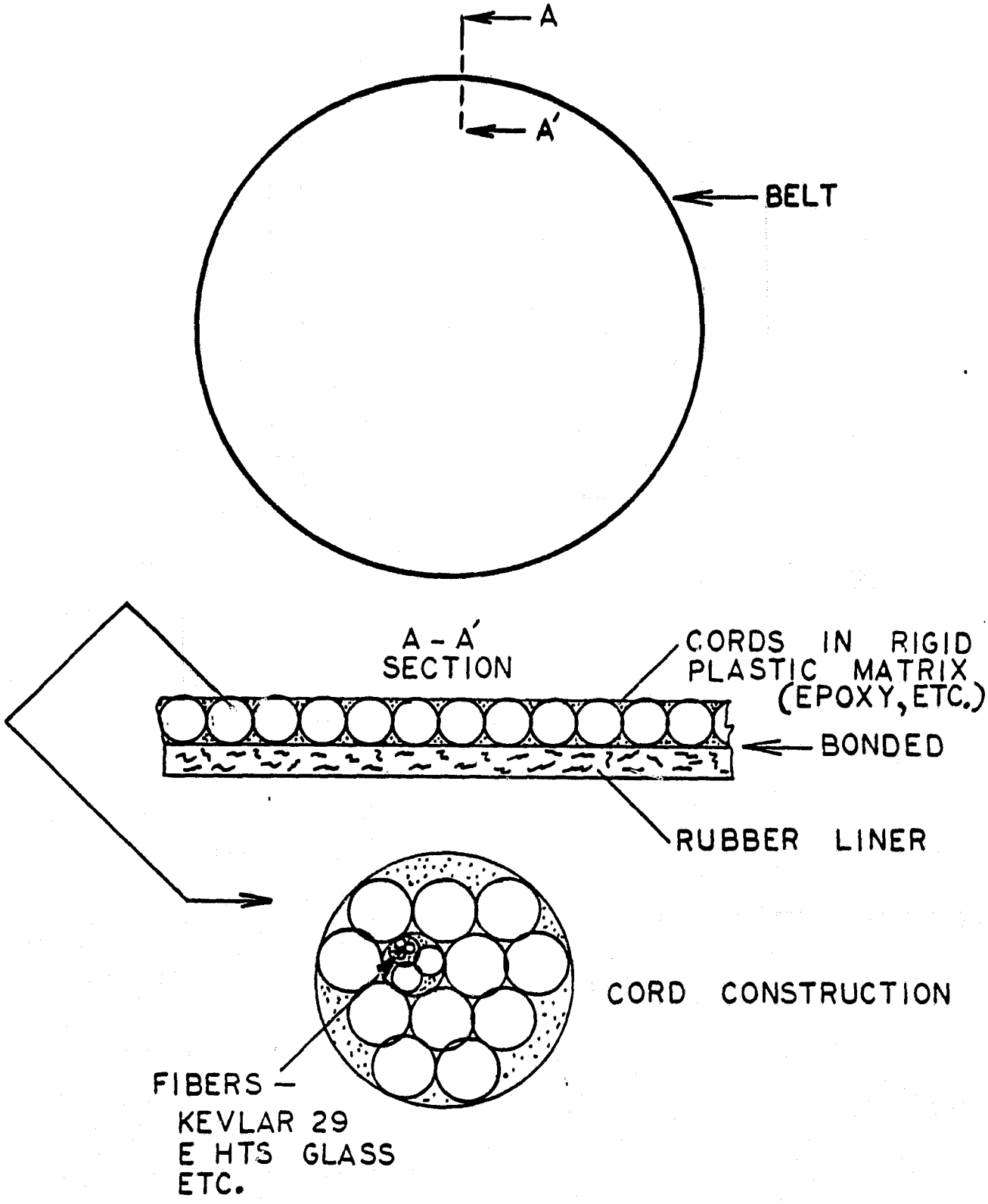

Figure IV-14 — FATIGUE RESISTANT BELT DESIGN

to a suitable rubber liner — neoprene, urethane, etc., to form the desired belt. Proper choice of the epoxy or other plastic would give relatively good assurance that the cord fibers would indeed stay in place, due to the rigidity of the plastic. It may be suitable to use vulcanization in the process — typical temperatures being 307° F — since various epoxy and some other plastics are not deteriorated by short time exposures at such temperatures. Also, some excellent bonding adhesives exist, i.e. for neoprene or urethane to epoxy. Such a circular belt should operate on the pulley with maximum bonding stresses corresponding to the bent beam formula, as given in Appendix A. Appendix B gives the other bending stress of the proposed belt construction when subjected to tension loads which straighten the belt between pulleys. Using 1.5 mm diameter aramid fiber cords results in bending stresses of less than 20% of the ultimate strength of the fibers. Infinite fatigue life due to bending stresses appear to be achievable, using the construction as proposed in Figure IV-14.

C. Transmission Gear Design

The design of the gears are discussed in Appendix C. Selection of the pulley size, speed ratio and the pulley center distance, together with the desired planetary carrier and maximum output speed, determine the desired transmission gear characteristics, as given in Table IV-4. The operating loads were determined for the various operating modes, considering the urban vehicle operation as previously given in Table III-1, and are summarized in Table IV-5. These requirements gave the gear design torques and speeds for the various required operating times. The most severe operating mode usually had a predominant effect on the selection of the necessary gear dimensions. The resulting gear design specifications are given in Appendix C. All gears are designed to give the overall integrated requirement of 2600 hours of desired operating life with at least a 90% reliability, using a stress safety factor of 1.5.

TABLE IV-4
GEAR SPECIFICATION DATA

Gear	No. of Teeth	Diam. Pitch	Nominal Center Distance mm	Oper. Pressure Angle Degrees	Gear O.D.(Extr) I.D.(Intr) mm	Root Diameter Min(Ext) Max(Int) mm	Bore or Rim Dia. Maximum mm	Operating Mode Most Severe	Speed RPM	Torque Newton-meter N-m	Tangential Tooth Load Newtons	Face Width Min. mm
①	26	20	65.41	21.47625	36.70 max	30.25	25.10	Max	21000	34.109	2045.6	15.49
②	76				98.88 max	92.43	87.27	Power	7184.2	99.702		13.46
③	22	12	107.92	21.45597	52.73 max	42.42	35.08	Max	7184.2	99.702	4240.5	18.29
④	79				171.20 max	160.86	152.40	Power	2000.7	358.02		17.78
④	79	12	116.84	20.56277	171.20 max	160.86	152.40	Max	2000.7	358.02	4266.0	17.78
Ⓑ	31				70.51 max	60.17	51.89	Power	5098.5	140.49		18.80
Ⓐ	39	10	112.73	21.30704	105.03 max	92.71	82.85	Max	9899.0	72.358	1448.2	5.84
Ⓕ	49				130.02 max	117.70	107.85	Power	7878.8	90.912		5.33
Ⓗ	33	10	108.71	21.07572	90.14 max	77.70	67.84	Max	7878.8	90.912	2153.7	7.87
ⒽⓄ	52				136.88 max	124.46	114.60	Power	5000	143.26		7.37
Ⓛ	33	10	108.71	21.07572	90.14 max	77.70	67.84	Max Grade Torque	1575.8	285.58	6765.5	23.88
ⓁⓄ	52				136.88 max	124.46	114.60		1000	450.01		23.37
Ⓢ	27	20	34.67	24.19501	37.77 max	31.32	24.89	Max Grade Torque	3275.4	95.188	1796.1	20.32
Ⓟ	26				36.55 max	30.10	23.75		1323.8	—		19.81
Ⓟ	26	20	34.67	18.81288	36.55 max	30.10	23.75	Max Grade Torque	1323.8	—	1864.1	19.81
Ⓡ	81				101.47 min	107.21	114.30		1575.8	285.58		

Table IV-4 — GEAR SPECIFICATION DATA

TABLE IV-5

DESIGN POWER, TORQUE, SPEED — DIFFERENTIAL BELT TRANSMISSION GEARS

	Normal Accel.	Normal Decel.	Low Cruise	High Cruise	Max. Power	Normal Start	Normal Stop	Max. Grade	Max. Stall	Reverse	Life Rating	Mode
	65	65	1300	850	3	65	65	26	5	26	2600	Hours
(1)	7.90	-7.90	4.97	14.14	75.00	0	0	47.11	0	-7.90	16.41	KW
	3.59	-3.59	2.26	6.43	34.11	0	0	21.43	0	-3.59	7.46	N-m
	21000.0	21000.0	21000.0	21000.0	21000	14000	14000	21000	14000	-21000	21000	RPM
(2)	7.90	-7.90	4.97	14.14	75.00	0	0	47.11	0	-7.90	16.41	KW
	10.50	-10.50	6.61	18.80	99.70	0	0	62.63	0	-10.50	21.81	N-m
	7184.2	7184.2	7184.2	7184.2	7184.2	4789.5	4789.5	21000	4789.5	-7184.2	7184.2	RPM
(3)	7.90	-7.90	4.97	14.14	75.00	0	0	47.11	0	7.90	16.41	KW
	10.50	-10.50	6.61	18.80	99.70	0	0	62.63	0	-10.50	21.81	N-m
	7184.2	7184.2	7184.2	7184.2	7184.2	4789.5	4789.5	7184.2	4789.5	-7184.2	7184.2	RPM
(4)	7.90	-7.90	4.97	14.14	75.00	14.67	-14.67	47.11	53.18	7.90	16.41	KW
	37.71	-37.71	23.74	67.50	358.02	105.02	-105.02	224.93	380.80	-37.71	78.31	N-m
	2000.7	2000.7	2000.7	2000.7	2000.7	1333.8	1333.8	2000.7	1333.8	-2000.7	2000.7	RPM
(B)	2.63	-2.63	4.97	14.14	75.00	14.67	-14.67	32.65	53.18	2.63	16.41	KW
	4.93	-4.93	9.31	26.49	140,49	41.21	-41.21	61.15	149.43	-4.93	30.73	N-m
	5098.5	5098.5	5098.5	5098.5	5098.5	3399.0	3399.0	5098.5	3399.0	-5098.5	5098.5	RPM
(A)	2.63	-2.63	4.97	14.14	75.00	14.67	-14.67	32.65	53.18	2.63	16.41	KW
	10.00	-10.00	9.50	15.16	72.36	20.90	-20.90	75.76	75.77	-10.00	26.38	N-m
	2513.7	2513.7	4949.5	8909.1	9899.0	6703.1	6703.1	4115.2	6703.1	-2513.7	5939.4	RPM
(F)	2.63	-2.63	4.97	14.14	75.00	14.67	-14.67	32.65	53.18	2.63	16.41	KW
	12.57	-12.57	11.93	19.04	90.91	26.26	-26.26	97.19	95.20	-12.57	33.14	N-m
	2000.7	2000.7	3939.4	7090.9	7878.8	5335.1	5335.1	3275.4	5335.1	-2000.7	4727.3	RPM
(H)	0	0	4.97	14.14	75.00	0	0	0	0	0	16.41	KW
	0	0	11.93	19.04	90.91	0	0	0	0	0	33.14	N-m
	2000.7	2000.7	3939.4	7090.9	7878.8	5335.1	5335.1	3275.4	5335.1	-2000.7	4727.3	RPM
(HO)	0	0	4.97	14.14	75.00	0	0	0	0	0	16.41	KW
	0	0	18.97	30.01	143.26	0	0	0	0	0	52.22	N-m
	1269.7	1269.7	2500.0	4500	5000	3385.7	3385.7	2078.6	3385.7	-2000.7	3000.0	RPM
(L)	7.90	-7.90	0	0	0	0	0	47.11	0	7.90	0	KW
	37.70	-37.70	0	0	0	78.77	78.77	285.58	285.6	-37.70	0	N-m
	2000.7	2000.7	1354.4	303.9	41.29	0	0	1575.8	0	-2000.7	1091.8	RPM
(LO)	7.90	-7/90	0	0	0	0	0	47.11	0	7.90	0	KW
	59.40	59.40	0	0	0	124.12	-124.12	450.0	450.0	-59.40	0	N-m
	1269.65	1269.7	859.5	192.9	26.20	0	0	1000	0	-1269.65	692.9	RPM
(C)	10.53	-10.53	0	0	0	14.67	14.67	79.77	53.18	10.53	0	KW
	50.27	-50.27	0	0	0	105.02	-105.02	380.76	380.77	-50.27	0	N-m
	2000.7	2000.7	2000.7	2000.7	2000.7	1333.8	1333.8	2000.7	1333.8	-2000.7	2000.7	RPM
(S)	2.63	-2.63	0	0	0	14.67	-14.67	32.65	53.18	2.63	0	KW
	12.57	-12.57	0	0	0	26.26	-26.26	97.19	95.20	-12.57	0	N-m
	2000.7	2000.7	3939.4	7090.9	7878.8	5335.1	5335.1	3275.4	5335.1	-2000.7	4727.3	RPM
(P)	0	0	0	0	0	—	—	—	—	0	0	KW
	—	—	0	0	0	—	—	—	—	—	0	N-m
	0	0	2013.3	5286.0	6104.2	4155.2	4155.2	1323.8	4155.2	0	2831.5	RPM
(R)	7.90	-7.90	0	0	0	0	0	47.11	0	7.90	0	KW
	37.70	-37.70	0	0	0	78.77	-78.77	285.58	285.6	-37.70	0	N-m
	2000.7	2000.7	1354.4	303.9	41.29	0	0	1575.8	0	-2000.7	1091.8	RPM

Note: Flywheel Run up (Initial) is assumed to comprise 130 hours of operating life of Transmission.

Table IV-5 — DESIGN POWER, TORQUE, SPEED-DIFFERENTIAL BELT TRANSMISSION GEARS

D. Bearing Selection

The bearing loads were calculated using the gear operating torques as given by the data of Table IV-5 and also the belt tension loads of Figure IV-12, when applicable, in a conventional manner. The bearings were then selected that would meet the shaft size requirements, as well as give adequate life, using catalog information of various bearing manufacturers. This was an interation procedure to try to obtain the minimum size bearings that would be adequate. This procedure is also complicated by the shaft critical speed calculations, which affect the shaft size. A summary of the bearings, giving their location, type, and size and their L_{10} life for the design rating point operation and maximum power or torque operation is given in Table IV-6. Some of the bearings are larger than appear currently to be needed but further refinement was believed to be unwarranted until more specific belt life operation is obtained. The drawings, Figures I-3, I-4, and I-5 show where all the bearings are located.

E. Transmission Efficiency

The transmission efficiency was obtained over the complete operating range of speeds and powers by computing the losses for each of the components as follows:

Gears:	(1) Sliding Friction of Mesh (2) Rolling Friction of Mesh (3) Windage Loss
Bearings:	(1) Sliding Friction (2) Rolling Friction
Clutch Plates, Pulleys, Belt:	(1) Windage
Seals:	(1) Sliding Friction
Pumps:	(1) Power Required for Lubricating and Actuating Oil

With eight gear meshes involving 16 gears supported by 22 bearings, the multiplicity of calculations for obtaining the losses for six different output powers

TABLE IV-6
BEARING SUMMARY

BEARING SUMMARY				DESIGN POINT MODE					MAXIMUM POWER MODE					CRITICAL SPEED
LOCATION	BEARING NUMBER	TYPE	BORE-O.D.-WIDTH	TORQUE N-m	SPEED RPM	RADIAL LOAD	THRUST LOAD	L_{10} LIFE HOURS	TORQUE N-m	SPEED RPM	RADIAL LOAD	THRUST LOAD	L_{10} LIFE HOURS	RPM
CLUTCH SHAFT	206	RADIAL BALL	30 x 62 x 16	—	21000	445	44.5	>30000	—	21000	445	44.5	> 30000	—
CLUTCH SHAFT	107	RADIAL BALL	35 x 62 x 14	—	21000	448	0	16686	—	21000	445	0	16686	—
ROTOR SHAFT	204	RADIAL BALL	20 x 47 x 14	7.461	21000	640.5	0	7541	34.11	21000	1544	0	539	—
ROTOR SHAFT	203	RADIAL BALL	17 x 40 x 12	7.461	21000	285.1	0	27117	34.11	21000	1099	0	471	—
JACK SHAFT	JJ-162112	CAGED ROLLER	25.40 x 33.34 x 19.05	21.81	7184	1076	0	>30000	99.70	7184	4919	0	253	—
JACK SHAFT	JJ-162112	CAGED ROLLER	25.40 x 33.34 x 19.05	21.81	7184	375.4	0	>30000	99.70	7184	1717	0	8450	—
PLANET CARRIER	JH-2212	ROLLER BEARING	34.92 x 44.45 x 19.05	78.31	2001	836.2	0	>30000	358.0	2001	3830	0	1094	—
PLANET CARRIER	JJ-283412	CAGED ROLLER	44.45 x 53.98 x 19.05	78.31	2001	569.3	0	>30000	358.0	2001	2611	0	23500	—
PLANET	FJJ-162117	NEEDLE ROLLER	16 x 21 x 17	0	2832	238	0	>30000	—	1324	3661	0	452*	—
SUN SHAFT	JJ-121616	CAGED ROLLER	19.05 x 25.4 x 25.4	33.14	4727	361.6	0	>30000	90.91	7879	631.6	0	> 30000	82400
SUN SHAFT	JJ-121616	CAGED ROLLER	19.05 x 25.4 x 25.4	33.14	4727	907.4	0	>30000	90.91	7879	2291	0	2871	82400
OUTPUT "HO"	14137A 14276	TAPERED ROLLER	34.925 x 69.012 x 19.845	52.22	3000	640.5	0	>30000	143.26	5000	1753	0	>30000	—
OUTPUT "LO"	14137A 14276	TAPERED ROLLER	34.925 x 69.012 x 19.845	0	693	0	0	>30000	52.22	1000	4386	0	>30000*	—
PULLEY "A" SHAFT	19150 19281	TAPERED ROLLER	38.1 x 71.438 x 15.875	26.38	5939	2635	206	14500	75.0	9899	6792	565	370	47460
PULLEY "A" SHAFT	HH84548 HH84510	TAPERED ROLLER	25.4 x 57.150 x 19.431	26.38	5939	1250	206	50060	75.0	9899	3296	565	1200	47460
PULLEY "B" SHAFT	19150 19281	TAPERED ROLLER	38.1 x 71.438 x.15.875	32.35	5098	2446	0	>30000	140.5	5098	6550	0	820	40350
PULLEY "B" SHAFT	HH84548 HH84510	TAPERED ROLLER	25.4 x 57.150 x 19.431	32.36	5098	925.2	0	>30000	140.5	5098	2475	0	17500	40350
"L"GEAR SHAFT	L507949 L507910	TAPERED ROLLER	57.150 x 87.312 x 18.258	—	1092	218.0	0	>30000	285.6	1576	4074	0	>30000*	—
"L"GEAR SHAFT	M86648A M86610	TAPERED ROLLER	30.950 x 64.292 x 21.433	—	1092	787.3	0	>30000	285.6	1576	2687	0	>30000*	—
TORQUE SENSOR	16009	RADIAL BALL	45 x 75 x 10	—	5939	0	565	>30000	—	9899	0	565	>30000	42560
			millimeters	Newton-meters		Newtons	Newton-				Newtons	Newtons		

* - Maximum Torque Grade Hole

Table IV-6 — BEARING SUMMARY

for three different input speeds for complete available output speed range is very large. Fortunately, the loss equations could be separated into speed dependent losses and load dependant losses. However, the bearing loss calculations required calculation of the bearing loads based on the arrangement geometry for each output power and speed.

It was assumed that the oil to the bearings operated in the bearings at a slightly higher temperature (63° C giving 18.8 CP viscosity) than the oil to the gear meshes (52° C giving 35.0 CP viscosity). The manner which is used to pass the oil to the bearing permits its relatively low flow to heat to the gear box temperature before injection. Since the bearing oil is then subjected to a large wetted area in the bearing, this oil increases in temperature more than the gear mesh oil. The gear mesh oil is brought directly from the external oil cooler to be ejected on the gear mesh teeth. A low gear box temperature of 60° C was assumed since no internal combustion engine heat is involved and the transmission has relatively high overall efficiency.

The transmission gear mesh losses due to the sliding friction of the gear teeth are shown in Figures IV-15, IV-16, and IV-17 over the operating range of powers and speeds. The gear losses are calculated from the sliding velocity of the gear teeth, using formula such as given by Shipley[9] but applied to a correlation of tests results as given by Benedict and Kelley.[10] The percent power loss is P,

$$P = \frac{50\ f}{\cos\Theta}\left[\frac{H_s^2 + H_t^2}{H_s + H_t}\right] \qquad \text{(IV-34)}$$

H = ratio of sliding velocity to Pitch line velocity

f = friction coefficient

Θ = pressure angle, degrees

Subscripts: s - value at start of contact
t - value at end of recess action

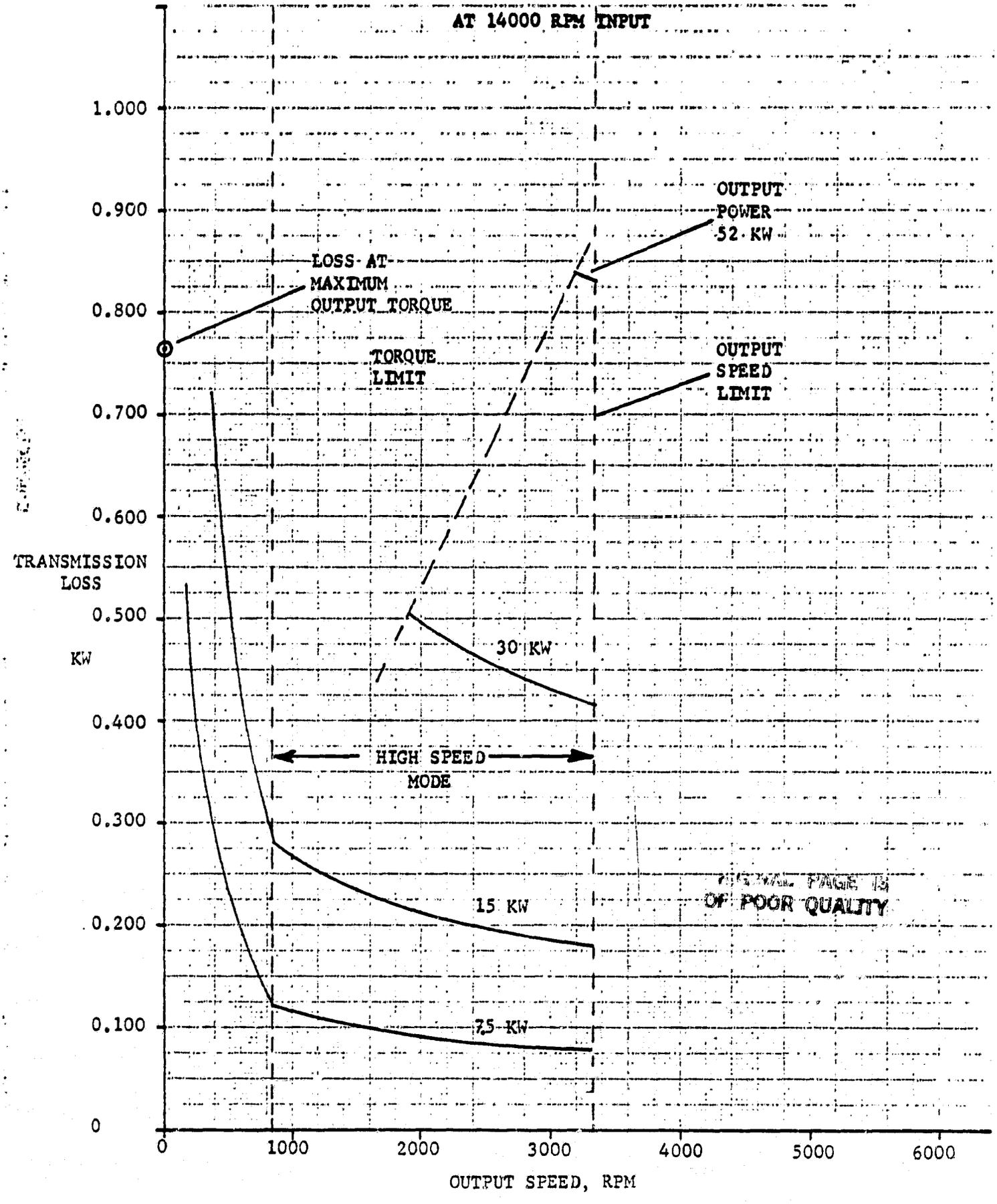

Figure IV-15 — GEAR MESH LOSS-SLIDING FRICTION AT 14000 RPM INPUT

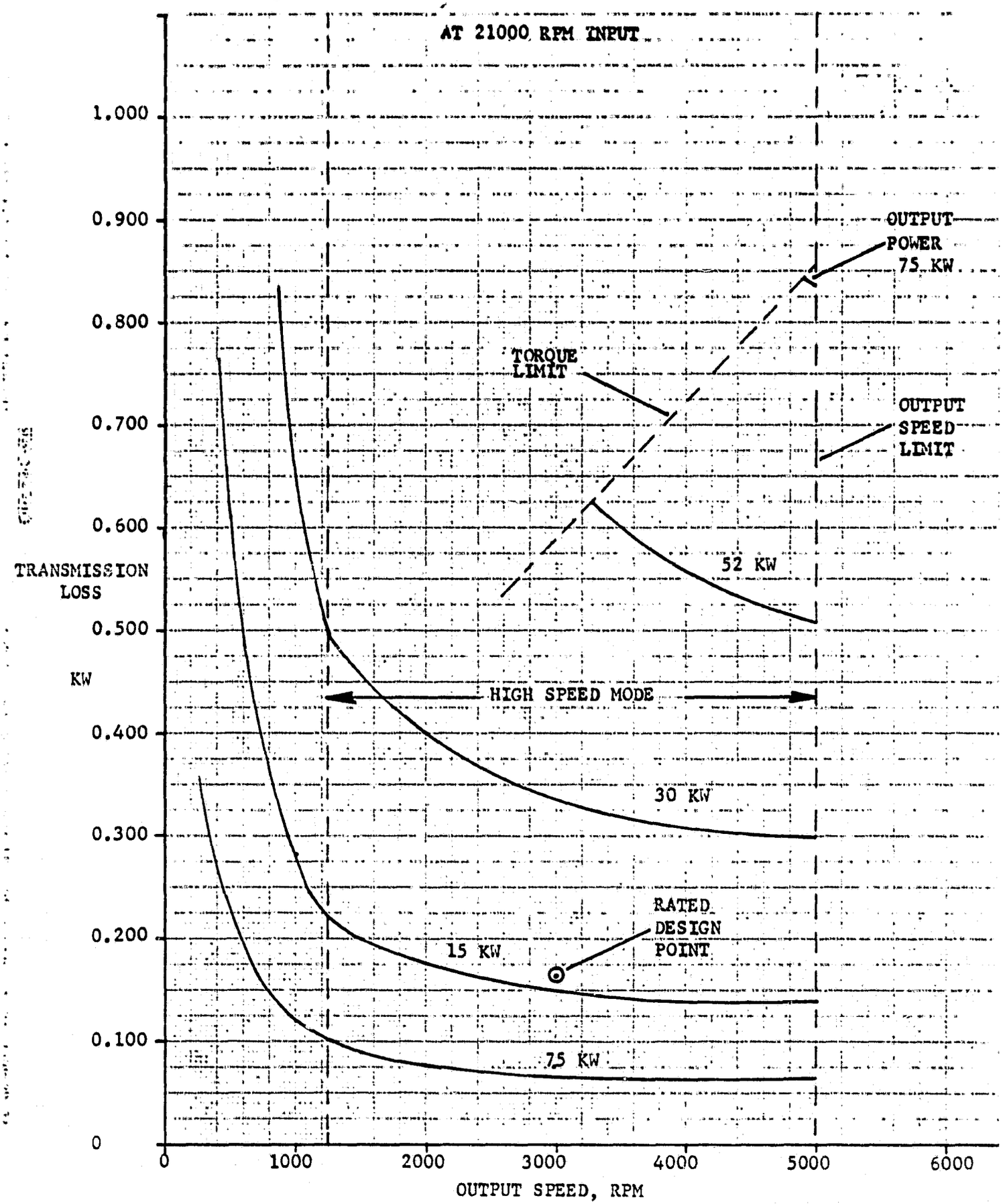

Figure IV-16 — GEAR MESH LOSS-SLIDING FRICTION AT 21000 RPM INPUT

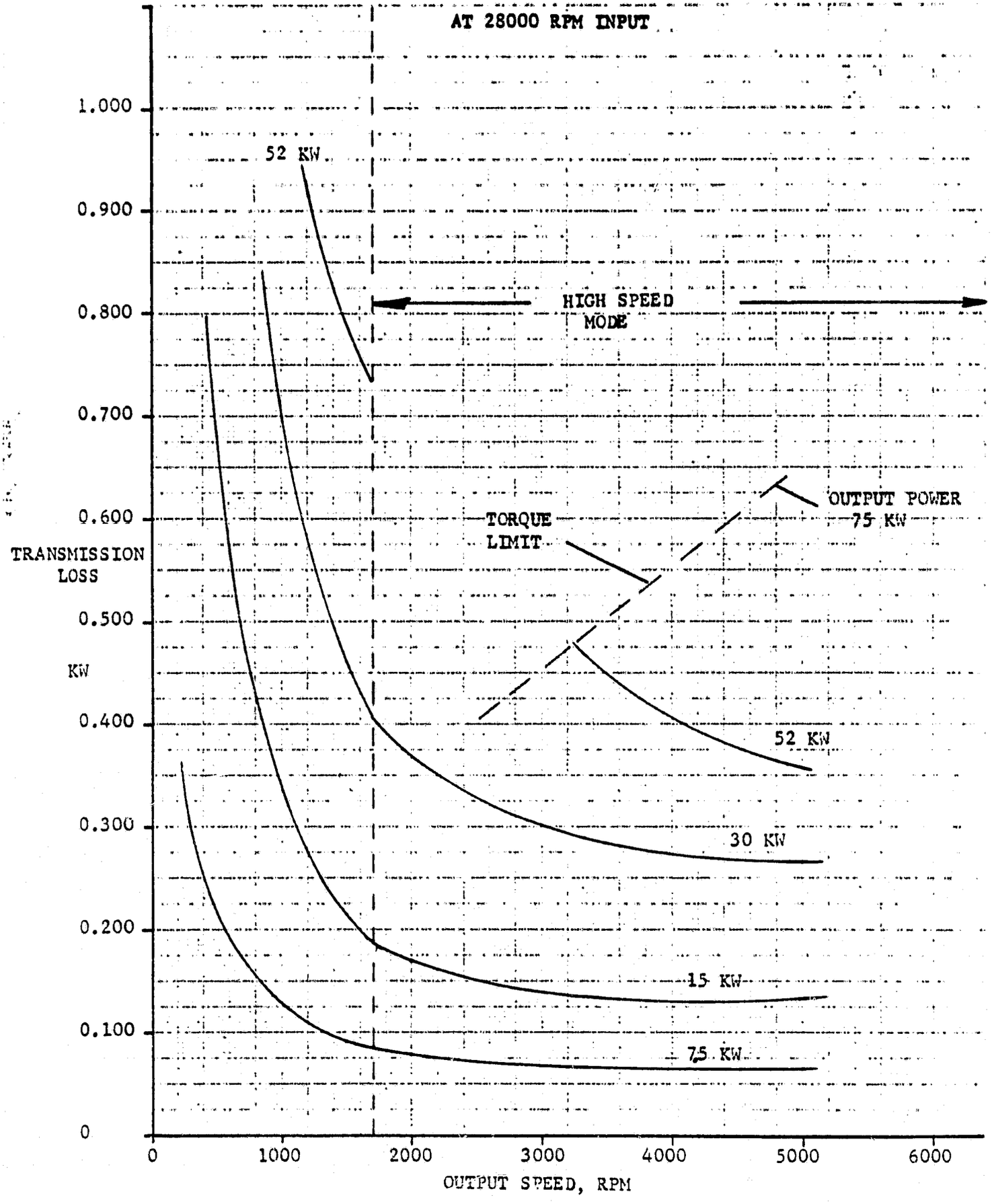

Figure IV-17 — GEAR MESH LOSS-SLIDING FRICTION AT 28000 RPM INPUT

$$f = 0.0127 \log_{10} \left[\frac{3.17 \times 10^8 W}{\mu_o V_s V_t^2} \right] \qquad \text{(IV-35)}$$

W = gear loading, lbs/inch face width

V_s = overall average sliding velocity, inches/sec.

V_t = sum of gear and pinion pitch line velocities, inches/sec.

μ_o = oil viscosity, centipoises

Calculations from these formulas give gear losses for the various meshes for the torques and speeds of each gear mesh. The largest losses under maximum loading occur in the planetary differential gears which operate in the low speed mode. However, in the high speed mode, such as involved in the maximum power-speed operation, the optimized spur gears are shown to have very low sliding friction losses indeed.

The gear rolling friction loss was computed using a method given by Anderson and Loewenthal.[11] The calculation separated out the mesh geometry factors from the speed and load variables so that it was possible to determine for each mesh a constant parameter that then needed modification for the speed and load to obtain the rolling friction loss.

Using the terminology of reference (11),

$$V_T = 0.1047\, n_p\, D_p \left[\text{Sin}\Theta - |X - X_p|\ (m_g - 1) / D_g \right] \qquad \text{(IV-36)}$$

V_T = rolling velocity, meters/sec, $X = l_1$ $X = l_2$ $X - l_4$ $X = X_p$

$$V_T = y\, n_p \quad - \quad - \quad - \quad - \quad - \quad - \quad - \quad y_1 \quad y_2 \quad y_4 \quad y_p \qquad \text{(IV-37)}$$

$$h = C_{11} \left[V_T \mu_g \right]^{0.67} w^{-0.067} R_{eq}\ 0.464 \qquad \text{(IV-38)}$$

$$P_R = C_2\, C_3\, V_T\, h\, \varphi_t\, F \qquad \text{(IV-39)}$$

Substitute V and h,

$$P_R = q\,Y \Big|_{X=l_1} - q_1 Y \Big|_{X=l_2} - q_2 Y \Big|_{X=l_4} - q_4 Y \Big|_{X=X_p} - q_p Y \qquad \text{(IV-40)}$$

P_R = power loss due to rolling traction, KW

$$q = C_2\, C_3\, C_{11}\, \mu_o^{0.67}\, R_{eq}^{0.464}\, F\, y^{1.67} \qquad \text{(IV-41)}$$

$$Y = n_p^{1.67}\, \varphi_t\, w^{-0.57} \qquad \text{(IV-42)}$$

$$\hat{P}_R = Y \left[(q_1 + q_2)\, l_3 + q_p l_s \right] / l_6 \qquad \text{(IV-43)}$$

$\hat{P}_R$ = total gear mesh power loss due to rolling traction, KW

Choose n_p, speed of pinion gear

$$V_T = y_p\, n_p \qquad \text{(IV-44)}$$

Obtain $Q_m = C_{13} \mu_o V_T^2$ and φ_t - Figure 3, Ref. (11) (IV-45)

Calculate $w_n = T_p / R_p \cos\theta$ (IV-46)

Calculate Y and P_R for each mesh and operating point for the rolling power loss. These losses are given for the flat belt transmission on Figure IV-18. The rolling mesh power loss decreases with increase in load but due to the slight effect of the $w^{-0.067}$ term only one curve is given for all powers except zero output. For output powers below about 7.5 KW, the rolling mesh losses become more significant than the sliding friction losses.

The bearing losses were computed using a SKF[12] formula that permitted ball bearings, roller, and tapered roller bearings to be computed on similar basis. The bearing torque loss is given:

$$M = 0.083\, f_1\, P_\beta\, d_m + 1.183 \times 10^{-6}\, f_o\, (\nu N)\, d_m^3 \qquad \text{(IV-47)}$$

$$f_1 = z\, (P_o/C_o)^y \qquad \text{(IV-48)}$$

P_o = Static equivalent load

C_o = Basic static load rating of bearing

z, y = Constants from Table 18[12]

$P_\beta = F_r$ or See P. 47[12]

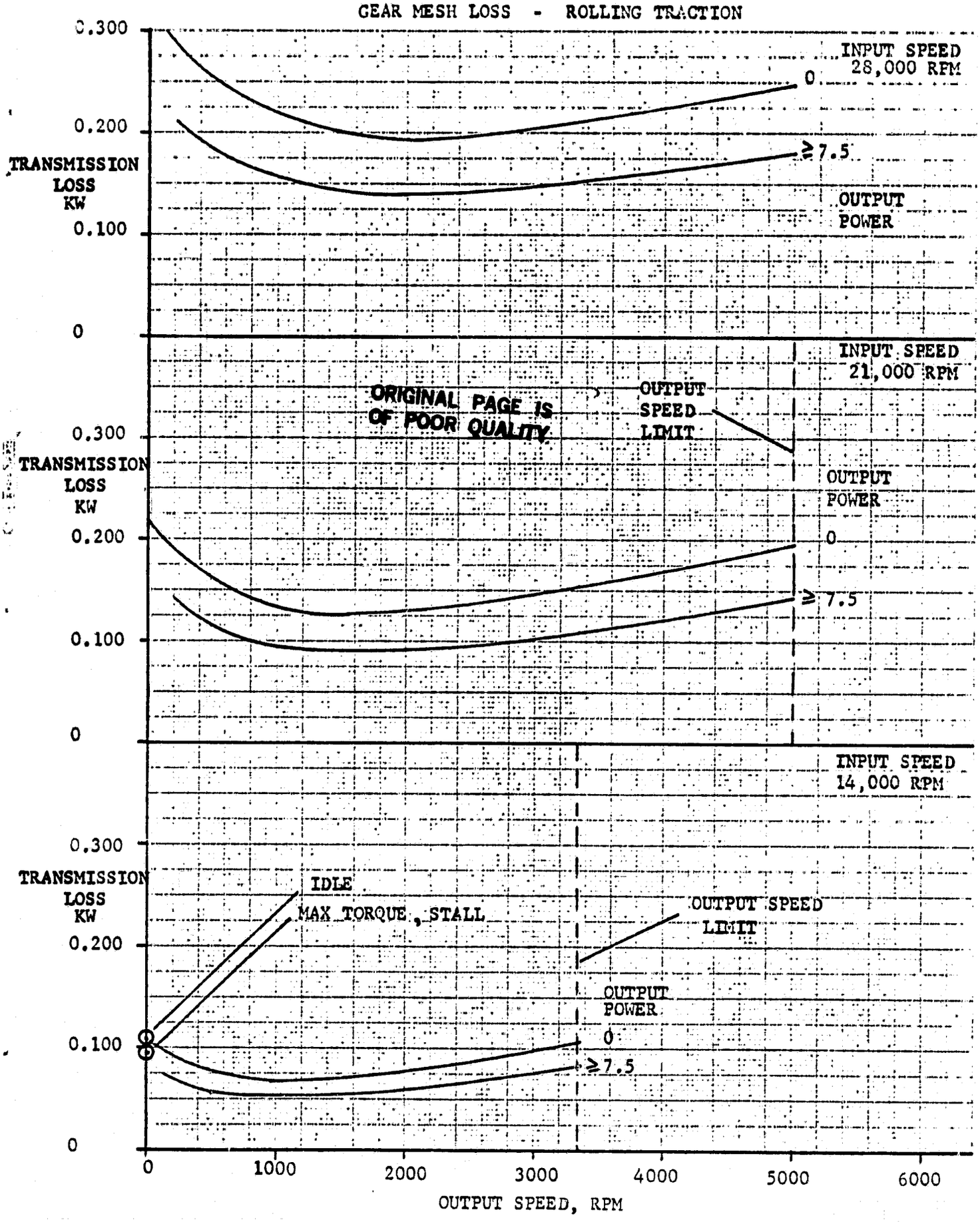

Figure IV-18 — GEAR MESH LOSS-ROLLING TRACTION

f_o = Constants from Table 19[12]

ν = Viscosity, centipoises

N = Speed, RPM

d_m = Mean diameter of bearing, inches

M = f.lbs., torque

Five ball bearings are used together with seven roller bearings and eight tapered roller bearings in the transmission package. For each operating point, the bearing loads were computed, and that portion of the bearing torque loss determined independently of the speed dependent loss. The bearing losses are shown on Figures IV-19, IV-20, and IV-21 for input speeds of 14,000, 21,000 and 28,000 RPM respectively over the operating range of output speed and power. The bearing losses are the largest loss component at the lower output powers and indicate how critical it is not to oversize the bearings in such a small high speed transmission. Due to the high critical speeds of the shafts, the transmission bearing losses may be reduced by using smaller diameter shafts and somewhat smaller bearings. The pulley belt load also affects the pulley bearing losses significantly at higher pulley speeds and any reduction in such loads due to a lighter belt, higher belt friction coefficient, etc. would reduce the pulley bearing losses. This is possible with the anticipated improvement in belts. However, these potential improvements are left for a future redesign.

The windage losses of the gears, the pulleys and clutch plates, as well as the seal losses, were calculated and are shown in Figure IV-22. The seal losses were very small, due to the use of lubricated seal surfaces and controlled gap seals - 15-30 watts loss being typical. At the lower transmission input speeds, all of these losses are quite small but become appreciable with the higher input speed at both low and high output speeds. Most of the loss is due to the gear

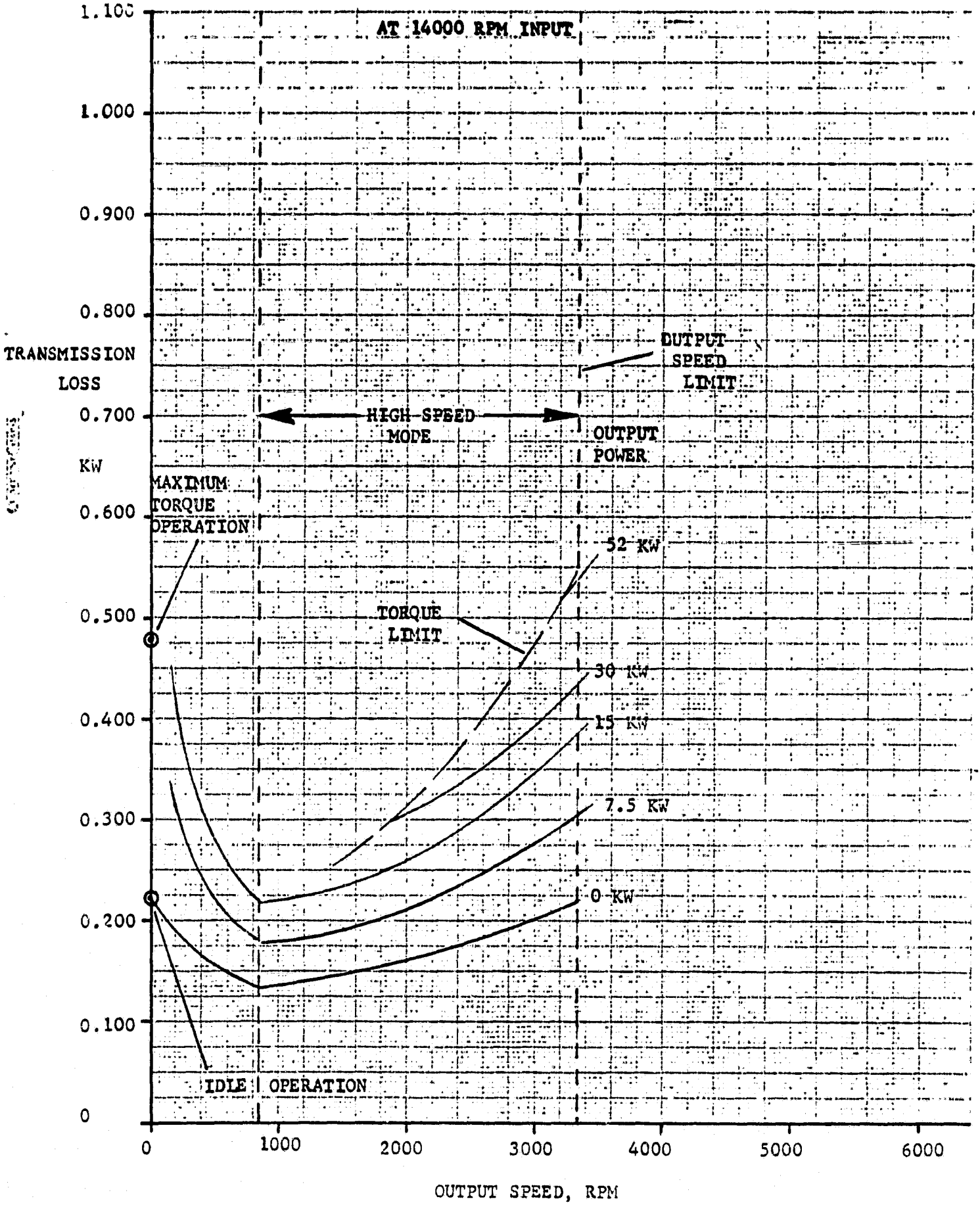

Figure IV-19 — BEARING LOSS AT 14000 RPM INPUT

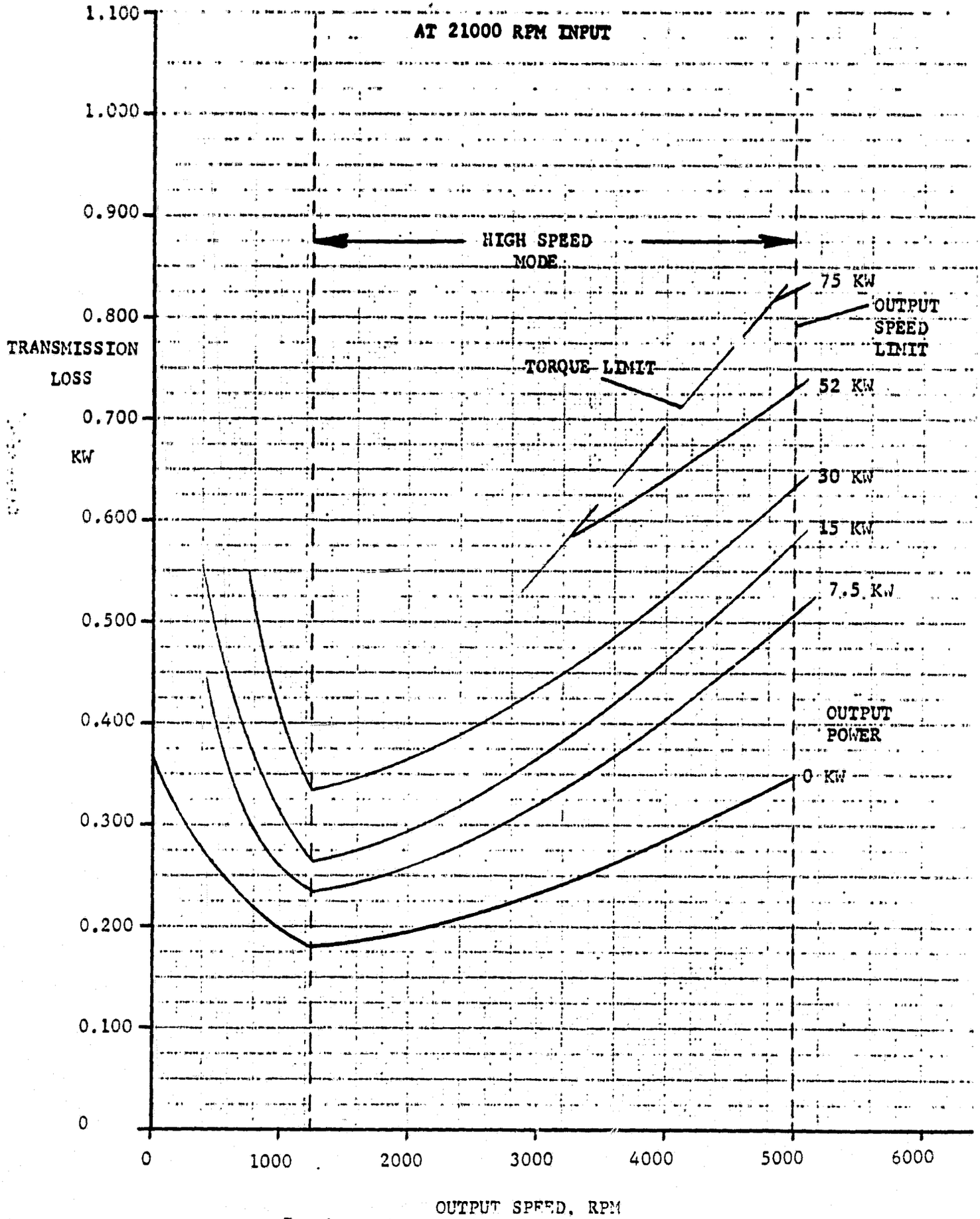

Figure IV-20 — BEARING LOSS AT 21000 RPM INPUT

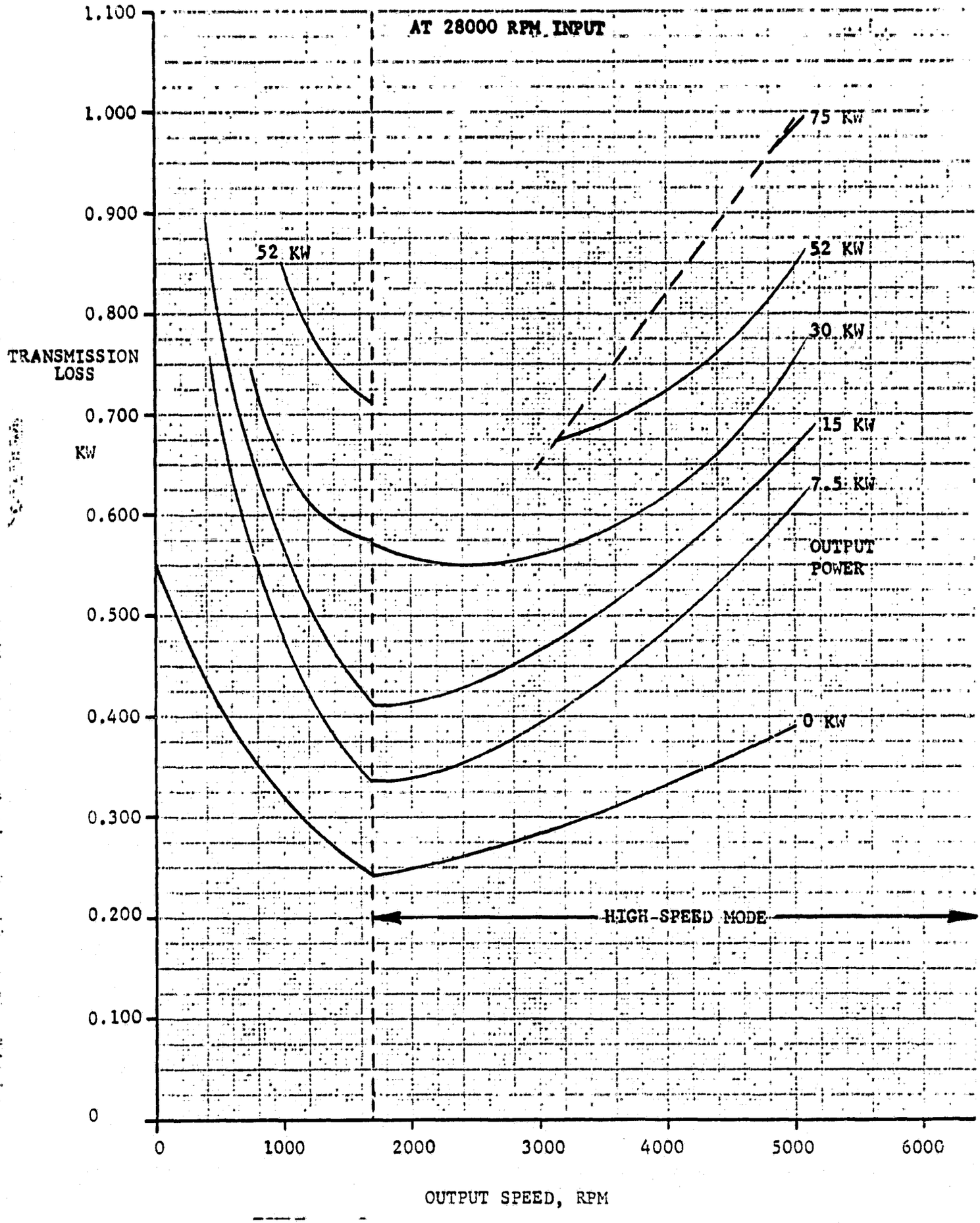

Figure IV-21 — BEARING LOSS AT 28000 RPM INPUT

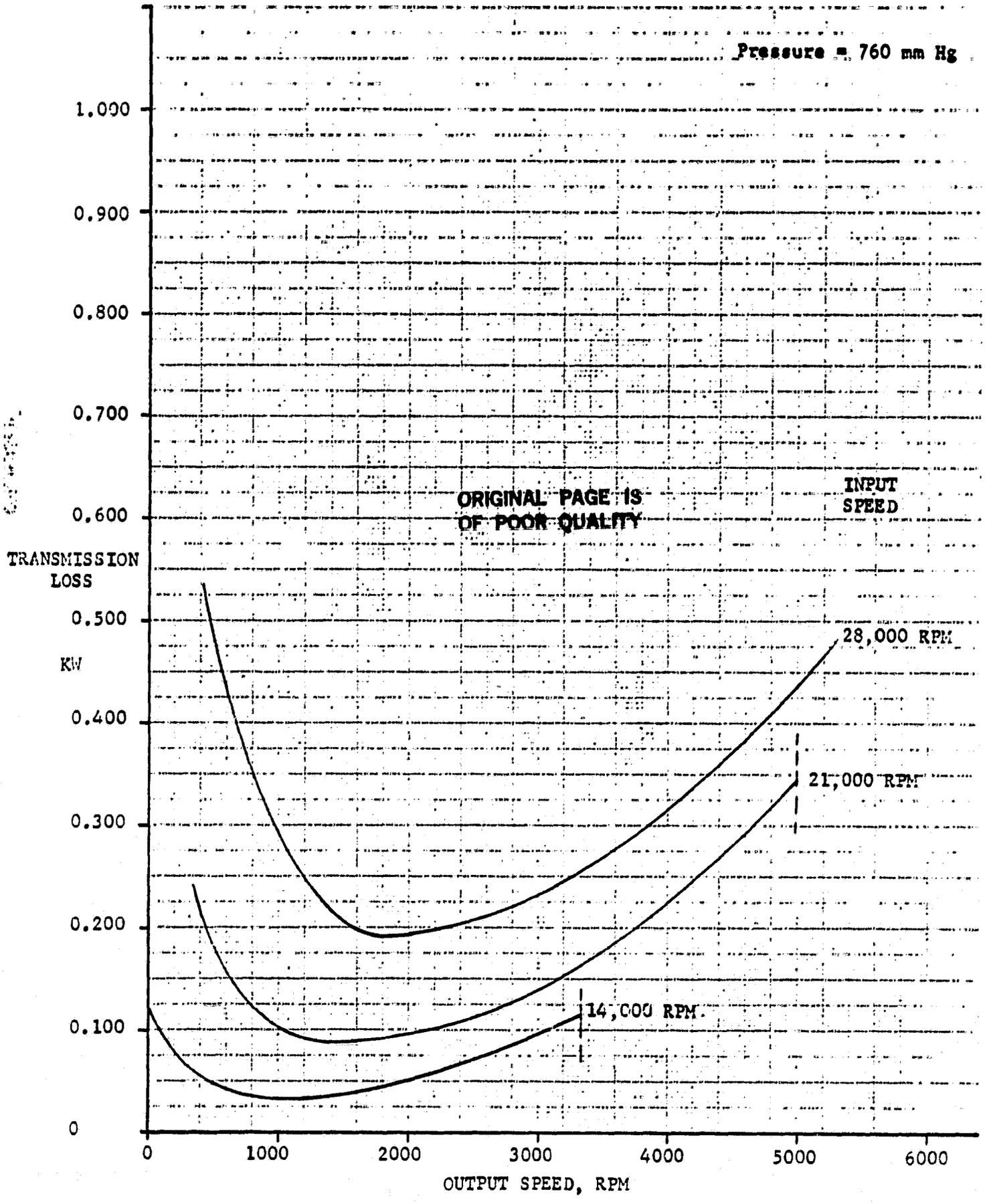

Figure IV-22 — WINDAGE AND SEAL LOSS

windage losses computed from an equation given by Anderson and Loewenthal[13] as follows, using the notation of reference[13]:

$$P_{w,g} = C_6 \, (1 + 2.3 \, F/R_g)(m_p/m_g)^{2.8} \, R_g^{4.6} \, (0.028\mu + C_5)^{0.2} \qquad \text{(IV-49)}$$

$P_{w,g}$ = gear power loss, KW

$$P_{w,p} = C_6 \, (1 + 2.3 \, F/R_g) \, n_p^{2.8} \, R_p^{4.6} \, (0.028\mu + C_5)^{0.2} \qquad \text{(IV-50)}$$

$P_{w,p}$ = pinion power loss, KW

This equation uses an effective gear box atmosphere density that is about 26 times ordinary air density, due to the oil mist in the gear box, based on tests with a helicopter gear box. The flat belt CVT is believed to have a relatively larger open volume, which should reduce the effective gear box atmosphere density, but to be conservative, no reduction in the loss was assumed here. These losses could also be reduced significantly by employing a small vacuum pump to reduce the ambient pressure in the gear box. The power consumption of such a vacuum pump calculates to give a saving of about .30 KW at the maximum loss conditions, including the power of the vacuum pump. This may be a future improvement, but the vehicle operation at normal urban speeds still gives reasonably low windage loss.

The oil requirements for the gears, bearings and belt pulley control actuators are analyzed in Appendix D. About 2.1 liters/min (0.6 GPM) is required for the gears, 0.4 liters/min (0.1 GPM for the bearings and a maximum transient flow of 9.0 liters/min (2.3 GPM) for the control actuator. An oil pump giving 8.0 liters/min (2.0 GPM) at 0.5 MPa (75 PSIG) with a 1.0 liter accumulator appears adequate. In addition, another small oil pump giving 0.1 GPM at 1.0 MPa (150 PSIG) with a 0.5 liter accumulator is needed for the torque balance pressure control. The total pump power of 0.10 KW is proposed to be supplied by a small separate electric motor driving gerotor type pumps.

The heat input to the oil and the required oil to air heat exchanger is also analyzed in Appendix D. Design for 2.1 KW (120 BTU/min) heat dissipation appears adequate. A heat exchanger of 1814 grams (4.0 pounds), not including fan (0.01 KW) sized at 305 mm x 293 mm x 142 mm appears adequate.

The total transmission power losses are presented on Figures IV-23, IV-24, and IV-25 for input speeds of 14,000, 21,000, and 28,000 RPM respectively over the operating range of output powers and speeds. The power loss curve at zero output power allows extrapolation to give gear box efficiencies for very low output powers. The resulting transmission efficiency curves over the same range of output powers and speeds are given on Figures I-8, I-9, and I-10. The principal objective of obtaining maximum efficiency at typical urban vehicle speeds (1000-3000 RPM output or 20-65 KMPH (12-40 MPH) appears to have been achieved. The efficiency at the rated design point of 16 KW output at 3000 RPM changes from 95.25% to 94.65% to 93.25% as the input speed varies from 14,000 RPM to 21,000 RPM to 28,000 RPM respectively. The transmission efficiency decreases significantly as the output power is decreased and output speed is increased. However, the normal vehicle cruise power increases with increasing speed to mitigate this effect and, depending on the associated electric motor controls, should permit operating the transmission at efficiencies over 90% at normal operating conditions.

F. Critical Speed and Shaft Torsional Vibration Calculations

Maximum rotational speeds of the shafts in the flat belt CVT are obtained at maximum output, using an appropriate control system which limits the input speed at idle and low speed operation.

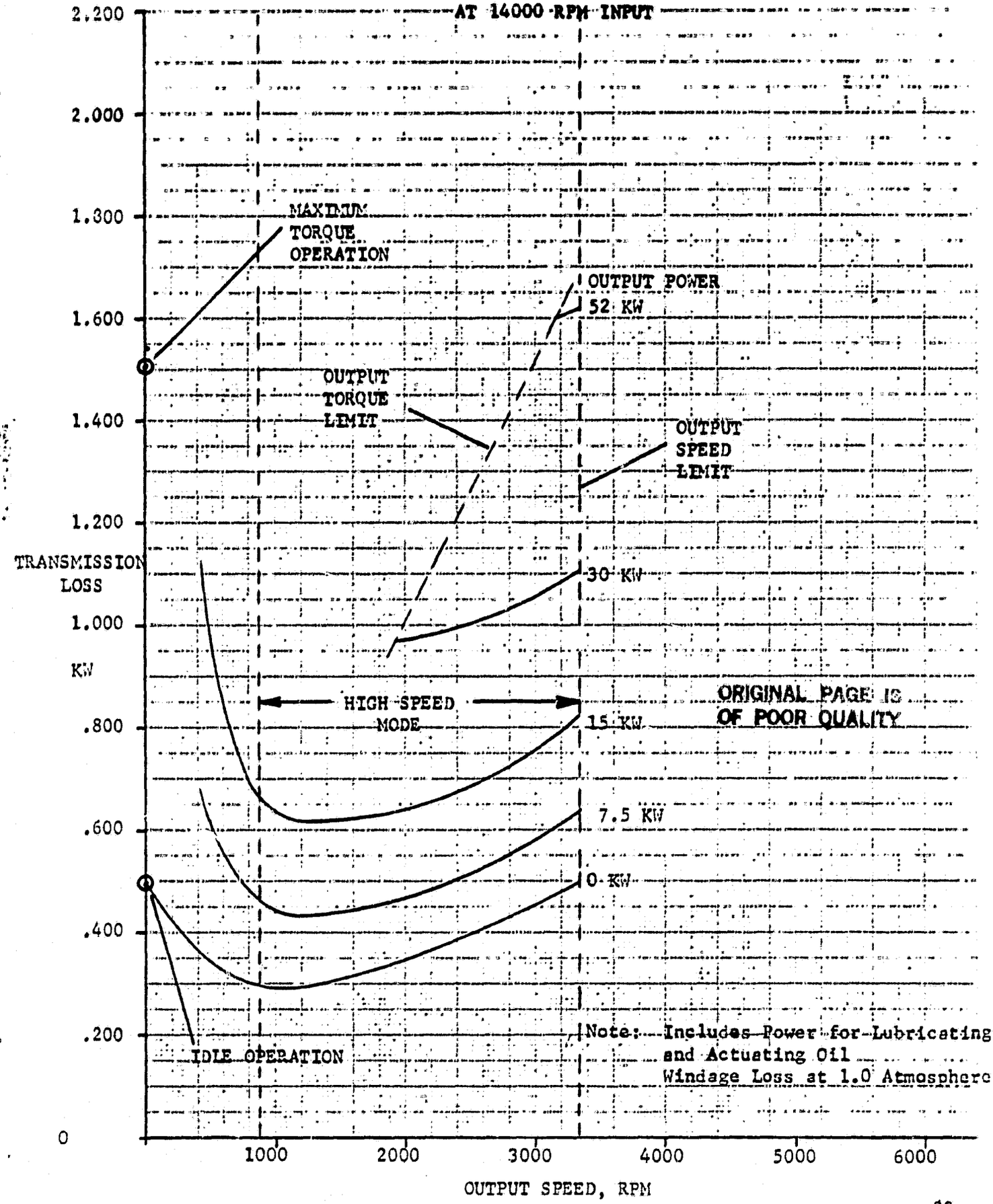

Figure IV-23 — TRANSMISSION POWER LOSS AT 14000 RPM INPUT

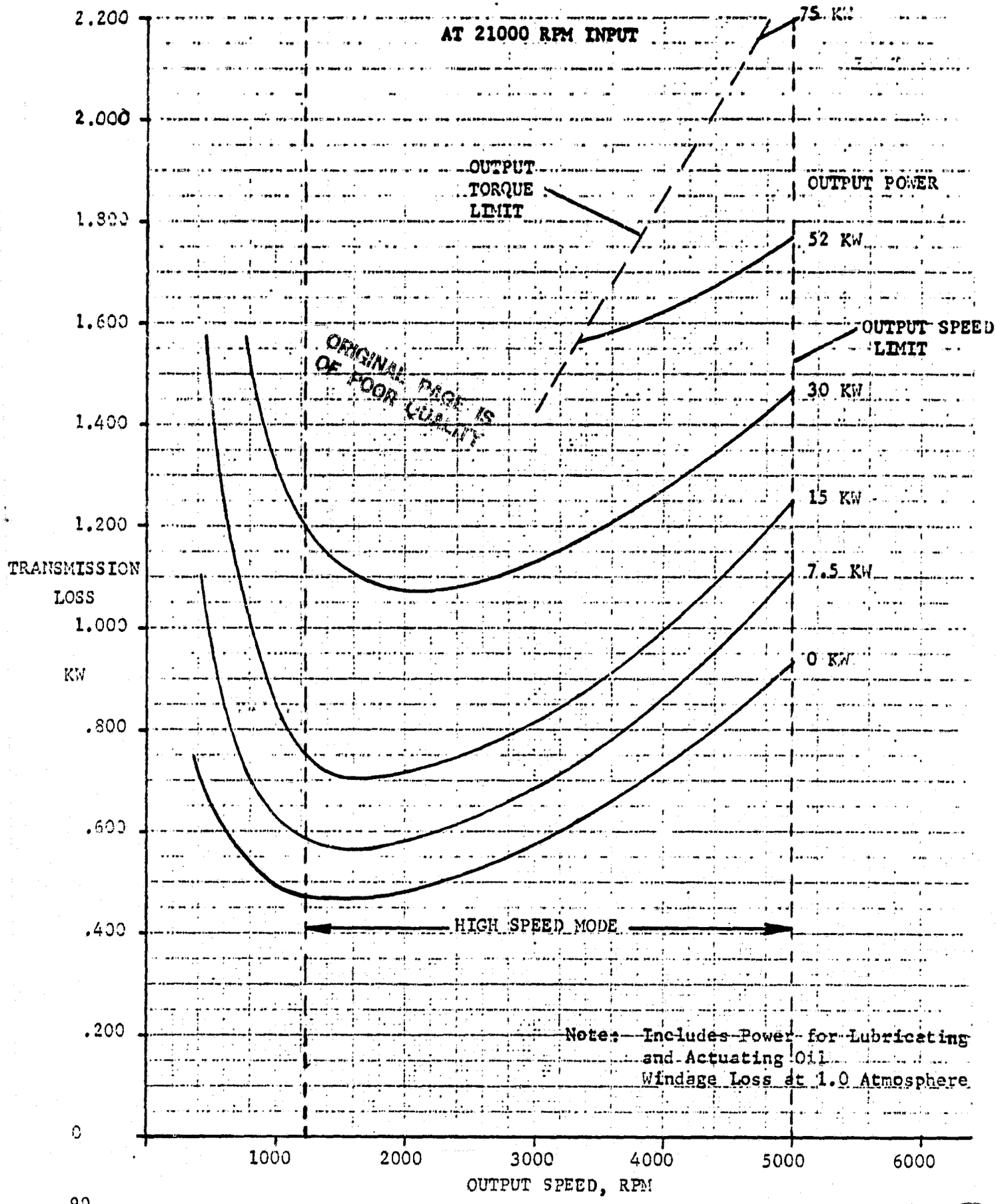

Figure IV-24 — TRANSMISSION POWER LOSS AT 21000 RPM INPUT

C-2

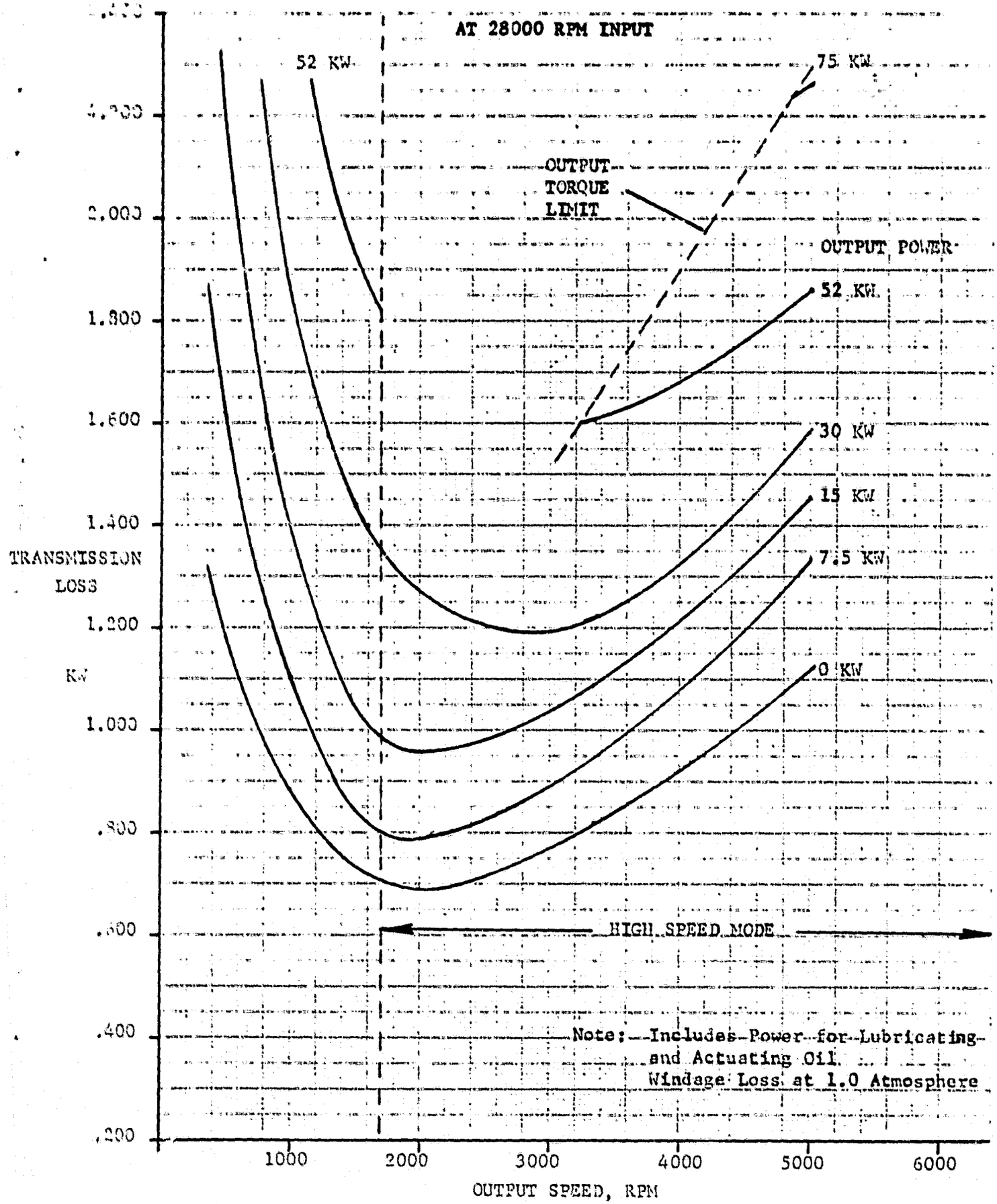

Figure IV-25 — TRANSMISSION POWER LOSS AT 28000 RPM INPUT

The shafts having the lowest critical speeds in the CVT are the shafts on pulleys A and B, due to their length and weight. These shafts are mounted on tapered roller bearings whose spring constants were obtained from the manufacturer. Fortunately, the spring constants of the bearings are sufficiently high to permit calculating the shaft critical speeds without correcting for the springs, as shown in Appendix E. Lumped weights were used for the shafts, gears and pulleys using the critical speed formula:

$$f = \frac{1}{2\pi}\left[g\frac{(W_1y_1 + W_2y_2 + \ldots)}{(W_1y_1^2 + W_2y_2^2 + \ldots)}\right]^{\frac{1}{2}}, \frac{1}{\text{sec.}} \qquad \text{(IV-51)}$$

W_1, W_2, ... = lumped weights

y_1, y_2, ... = deflections due to lumped weights

Using Roark,[8] the deflections on all shafts were calculated for the lumped weights at each weight position for use in the above formula.

Using the bearing spring rates only, the critical frequency is shown to be over 100,000 RPM on shafts of pulley A and B. Using the above formula the critical speeds of pulley A shaft and pulley B shaft is calculated to be 47,460 RPM and 40,350 RPM, respectively — well in excess of their maximum operating speeds of 9,899 RPM and 6,797 RPM, respectively. Also, the critical speed of the shaft attached to the sun gear of the differential and gears H and F was calculated to be 82,400 RPM, well in excess of its maximum speed of 7,879 RPM.

The torsional vibration frequency of the pulley shafts coupled with a belt is estimated in Appendix F by determining the equivalent spring constant of the belt, computing an overall equivalent spring constant and lumping inertial elements. The lowest torsional frequency of this system is computed to be 25390 RPM, which is significantly more than the maximum pulley A shaft speed of 9,899 RPM.

G. Flywheel Clutch Design

It is proposed to use an electric clutch between the flywheel and the transmission operating at flywheel speeds (up to 28,000 RPM), to be able to disconnect the flywheel for minimum losses with an idle vehicle. Investigation of such clutches revealed that no manufacturer currently makes an electric clutch for speeds over 15,000 RPM.

Clutches using multiple plates that are frictionally engaged must be installed with a loose fit at their I.D. and O.D. to prevent binding upon clutch engagement and disengagement. However, this loose fit will then cause all the clutch plates to be moved into a similar unbalance position about their rotating center, resulting in unbalanced rotor loads on the shaft bearing that, depending on the plate clearances, can severely limit the maximum clutch rotating speed. However, the deliberate unbalance of each plate by a small amount and their appropriate stacking can give an overall dynamic balance, as discussed in the analysis of unbalance loads of clutch plates - Appendix G. Each unbalanced plate will take a specific position, due to said unbalance, which is well defined. Hence, it now appears that in using such a design approach the clutch as shown in Figure IV-26 may be designed for very high speeds with reasonable bearing loads.

H. Flat Belt CVT Controls

The speed control system was described generally in Section III of this report, and is given schematically in Figure I-7. As shown on Figure I-7, the operator moves a spool in the speed servo valve to obtain either an increase or decrease in the transmission torque output. A spring in the speed servo valve provides a driver "feel". Without driver input, the rotary actuator in pulley B is moved to the maximum radius position, resulting in the belt in pulley A being

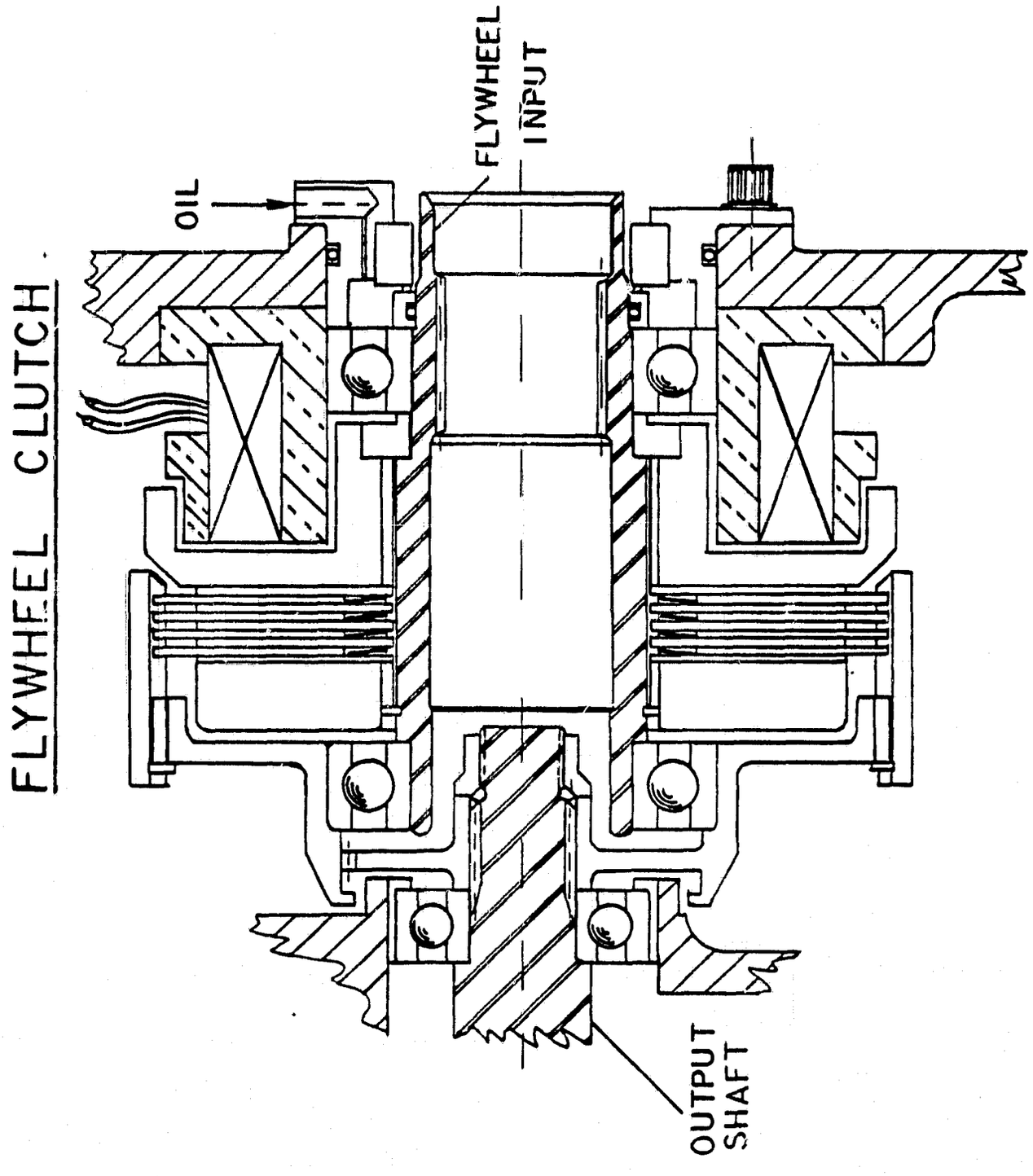

Figure IV-26 — ELECTRIC CLUTCH FOR VERY HIGH SPEED

at the minimum radius position. This operating condition will give essentially zero output speed when the driver engages the synchronizer into the forward drive mode. This then gives the low speed operating mode, with the synchronizer connecting the low output gear (LO) to the low speed gear (L). As the operator moves the spool of the speed servo valve against the spring, the low pressure oil, P_2, enters the rotary actuator of pulley B and leaves the rotary actuator of pulley A. Thus the rotary actuator pressure differential in pulley B decreases relative to the pressure differential in pulley A, and the drive elements are positioned to a larger radial position in pulley A and to a smaller radial position in pulley B. With constant pulley B speed (due to the D.C. motor and flywheel input speed), pulley A then decreases in speed, causing the output speed to increase in the low speed operating mode. Both rotary actuators are subjected to the same pressure, P_1, which operates in both pulleys to increase the radial position of the belt drive elements. The pressure, P_1, is supplied from the torque pressure balance regulator from a higher discharge pump "1" than the pump "2" supplying the P_2 pressure oil. P_1 is made proportional to the torque at pulley A, as previously described in Section IV. B. 3, so as to load the belt only as necessary to prevent slippage. The torque pressure balance regulator is designed to operate in either direction as necessary for the high speed operating mode versus the low speed operating mode, as well as reverse versus forward speed and power from wheels versus power to wheels. The P_1 flow from the torque pressure balance regulator to the rotary actuators is small — only required for leakage makeup — since P_1 oil flows from pulley A to pulley B actuators, and vice versa, in any speed change operation. However, the supply P_2 oil must be adequate to fill the rotary actuators in one pulley in less than two seconds. A small accumulator permits a relatively small pump to supply the necessary flow, as shown in Appendix D.

The centrifugal force of the belt drive elements is shown to be significant in loading the belt at high pulley speeds so that a counter balance is used to compensate for such forces as discussed in Section IV. B. 3. As shown in Figure I-7, the discharge pressure at the torque pressure balance regulator is P_2 whenever P_1 is larger than P_2. Hence, the differential pressure applied to the rotary actuators is P_1-P_2 for $P_1 > P_2$. However, as the pulley A speed increases, the ball centrifugal counter balance causes the torque sensor input to decrease. If the torque demand is sufficient so that P_1 is greater than 75 PSIG chosen for P_2, there is no P_c signal. However, if the torque is low and the speed high, the resulting P_1 is reduced below 75 PSIG by using a P_c input to the follow-up regulator. The P_c signal is generated as shown schematically on Figure IV-27 by the use of a voltage signal from a small generator driven at a speed related to the speed of pulley A, which operates on P_1 and P_3 to give the desired P_c characteristic versus transmission output speed. The desired characteristic for P_c varies, dependent on low speed mode or high speed mode operation to account for the fashion in which the speed of pulley A changes. The follow-up regulator permits obtaining P_1 pressures smaller than P_2 so that the rotary actuators will operate to reduce the belt tension caused by the centrifugal loading of the drive elements. Hence, with P_2 being held essentially constant at 75 PSIG, P_1 may be varied from 150 PSIG to essentially zero as desired, to compensate for the drive element centrifugal loading of the belt. By varying the belt tension as needed to prevent belt slippage for various output torques, the bearing loads are reduced and the overall operating efficiency improved.

The shift from the low speed to the high speed mode and vice versa occurs when the drive elements in pulley A have reached their maximum radius, at which time

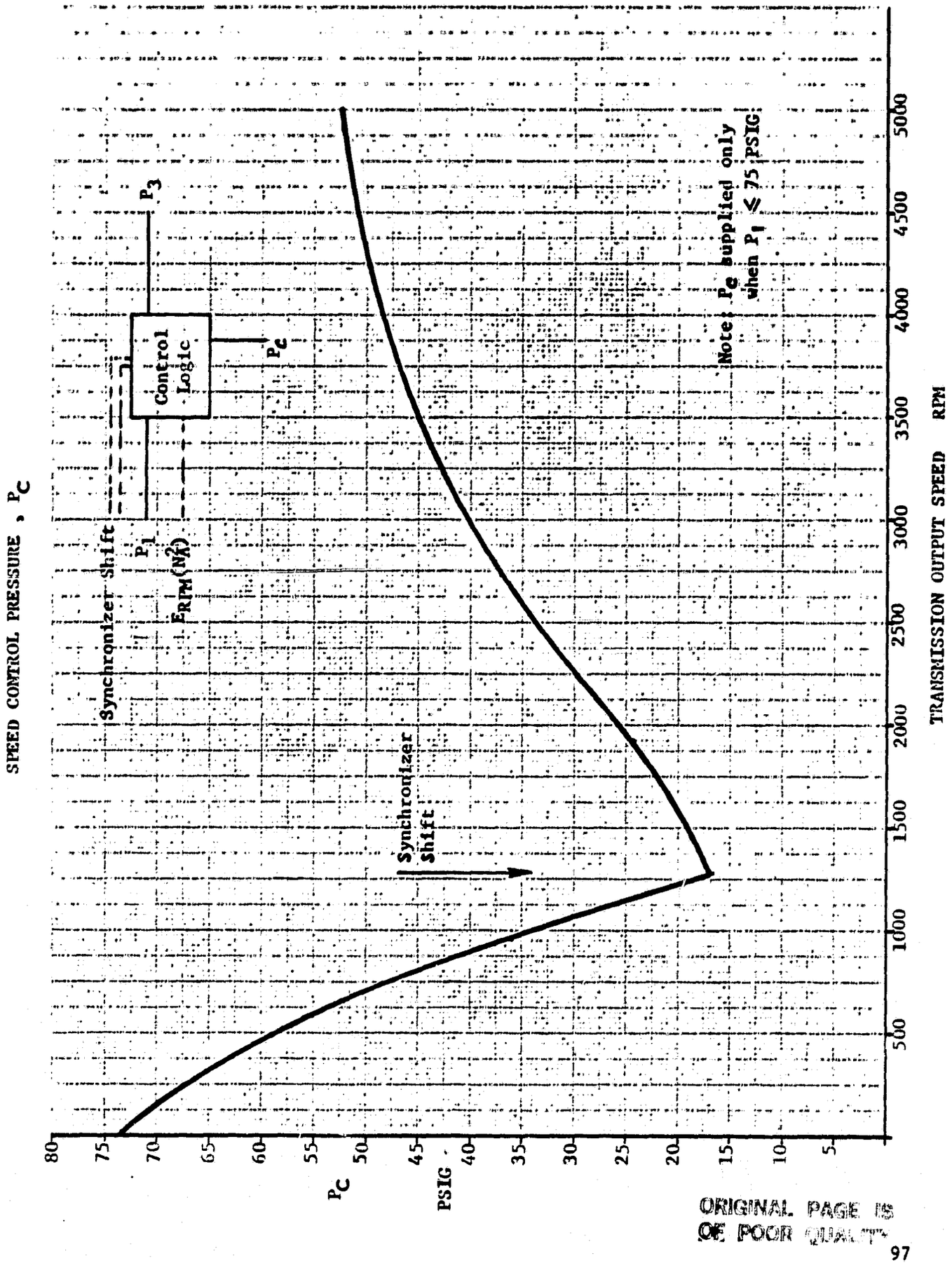

Figure IV-27 — SPEED CONTROL PRESSURE, P_c

the low speed and high speed gears are traveling at the same RPM. A solenoid arrangement is shown in Figure IV-28 to operate the synchronizer electrically and rapidly in an automatic fashion. Relatively small solenoids may be used, providing that a push-pull arrangement is used. Solenoids develop their maximum push or pull in a closed position, which is (depending on the stroke) several times the open position push or pull. Hence, while solenoid "C" can seat the actuator in the high speed mode, it cannot unseat it easily from the low speed mode engagement and requires the help of the more effective solenoid "D" to push it free. Similarly, solenoid "A" requires the help of solenoid "B" to transfer into the low speed mode from the high speed mode. Simultaneous operation of solenoids "B" and "D" only causes the synchronizer to disengage the output shaft from the transmission. The solenoids are shown full size in Figure IV-28 and would deliver 4 pounds axial force to operate the synchronizer. It is estimated that the shift operation should not exceed 30 milliseconds. Using 100% rated coils at 24 VDC requires a momentary power consumption of 6.0 watts per coil or 12 watts for two coils at any one time. The required solenoids have the following dimensions (L = 44 mm, W = 22 mm, H = 25 mm).

I. Lubrication Considerations

Lubrication of gear meshes and bearings is required in the transmission. The oil flow to each mesh and bearing is based on the maximum power loss as calculated in determining component efficiencies. The oil flows are given in Appendix D. A total oil flow of 8 liters/min. (2.0 GPM) is used in the transmission. It is assumed that the very small oil flows to the bearings will result in the bearings and their oil operating at about 66° C (150° F). Such temperatures are somewhat higher than the assumed mean gear box temperature of 60° C (140° F), while the gear mesh oil at 52° C (125° F) is somewhat lower in temperature due to it being brought in directly from the external heat exchanger

SYNCHRONIZER ACTUATOR

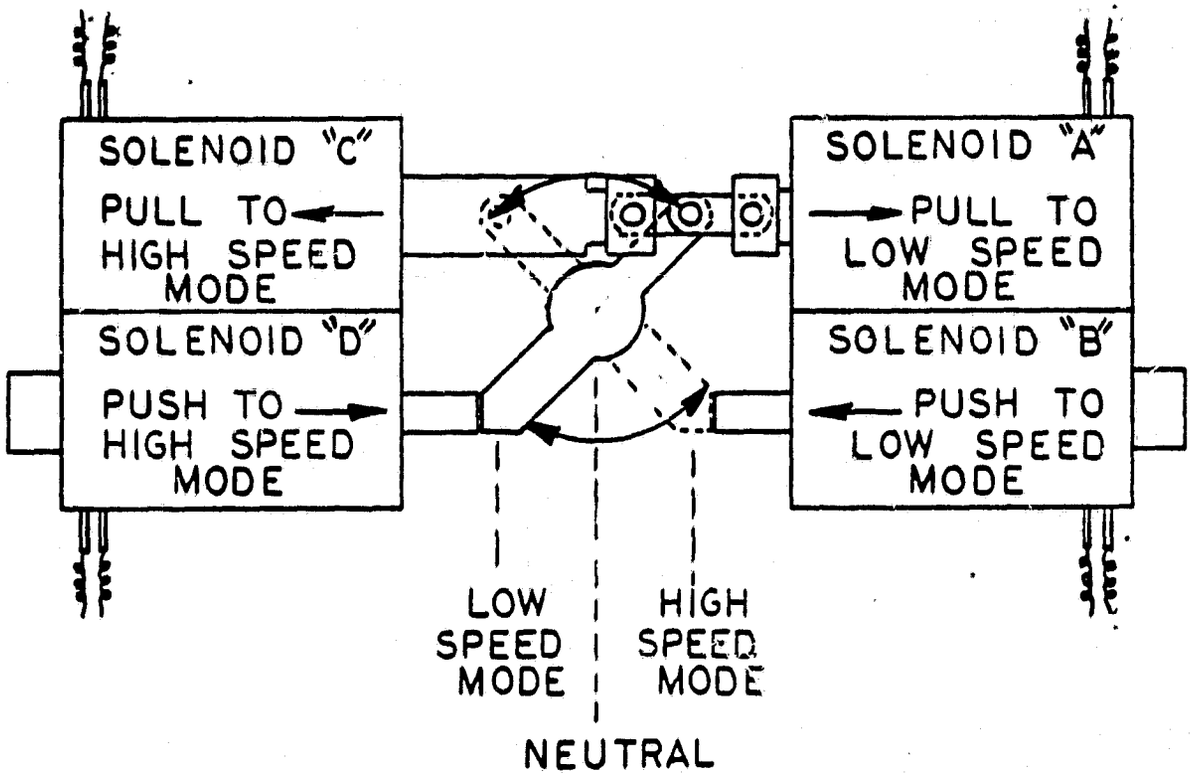

Figure IV-28 — SYNCHRONIZER ACTUATOR

to be discharged on the gear mesh. It should be possible to control to such temperatures quite well after start up by bypassing the oil heat exchanger until adequate oil temperature is achieved.

Out of mesh lubrication oil jets would be employed with all gears except the planetary differential using at least 0.34 MPa (50 PSIG) pressure. The planetary differential gears are fed from the center of the sun shaft using holes in the sun gear to the root section of each tooth. The ring gear receives a portion of this oil and oil from bearing elements as well. The lubrication at the bearings is controlled in some cases by dams and drains to prevent overloading the bearing, and in other cases by the natural restriction imposed by the flow through a journal bearing before being collected to pass through a rolling element bearing. The viscosity of the oil is dependent on the oil grade as well as temperature. Considering the relatively low maximum and normal operating temperature, the viscosity of SAE 20 oil was used to calculate reasonable bearing losses, yet providing sufficient viscosity to minimize the gear losses. In practice, an ATF oil of similar viscosity should give similar losses.

J. Seals

Oil must not leak into the pulley section from the gear box, since it could cause the belt to slip. The two pulley shafts propose to use controlled clearance seals which are ground to a clearance with the shaft of about 0.025 mm on a radius. The gear box is vented to a low pressure point, such as to the fan blown cooling air for the D.C. motor, to maintain a positive pressure differential between the pulley case and the gear box. The small air leakage at the controlled clearance seals then prevents oil from entering the pulley section. Conventional pressure balanced oil lubricated carbon graphite rubbing seals are used on the input shaft to gear (1), both on the D.C. motor side and

the flywheel side. A very good seal is required on the flywheel side, since the flywheel is normally operated at a very low pressure (1.0 mm Hg) to reduce drag losses. Other rubbing seals are used to seal the oil to the rotary actuators. The rotating seals on the end of the pulley shafts do not have to be leak free since the higher pressure oil merely leaks into the lower pressure oil and the lower pressure oil would leak into the gear box. Hence, these oil seals can have relatively low torque losses.

K. Transmission Size, Weight, and Construction

The maximum dimensions of the transmission are 483 mm (19 inches) across the pulley enclosure, 485 mm (19 inches) in breadth, and 300 mm (12 inches) in depth, as shown on Figures I-3, I-4, and I-5. The center distance between the flywheel or D.C. motor input and the output shaft is 282 mm (11.1 inches) and the center distance between the two pulley shafts is 229.6 mm (9.04 inches).

The weights of all elements, as shown in Figures I-3, I-4, and I-5 of the proposed flat belt transmission, were calculated. A total transmission weight of 44,450 grams (98.0 pounds) was computed, not including the front flywheel housing of 2,360 grams (5.2 pounds), which is included in the figures. The transmission weight breakdown is given in Table IV-7.

TABLE IV-7

TRANSMISSION WEIGHT BREAKDOWN

	grams	pounds
Housing, Cast Aluminum	10,524	23.2
Pulley Cover, Aluminum	908	2.0
Pulley A, Shaft & Bearings	7,212	15.9
Pulley B, Shaft & Bearings	5,942	13.1
Output Shaft, Bearings, Synchronizer & Gears	6,985	15.4
Input Electric Clutch, Bearings	4,717	10.4
Other Elements - Differential, etc.	8,162	18.0
Total Transmission Weights	44,450	98.0

Further study should make possible a weight reduction of perhaps 10-15 pounds by reducing the size of certain shafts, bearings and wall thickness of the structure, as well as other components. Also, the use of cast magnesium may be feasible, which could reduce the weight by 6-7 pounds.

A three piece cast aluminum housing structure is shown which permits the gearing to be assembled easily and gives relatively simple castings. The fore and aft housing are bolted to or through the center housing. The resulting structure is very rigid and strong and capable of supporting a flywheel as well as the differential to the wheels of the vehicle without any significant deflection. A cover for the pulley section is fastened to the front housing. When the cover is removed, the belt may be replaced in a simple direct fashion by positioning the belt drive elements in each pulley to their minimum radial position, to allow the belt to be installed over the pulley rim. A wrench socket is shown in the end of each pulley shaft to permit the inner guideway plates to be rotated relative to the outer guideway plates against the load of a spiral spring to replace a belt. The spiral spring assures that the belt will always be slightly tensioned on the pulleys to prevent shock loading when starting.

While the drawings are largely self explanatory, the transmission may be modified rather easily. The output speed may be changed by replacing gears (L), (LO), (H) and (HO). Space exists for incorporating a "high speed accelerator" by extending the shaft on the gear (LO), as will be later described. The bearing at the flywheel input may be used to support the flywheel and the bearings on the output shaft could permit overhanging and supporting an output gear in the wheel differential.

L. Maintainability

The transmission is designed to require very little maintenance. The torque sensor on pulley A prevents excessive loads to be applied to the gears, bearings, and belt when power is transmitted to the wheels. Conversely, excessive torque transients from the wheel would normally cause only a momentary belt slippage and, in the worse case, fail the belt due to frictional heating, without damaging the remainder of the transmission. But this is not regarded as a significant problem, and a long belt life should be possible. Also, replacement of a relatively low cost belt is direct and simple and does not require removal of any rotating parts or opening the oil-wetted section.

The oil used in the transmission will become contaminated with time, but little or no makeup should be necessary with normal filtration. It may be desirable to change the oil filter occasionally, but considering the relatively low operating temperature, 60° C (140° F), without the heat of an internal combustion engine, the time between changes would probably be very long indeed.

The maintainability of the transmission should be excellent.

M. Noise Generation and Abatement

The minimum objective in abatement of noise from the transmission would be to meet required domestic and international standards for vehicles and their operation. Table IV-8 lists these standards.

While the normal power (15 KW) and maximum power (75 KW) transmitted is not large for the size of gear box, a large number of gears (16) and bearings (22) are involved in an aluminum gear box. Aluminum is very low in damping capacity as compared to graphitic or grey cast irons, or magnesium when stressed;[14] so that acoustical treatment of the gear box, in all probability, would be essential to meet noise standards. Table IV-9 gives comparative damping

TABLE IV-8

SOUND LEVEL REQUIREMENTS OF VEHICLES

DOMESTIC STANDARDS

ANSI/SAE	Title
J986b-1977	Sound Level for Passenger Cars and Light Trucks
J1030-1977	Maximum Sound Level for Passenger Cars and Light Trucks
J1074-1974	Engine Sound Measurement Procedure

INTERNATIONAL STANDARDS

ISO/Dis	Title
362	Acoustics - Measurement of Noise Emitted by Road Vehicles
5128	Acoustics - Measurement of Noise Inside Motor Vehicles
5130	Acoustics - Survey method for the Measurement of Noise Emitted by Stationary Road Vehicles

Reference (15)

TABLE IV-9

ACOUSTICAL DAMPING CAPACITY OF CONVENTIONAL MATERIALS

Material Alloys	Mode of Vibration	Damping Capacity $\Delta E/E \times 10^{-3}$	Ranking
Engr. Cast Iron	Torsional	4,000 to 6,000	1
Carbon Steels	Transverse Longitunal	20 to 90 1 to 22	2
Alloy Steels	Torsional Longitudinal	15 to 45 15 to 180	3
Aluminum Alloys	Transverse Torsional	1 to 20	4

Reference (16)

capacity of conventional materials. Studies of gear case assemblies have shown the primary sound emissions to result from structure borne vibration with internal airborne sound of a secondary minor influence.[17] The structure borne noise is characterized by a very large number of tones and overtones relating to the shaft rates, tooth mesh frequencies, plate disk modes, sum and difference tones and complex interaction modes.

There are many techniques to reduce the primary noise generation, prevent resonance and attenuate the noise output. The gears are designed to use overlapping teeth in the meshes so as to minimize the higher frequency noise generated by the gear teeth. The construction of the gears must be accurate and their installation precise, with low tolerances, to obtain the proper gear action. A "noisy" automotive gear box is often caused by worn bearings that then cause misalignment of the gears. Holes that are used to reduce the weight of a gear disc are also quite effective in preventing resonance of the gear disc. However, dampening rings are necessary in some cases to prevent "ringing" or resonance of the gear. The pulley gear (A) is probably most susceptible of all the transmission gears to "ringing", due to it's cylindrical section.

The general concern with machinery noise attenuation has resulted in the development of many excellent acoustical control composites which can be wrapped or adhered directly to the structure or covers. While any major noise generating source in the transmission would be investigated and its noise production reduced if feasible, major reliance would be made on using sound dampening laminates directly on the transmission case and attached equipment. The relatively small transmission and associated equipment size makes reasonable such an approach. If further noise silencing is required, the transmission and associated equipment may also be housed in an appropriate plastic case, which is treated to reduce the transmitted sound.

The noise output from the D.C. electric motor associated with the transmission must be considered carefully. Here, it is necessary to use a cooling air flow which prevents the motor from being completely enclosed and which allows the air borne noise to be significant, particularly since the motor is attached directly to the transmission. The ducts to and from the motor may need special treatment to reduce its output noise.

The construction of the transmission housing using engineering cast iron (nodular, grey) in place of the proposed aluminum would increase the transmission weight by about 25-30 pounds but would have advantages in reducing the transmission cost somewhat and require less sound attenuation. Likewise, the construction of the transmission housing, using a magnesium casting[14] such as AZ91B, would reduce the casting weight by about one third with costs similar to the aluminum. However, galvanic corrosion must be considered. The overall cost effectiveness of using cast iron or magnesium versus aluminum would have to consider the many other factors, such as energy savings due to weight reduction, interest expense of increased initial costs, etc. There is definitely a need for further study in this area.

N. Scalability of the Transmission

The belt and pulley size are the basic parameters in scaling up or down for various output torques or powers, as given in Table IV-10. It will be shown that the output power or torque (for the same output speed range) varies with the 1.5 power of the pulley dimensions:

$$P_p \propto D_p^{1.5} \qquad P = \text{power, } D = \text{diameter, } p = \text{pulley} \qquad \text{(IV-52)}$$

This contrasts with the commonly accepted power or torque available from gearing which (for the same output speed) varies with the 2.0 power of the gear dimensions:

$$T_g \propto D_g^2 W_g \qquad T = \text{torque, } W = \text{face width, } g = \text{gear} \qquad \text{(IV-53)}$$

$$P_g \propto T_g N_g \qquad N = \text{speed} \qquad \text{(IV-54)}$$

Using $N_g D_g$ = constant (constant gear velocity) (IV-55)

and $W_g \propto D_g$ strength considerations (IV-56)

There is obtained:

$$P_g \propto D_g^2 \quad \text{(IV-57)}$$

In the belt pulley drive, the chief critical parameters are the maximum belt loading, F_1, and the maximum stress, σ, imposed on the belt drive element. The torque of the pulley is proportional to the maximum belt loading, F_1, and the pulley diameter, D_p, for the constant operating friction coefficient and proportional loads relative to belt contrifugal forces.

$$T_p \propto F_1 D_p \quad \text{(IV-58)}$$

The belt width W_b, is proportional to the maximum belt loading, F_1, giving

$$T_p \propto W_b D_p \quad \text{(IV-59)}$$

The possible belt width is dependent on the drive element stress, σ, which is caused by the resulting radial loads on the drive element — a beam simply supported at its two ends. The stress, σ, in such a beam is related to a dimension, d, proportional to the pulley diameter

$$d \propto D_p \quad \text{(IV-60)}$$

and the moment on the beam, M, which is proportional to the product of the maximum belt loading, F_1, and the beam length, W_b,

$$M \propto F_1 W_b \quad \text{(IV-61)}$$

Thus, $\sigma \propto M/d^3$ - beam formula (IV-62)

Then, $\sigma \propto F_1 W_b / D_p^3$ (IV-63)

Using $W_b \propto F_1$, Substitute in Eqn. (IV-63) (IV-64)

$$W_b \propto \sigma^{3/2} D_p^{3/2} \quad \text{(IV-65)}$$

For constant design stress,

$$W_b \propto D_p^{3/2} \quad \text{(IV-66)}$$

Thus, substituting into Eqn. (IV-59),

$$T_p \propto D_p \tag{IV-67}$$

The pulley power is given:

$$P_p \propto N_p\, T_p \tag{IV-68}$$

Substituting for T_p from Eqn. (IV-67) into Eqn. (IV-68)

$$P_p \propto N_p\, D_p \tag{IV-69}$$

For constant maximum belt velocity, $V_b \propto N_p\, D_p = K$ (IV-70)

Using Eqn. (IV-70) in Eqn. (IV-69)

$$P_p \propto D_p^{3/2} \tag{IV-71}$$

Thus, for the same input and output speeds, for constant stress and belt velocities, the physical size of the CVT may be scaled from the present unit as follows:

The width of the transmission depends on the width of the belt, gears, and bearings. The pulley center distance determines the gear sizes which, using the 1.5 power relation, increases more rapidly than the 2.0 power relation applicable to gears. Hence, the gear, bearing and structure width (including pulley guideway plates, etc.) will vary as follows:

$$W/W_{REF} = (D/D_{REF})^{2.0} \Big/ (D/D_{REF})^{1.5} = (D/D_{REF})^{0.5} \tag{IV-72}$$

Case I (Exhibit A) $W = 300\ (133/222)^{0.5} = 232$ mm

Case 2 (Exhibit A) $W = 300\ (715/222)^{0.5} = 538$ mm

The dimensions for the CVT scaled for the cases 1 and 2 of Exhibit "A"'are given on Table **IV-10.** These dimensions reflect the use of belts that are loaded to only 8-9% of their ultimate strength in a transient maximum load condition. With new materials and better design, the state of the art is advancing rapidly in obtaining smaller stronger belts. This could make for major reductions in the size of larger powered equipment. However, the assumption made herein was to use the currently available "best-state-of-the-art" belt.

TABLE IV-10

SCALED DIMENSIONS OF FLAT BELT CVT

CASE	VEHICLE WEIGHT	MAXIMUM CVT OUTPUT	PULLEY DIAMETER	PULLEY FACE DIMENSIONS	TRANSMISSION WIDTH
REFERENCE CURRENT DESIGN	1700 KG 3750 LBS	450 N-m 330 lb-ft	222 mm 8.74 in	255 x 484 mm 10.04 x 19.06 in	300 mm 11.8 in.
1.	790 KG 1750 LBS	210 N-m 155 lb ft	133 mm 5.24 in	153 x 290 mm 6.02 x 11.4 in	232 mm 9.1 in.
2.	10000 KG 22000 LBS	2600 N-m 1900 lb ft	715 mm 28.14 in	821 x 1558 mm 32.33 x 61.4 in	538 mm 21.2 in.

Assumptions:

1. Maximum Belt Velocity - Constant
2. Maximum Gear Tip Velocity - Constant
3. Belt Drive Element Stress - Constant
4. Belt - Best Current "State of the Art"

O. The Accelerator Modification

A low speed and a high speed accelerator, such as shown in Figure IV-29, could be added to the transmission with little modification that would give substantially greater transient output torques without increasing the loads through the belt and pulley system. In the planetary differential gearing, torque is transmitted either from the carrier to the ring gear by restraining the sun gear or from the carrier to the sun gear by restraining the ring gear. Hence, to increase the output torque in the low speed mode, a power absorbing element such as a slipping clutch may be applied to the sun shaft, increasing the torque to the ring gear (R) and low speed gear (L) and hence to the low speed output gear (LO). Likewise, to increase the output torque in the high speed mode, a power absorbing element, such as a slipping clutch, may be applied to the output gear (LO) connected to the low speed gear (L) and ring gear (R). This permits power to be transmitted through the planetary differential gearing to the sun shaft and high speed gear (H) in the high speed mode operation in addition to the power transmitted through the belt drive to gear (H) from gear (A).

Calculations on these approaches showed that oil flows of about 7 GPM and 10 GPM are needed for cooling the low speed and high speed accelerators respectively, to double the output torque. Transient losses are involved when using such clutches, the magnitude of the loss depending on the output speed and operation duration. Using only the high speed accelerator, a preliminary calculation, using the output powers given on Figure IV-30, resulted in acceleration of a 1700 KG vehicle, as shown in Figure IV-31.

While use of a concept such as the accelerator clutches improves the performance of the vehicle significantly, there are good reasons to believe that it will be possible in the near future to transmit much larger powers through belts. This would give less overall transmission elements and largely eliminate the losses involved with the accelerator operation, even though this operation is involved in high power short time transients only. Consequently, this approach is not proposed in the initial transmission, as shown in this report.

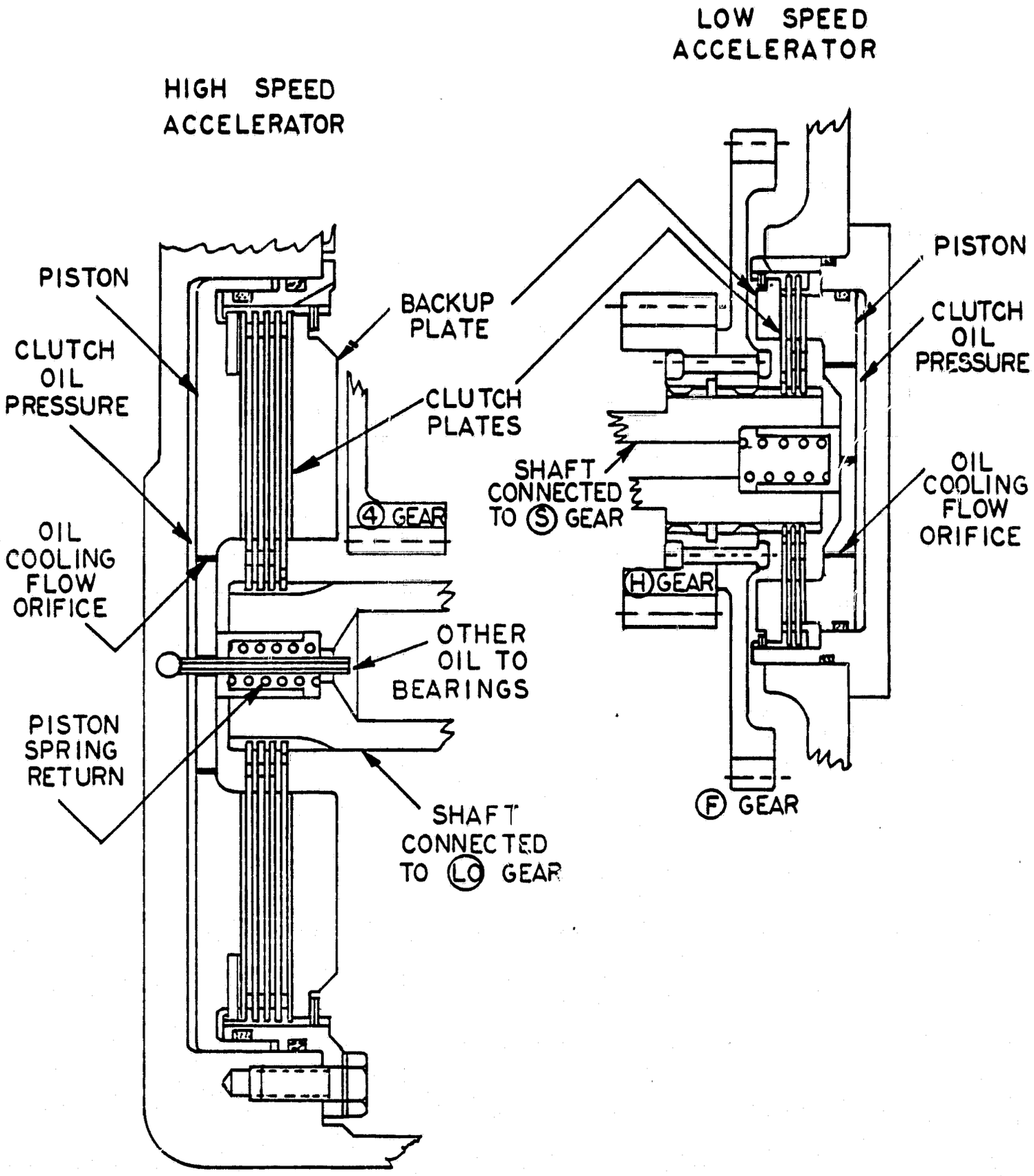

Figure IV-29 — ACCELERATOR CLUTCH DESIGN

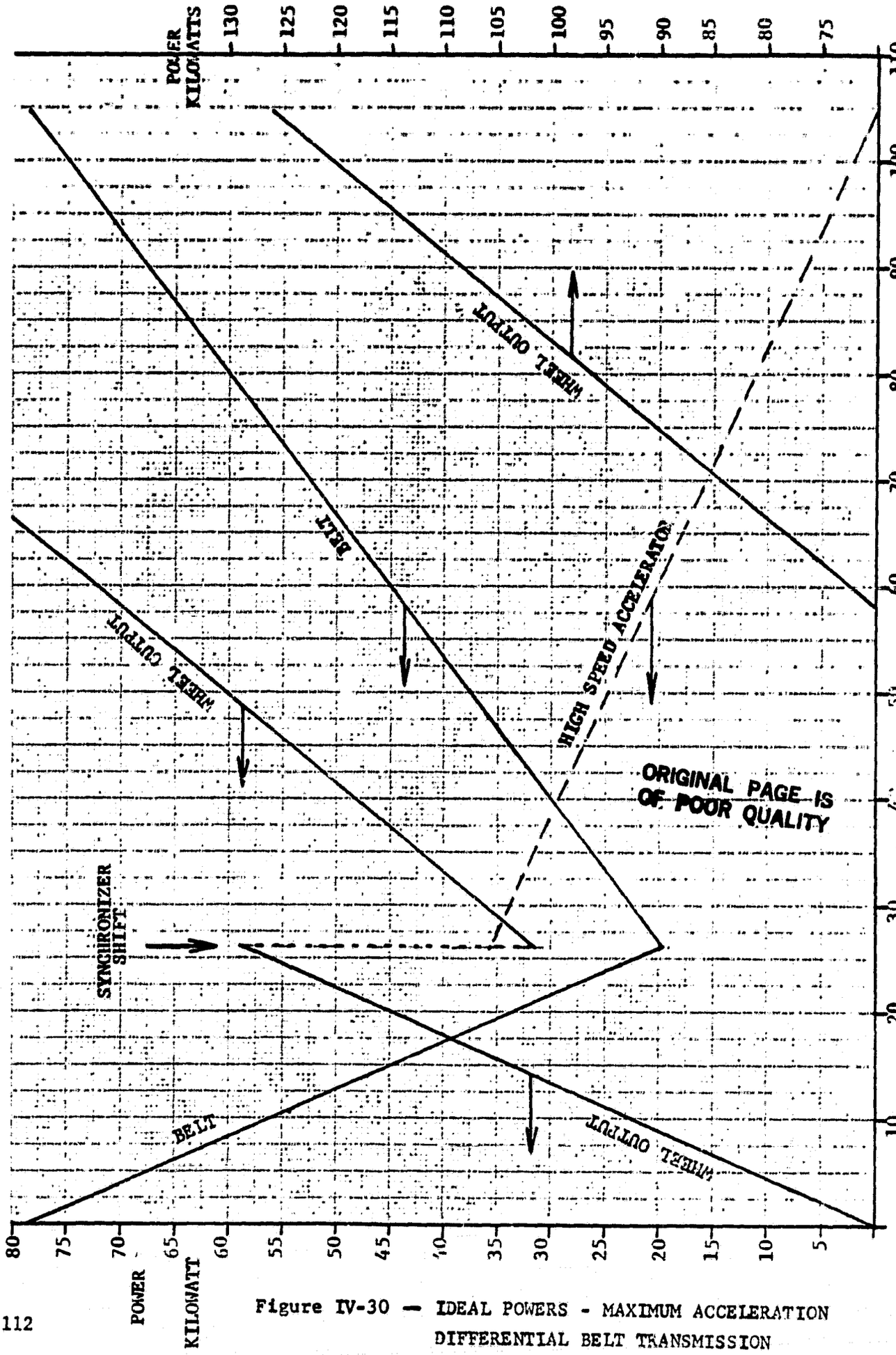

Figure IV-30 — IDEAL POWERS - MAXIMUM ACCELERATION
DIFFERENTIAL BELT TRANSMISSION

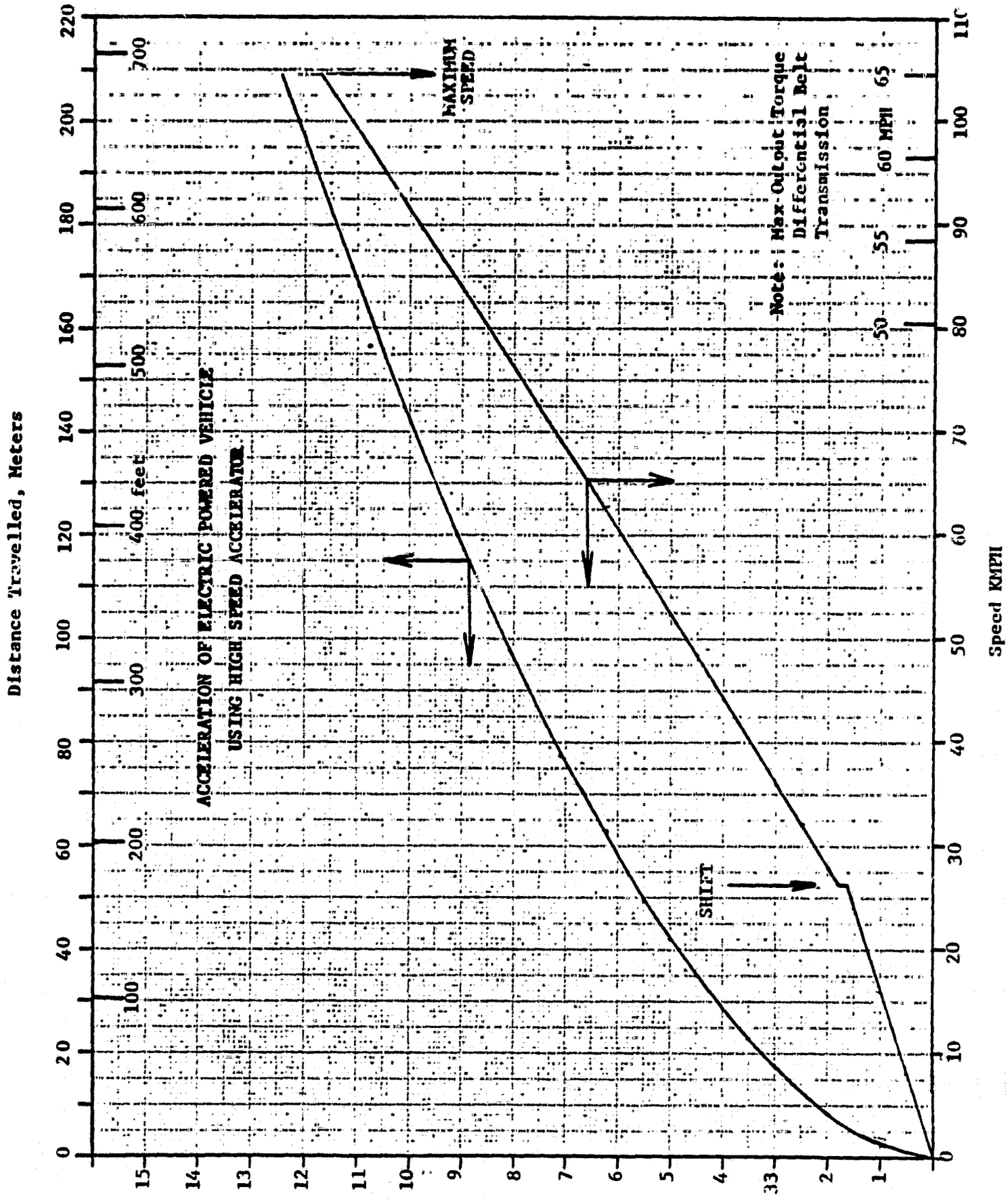

Figure IV-31 — ACCELERATION OF ELECTRIC POWERED VEHICLE USING HIGH SPEED ACCELERATOR

V. TECHNOLOGY REQUIREMENTS OF THE FLAT BELT CVT

Substantially all the technology requirements of the described flat belt CVT may be met in current "state of the art" equipment. The bearings, seals, O-rings, and fasteners are all relatively standard components, having been selected from manufacturer's catalogs. The gears, shafts, splines, pulleys, and housing should involve no new manufacturing problems, since the materials, designs, and tolerances are conventional. However, four components of the transmission do require some special attention and development. The drive belt used in the pulley system was sized, using belt manufacturers' recommendations. Such a belt is not currently available but could be supplied by at least two companies. However, this contractor believes that another belt fabricated as described in this report could demonstrate much improved life relative to other belts.

The drive elements used in the pulley are to be fabricated either from a magnesium extrusion or from magnesium castings. The desired wall thickness appears to be somewhat difficult to obtain but should be obtainable with some work.

The transmission shows the use of a very high speed clutch (28,000 RPM), which is not currently manufactured. Considerable analyses were made in this study to show how such a clutch could be made to operate successfully. This was coordinated with a clutch manufacturer and it is believed that such a unit is practical.

The transmission proposes the use of a high speed D.C. motor (28,000 RPM maximum). While such a motor is not currently commercially available, one manufacturer has made some preliminary successful tests with such a motor and a number of companies are known to be working in this general area. It is believed that such a motor will be available in the near future.

VI. ALTERNATE APPLICATIONS OF THE FLAT BELT CVT

A. Electric Vehicle Without Flywheel Energy Storage

By eliminating the flywheel input, the same transmission could be used as given previously and could be powered in the same way by a D.C. motor.

The proposed transmission does not require a motor that generates a large torque at low speed, such as normally required with traction-type motors. The regenerative power transfer through the planetary differential permits a very low motor torque to generate the maximum required output torque at the "stalled" condition. Hence, there is no particular need to use a series connected motor which would give the maximum stalled torque in a given frame size. Also, if the pulley belt should break or the hydraulic system for loading the pulleys fail, a series wound motor could give excessive speed in the transmission. DC shunt wound, compound wound or permanent magnet motors can all be used in the proposed system with safety, due to their limited maximum speed. When designed for very high speed and power, they can be much more efficient than low speed motors. Thus, trade literature on such motors indicates that it would be difficult to obtain over 83-84% efficiency at rated speeds under 3600 RPM in 10-20 KW motors, but 90% efficiency has been obtained at 8,000 RPM (30 KW), and new designs using the rare earth permanent magnet motors aim at 93% efficiency (23 KW) at 26,000 RPM. The electric motor weight and size per KW appears to be inversely proportional to the speed in such motors. Hence, the design use of the motor at maximum speed results in a lighter weight configuration, but the operation must consider the motor efficiency at lower loads.

The known efficiency characteristic of the lower speed DC compound, shunt, and permanent magnet motors indicate that the motor efficiency is nearly constant for a 2 to 1 change in torque or 2 to 1 change in power at constant

applied voltage, as shown on Figure III-7. The output power increases with decreasing output speed as the load is increased, holding the applied voltage constant. The motor power level may be increased by increasing the applied voltage and by increasing the resistance in the field circuit of a shunt motor, as described in Figure III-8. The torque sensor in the transmission provides a hydraulic pressure proportional to the output torque, which then may be used to increase the D.C. motor input speed and power by decreasing the field current, as mentioned previously in Section III.C. The D.C. motor control is essentially the same, with or without the flywheel. However, the D.C. motor must be sized to provide the desired vehicle acceleration, as well as the necessary cruise power and, hence, must be substantially larger than the D.C. motor with flywheel. However, it will be necessary to have specific characteristics of a suitable D.C. motor to design its most optimum control.

B. Hybrid Electric Vehicle With An Internal Combustion Engine

A hybrid arrangement using a combustion engine instead of the flywheels for acceleration and high power vehicle operation can use the current flat belt CVT design by eliminating the flywheel and its clutch and driving pulley B shaft directly through a clutch from the engine. In this case, pulley B shaft would then be modified and installed with oil seals to permit passing the rotary actuator control oil to and from the pulley shaft and the center gear box housing instead of through the end of the shaft, as now shown. A maximum combustion engine speed of 5,100 RPM would then give the desired maximum transmission output speed of 5,000 RPM without changing the transmission gearing. The gearing to the high speed electric motor would remain identical to permit vehicle operation by the electric motor only at low powers and in part at high powers in the same fashion as proposed with the electric motor-flywheel arrangement.

It is desired to operate the internal combustion engine at its minimum SFC over the range of torques, as shown in Figure VI-1. The belt drive control to accomplish this was described previously in Section III-B, using Figures III-5 and III-6. It is necessary to supply the schedule control with a control oil pressure, P_E, which is proportional to the engine output torque, not the transmission output torque. A hydraulic pressure, P_1', may be generated, as shown in Figure VI-2, that is proportional to the transmission output torque by using a voltage generator at the sun shaft (geared to pulley A shaft) that gives an output voltage which is a function of the speed of pulley A. The hydraulic pressure, P_1', must then be modified by the speed ratio between pulley A and pulley B to obtain a pressure proportional to the engine torque as needed for the control in Figure III-6. This may be accomplished by employing an additional voltage generator operated by gearing to pulley B or the engine shaft, which is used with the voltage generator at the sun shaft to operate a differential solenoid, as shown schematically in Figure VI-2, to obtain a hydraulic pressure, P_E, proportional to the engine output torque.

Various other control approaches are also possible, but the above scheme is relatively direct, and with due consideration to dampening the pintle movements, using relatively friction free elements, and consideration of necessary flow rates and solenoid characteristics, it is believed to be a practical control configuration when operating the CVT in the direct high speed mode. It is proposed that operation in the low speed mode be accomplished only with the electric motor, disconnecting the engine drive by means of a clutch. The electric motor is capable by itself of generating the maximum necessary torques due to the differential planetary gearing, as has been previously discussed.

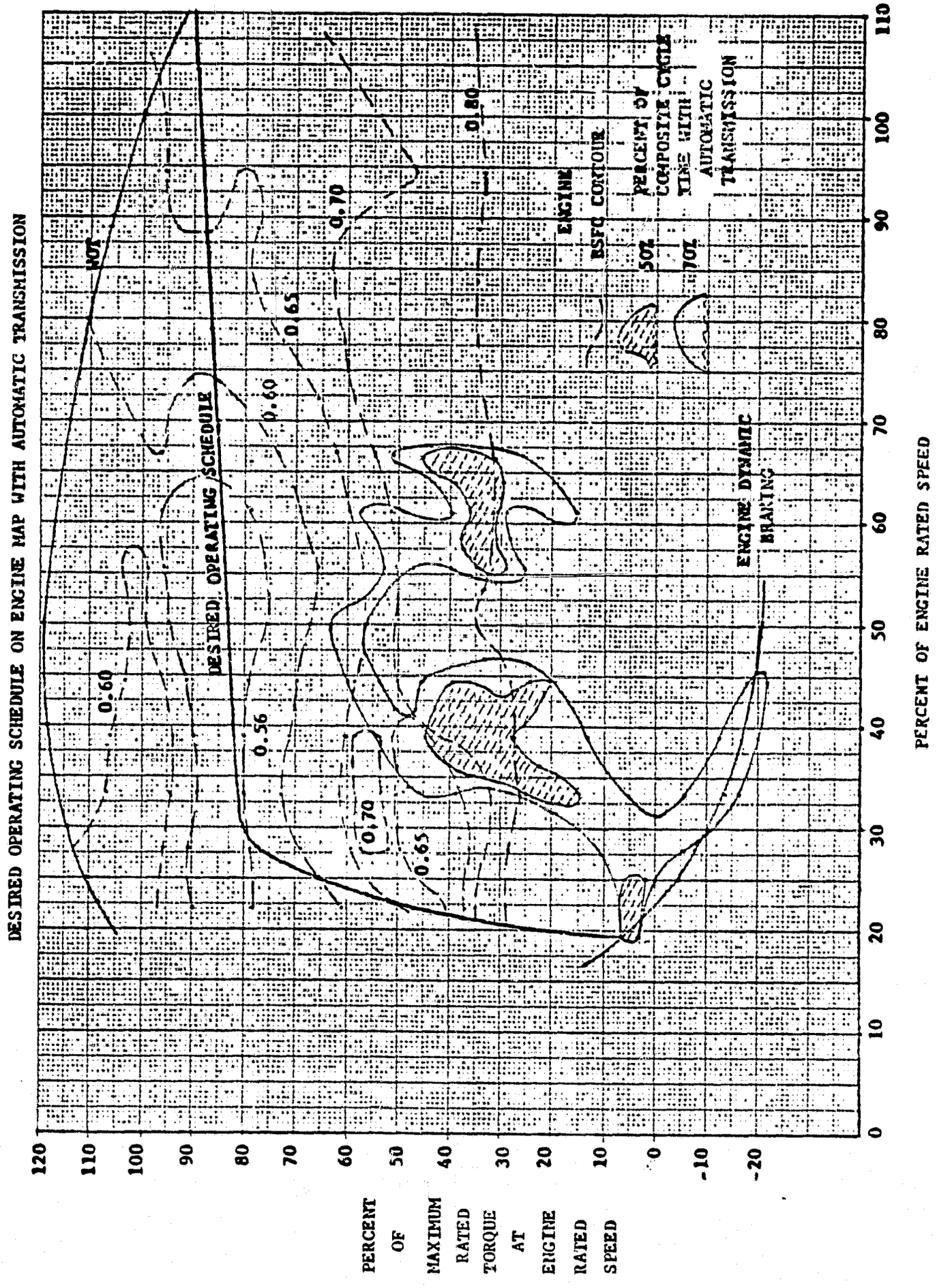

Figure VI-1 — DESIRED OPERATING SCHEDULE ON ENGINE MAP

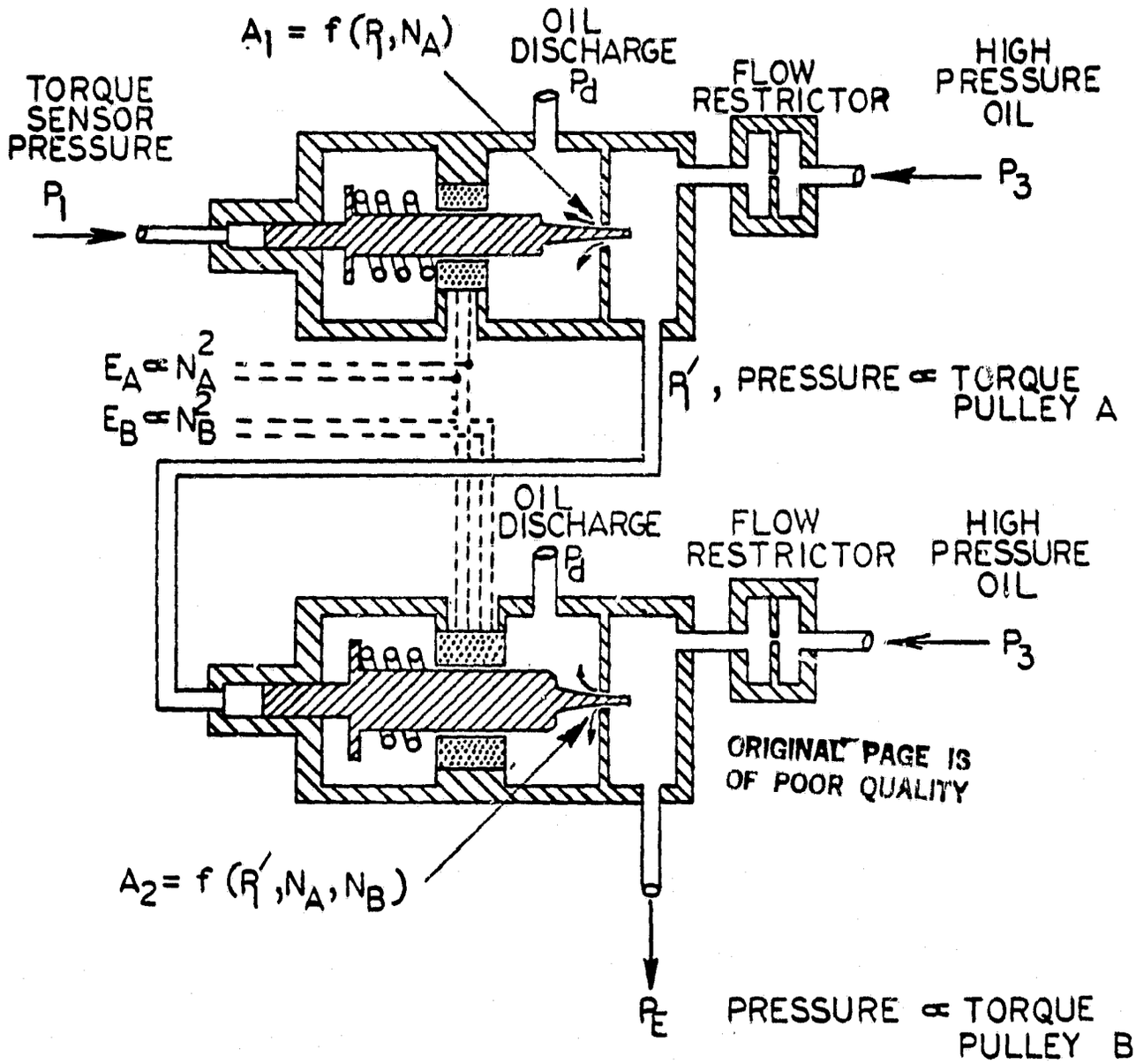

Figure VI-2 — ENGINE TORQUE BALANCE PRESSURE CONTROL

APPENDIX A

BENDING STRESS OF BELTS PASSING AROUND PULLEYS

This derivation is based on the assumption that the cord bends as a simple solid beam, but uses Castigliano's theorem[18] to determine from the strain energy of bending, the maximum bending stress in the cords passing over the minimum radius pulley.

A tensile force is applied to the belt which is shared by the cords of the belt. This tensile force results in pressing the fibers of a cord together and prevents fiber slippage, due to the friction between fibers when the belt is bent around a pulley. With sufficient bonding material and friction, it then appears reasonable to assume that the cord will act as a simple beam in bending. This stress has been given as follows:[19]

$$S_b = Ec/r \qquad \text{(A-1)}$$

The analysis, using Castigliano's theorem, gives the stress S_b' as follows:

$$S_b' = 84.256\ (.1817\ L - 1.1416\ r)Ec\ /\ L^2 \qquad \text{(A-2)}$$

L = length of belt

r = pulley radius

E = modulus of elasticity of material

c = distance - neutral axis to outer surface

This analysis assumes the belt to be initially without bending stress in the form of a circle and uses the formula for the deflection and stress in a thin ring as pulled by two opposing forces to give smaller radii ends. Consider the belt as a thin solid ring of Figure A-1 having a diameter of L/π , L = belt length.

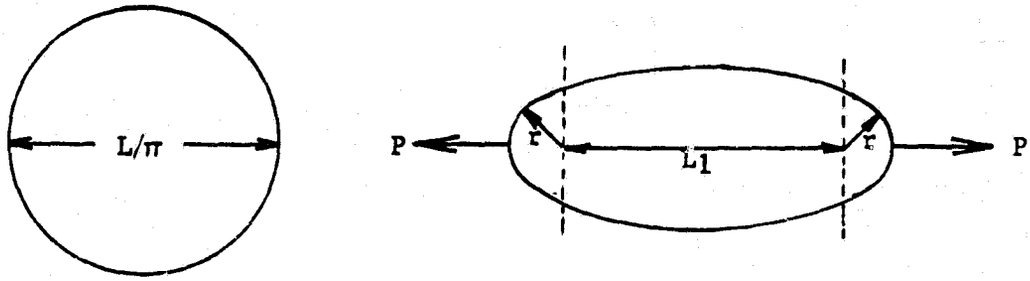

Figure A-1 – BELT DEFLECTION

Subject the ring to two opposing forces, P, to deform the ring as shown. The resulting deflection, δ , in the horizontal direction may then be defined as follows:

$$\delta = 2r + L_1 - L/\pi \qquad \text{(A-3)}$$

$$L = 2\pi r + 2L_1 \qquad \text{(A-4)}$$

$$L_1 = L/2 - \pi r \qquad \text{(A-5)}$$

Substitute for L_1 in Eqn. (A-3)

$$\delta = .1817\ L - 1.1416\ r \qquad \text{(A-6)}$$

Then from Reference (18)

$$\delta = 0.149\ (P / EI_z)\ (L / 2\pi)^3 \qquad \text{(A-7)}$$

I_z = cross section moment of inertia

The maximum moment on the belt is (Reference 18)

$$M = 0.318\ P\ L / 2\pi \qquad \text{(A-8)}$$

The well known equation for bending stress in any beam is

$$S_b = Mc / I_z \quad , c = d_c / 2, \text{ (round cord)} \qquad \text{(A-9)}$$

Substituting and collecting terms, equation (A-10) is given:

$$S_b'/d_c = 42.128\ (.1817\ L - 1.1416\ r)\ E/L^2 \qquad \text{(A-10)}$$

or
$$S_b' = 84.256\ (.1817\ L - 1.1416\ r)\ Ec/L^2 \qquad \text{(A-2)}$$

Given data on the characteristics of fibers useful for belt cords then permits comparison of the allowable cord diameters to give a specified fraction of the tensile ultimate strength suitable for adequate life due to bending fatigue.

Table A-1 gives data for some well known fibers. The large elongation of Nylon and Dacron is unattractive for a highly loaded belt. The fraction of the ultimate strength possible to use for the desired fatigue life in bending of Kevlar 29 and E-HTS is not known. The fatigue life of National Standard carbon steel rocket wire is excellent, the percent of the ultimate tensile strength apparently increasing as the wire diameter is decreased.

TABLE A-1

CORD BENDING STRESS

Material	Density G/cm^3	Elongation to Break-%	Modulus E M Pa	Tensile Ultimate Strength S_u M Pa	Formula S/c L=900mm R=50mm	c mm S=20% S_u	Cord Diameter D mm S=20% S_u	New Formula S_b M Pa	Old Formula $S_b=Ec/r$ M Pa
Kevlar 29 Fiber	1.44	2.5	62069	2758	687.28	0.803	1.606	551.6	996.8
Nylon 728 Fiber	1.14	18.3	5516	986	61.08	3.23	6.46	197.2	356.3
Dacron 68 Fiber	1.38	14.5	13790	1120	152.70	1.47	2.94	224.5	405.4
E-HTS Fiber	2.55	3.5	68950	2413	763.48	0.63	1.26	481.0	868.8
Rocket-Wire (NS) 0.10mm diameter	7.84	2.0	200000	3965	2214.58	0.36	0.71	793.0	1440

However, if the configuration dimensions for the flat belt proposed herein were used (L = 900 mm, r = 47.5 mm) and it is assumed that the fatigue life due to bending is unlimited at 33% of the Kevlar 29 ultimate strength.

Using Eqn. (A-10),

$$d_c = (0.33)(2758)(900)^2 / 42.128\ (62069) \left[(.1817)\ 900 - 1.1416\ (47.5)\right]$$

$$d_c = 2.57 \text{ mm } (.100 \text{ inches})$$

The diameters of cords and wires of the other materials may be calculated similarly.

Other stresses are also involved, and if it is assumed as a result the bending stresses should be limited to 20% of the ultimate strength for unlimited life, a table comparing maximum cord sizes may be prepared considering various cord or tensile elements. As shown in Table A-1 the Kevlar 29 fibers are very attractive, considering their low density and high strength, but the E-HTS and Rocket-Wire materials could also be used.

A material being subjected to cyclic stresses which give a zero mean average applied stress has a longer fatigue stress life than the same material subjected to cyclic stresses with the same maximum value but a non-zero mean average applied stress. Thus, a rigid ring belt construction (Figure IV-14), which could be expected to have rather complete cyclic stress reversals with resulting low mean average applied stress, should have a longer fatigue life than a non-rigid belt construction which does not have as complete cyclic stress reversals.

APPENDIX B

BENDING STRESS OF BELT PASSING BETWEEN PULLEYS

This calculation is involved with the axial forces necessary to straighten a curved beam. Consider the belt to be a thin beam originally in the form of a circle and then deformed by passing over pulleys A and B as shown in Figure B-1.

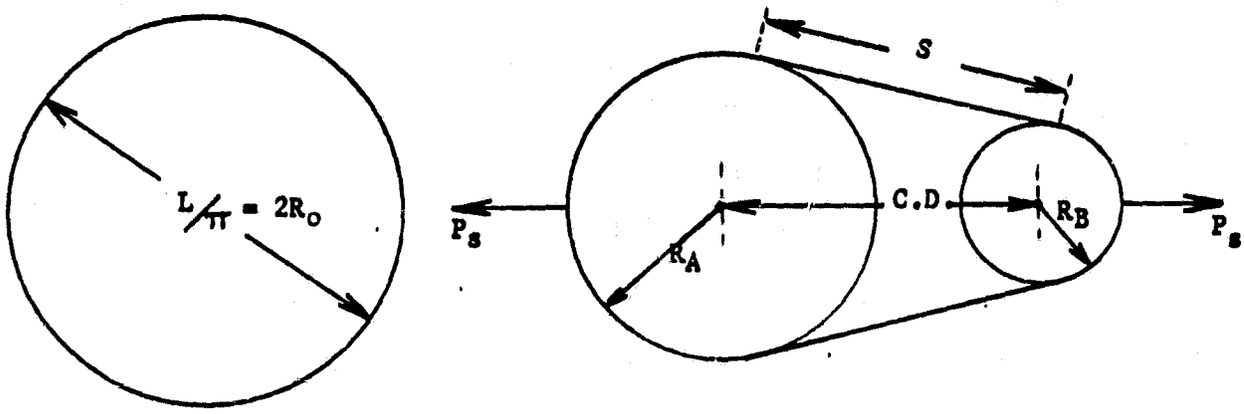

Figure B-1 — BELT DEFORMED OVER PULLEYS

The straightened section of length S is bent from a circular arc as shown in Figure B-2.

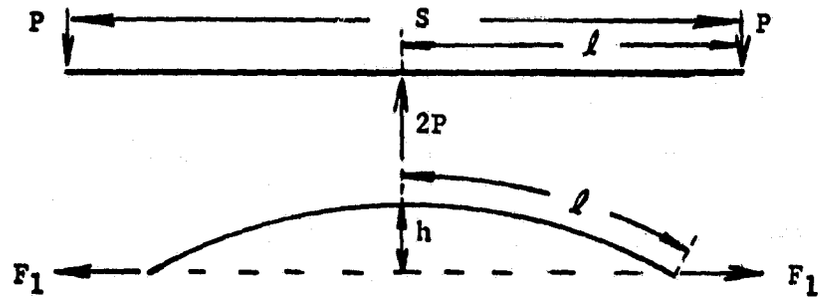

Figure B-2 — BELT STRAIGHTENED FROM CIRCULAR ARC

Assume that bending a straight beam of length S to have the same deflection h by application of force P gives an equivalent bending stress on the beam. A pulley system having a belt length, L, and center distance between pulleys of C.D. has a slant length S equal approximately to the center distance, D.C.

However, the specific geometry is given by

$$S = C.D. \cos \varphi \qquad (B-1)$$

$$\varphi = \sin^{-1} (R_A - R_B) / C.D. \qquad (B-2)$$

$$L = 2S + R_A (\pi + 2\varphi) + R_B (\pi - 2\varphi) \qquad (B-3)$$

Let $C.D. = 225$ mm

$R_A = 100$ mm

$R_B = 50$ mm

Then $\varphi = \sin^{-1} (100-50) / 225 = 12.84$ degrees (B-4)

$$S = 225 \cos 12.84 = 219.37 \text{ mm} \qquad (B-5)$$

$$L = 2(219.37) + 100 \left[\pi + 2 (.224)\right] + 50 \left[\pi - 2 (.224)\right] \qquad (B-6)$$

$L = 932.4$ mm

$$R_o = L/2\pi = 932.4 / 2\pi = 148.4 \text{ mm} \qquad (B-7)$$

From geometry of circular arc section

$$h = R_o - R_o \cos \theta /2 \qquad (B-8)$$

where $\theta = S/R_o = 219.37/148.4 = 1.478$ radian $= 84.7$ degrees (B-9)

Substitute in (B-8)

$h = 148.4 (1-\cos 84.7/2) = 38.73$ mm

Using the straight beam deflection formula

$\ell = S/2 = 109.69$ mm

$$h = P \ell^3 / 3 EI \qquad (B-10)$$

$$P = EI (38.73) (3) / (109.69)^3 = EI / 11357 \qquad (B-11)$$

The maximum moment due to P is

$$M = P\ell = EI (109.69) / 11357 = EI / 103.54 \qquad (B-12)$$

Equivalent moment due to F_1 is

$$M = hF_1 = EI / 103.54 \qquad (B-13)$$

Maximum stress due to straighten section is then

$$s_s = M\,c\,/\,I = EI\,c\,/\,I\ (103.54) \qquad \text{(B-14)}$$

$$s_s = E\,c\,/\,103.54 \qquad \text{(B-15)}$$

The bending stress to straighten the belt is directly proportional to the cord diameter.

Consider $d = 1.5$ mm (0.0591 inches), cord diameter

$c = .75$ mm

For $E = 62069$ M Pa — Kevlar 29 fiber, using Eqn. (B-15)

$s_s = 62069\ (.75)\ /\ 103.54$

$s_s = 449.60$ M Pa = 65215 psi

The ultimate strength of Kevlar 29 fiber

$s_u = 2758$ M Pa

The operating fractional ultimate strength is:

$$s_s\ /\ s_u = .163 \qquad \text{(B-16)}$$

An infinite fatigue life is obtained in most strong materials with stress fractions of less than 30 - 40%.

The force F_1 necessary to straighten the beam or belt is from equation (B-13) per cord,

$$F_1 = EI\ /\ (103.54)\ h \quad , I = \pi\ (d/2)^4\ /\ 4 \qquad \text{(B-17)}$$

$$F_1 = 62069\,\pi\ (.75)^4\ /\ 4\ (103.54)(38.73)$$

$F_1 = 3.846$ Newtons (.865 lbs)

If a single layer of cords are placed side by side, the number in a 37.5 mm wide belt is

$$N = 37.5\ /\ 1.5 = 25 \text{ cords} \qquad \text{(B-18)}$$

If the cord has a actual Kevlar cross section of 35%, the ultimate strength of the belt would be

$$F_u = 0.35\ S_u N \pi c^2 \qquad \text{(B-19)}$$

Breaking Strength $= 2758\ (25)\pi\,(0.75)^2\ (.35) = 42655$ Newtons
$= (9600$ lbs)

A maximum tensile force of 3100 Newtons as calculated for the belt drive appears very conservative, being only 7.3% of the average breaking strength.

APPENDIX C

DESIGN OF GEARS

1. GENERAL

All of the gears were designed using criteria that is based on over twenty five years of experience devoted to all types of gearing. In general, methods and formulae used are based on "American Gear Manufacturers Association" design procedure. The stress/life curves used to determine the allowable stresses were developed several years prior to the 1966 AGMA Standard 411.02, "Design Procedure for Aircraft Engine and Power Take-Off Spur and Helical Gears", but conform very closely to tables 4 and 5 in the AGMA publication. Figure C-1 shows the curves of the material and processing as specified, modified for 90% reliability.

Spur gears are used throughout the transmission. For the face widths required, excessive helical angles would have been required to get the tooth overlap advantage associated with helical gears. The high helix angles would also have resulted in substantial gear thrust loads on the bearings.

Gear tooth meshing noise is controlled by the design features of the gearing and quality of the gears. Center distances and tooth addendums have been modified to provide smoother, quieter gear tooth meshing through reduced approach and increased recess tooth action, as well as to balance stresses on the pinion and gear at each mesh.

All of the external gears are specified to be made from SAE 9310 steel with the teeth case hardened by carburizing. The case hardness is selected to be Rockwell 15N-90 minimum with a core hardness of Rockwell C 33-43. The gear teeth active surfaces are specified to have

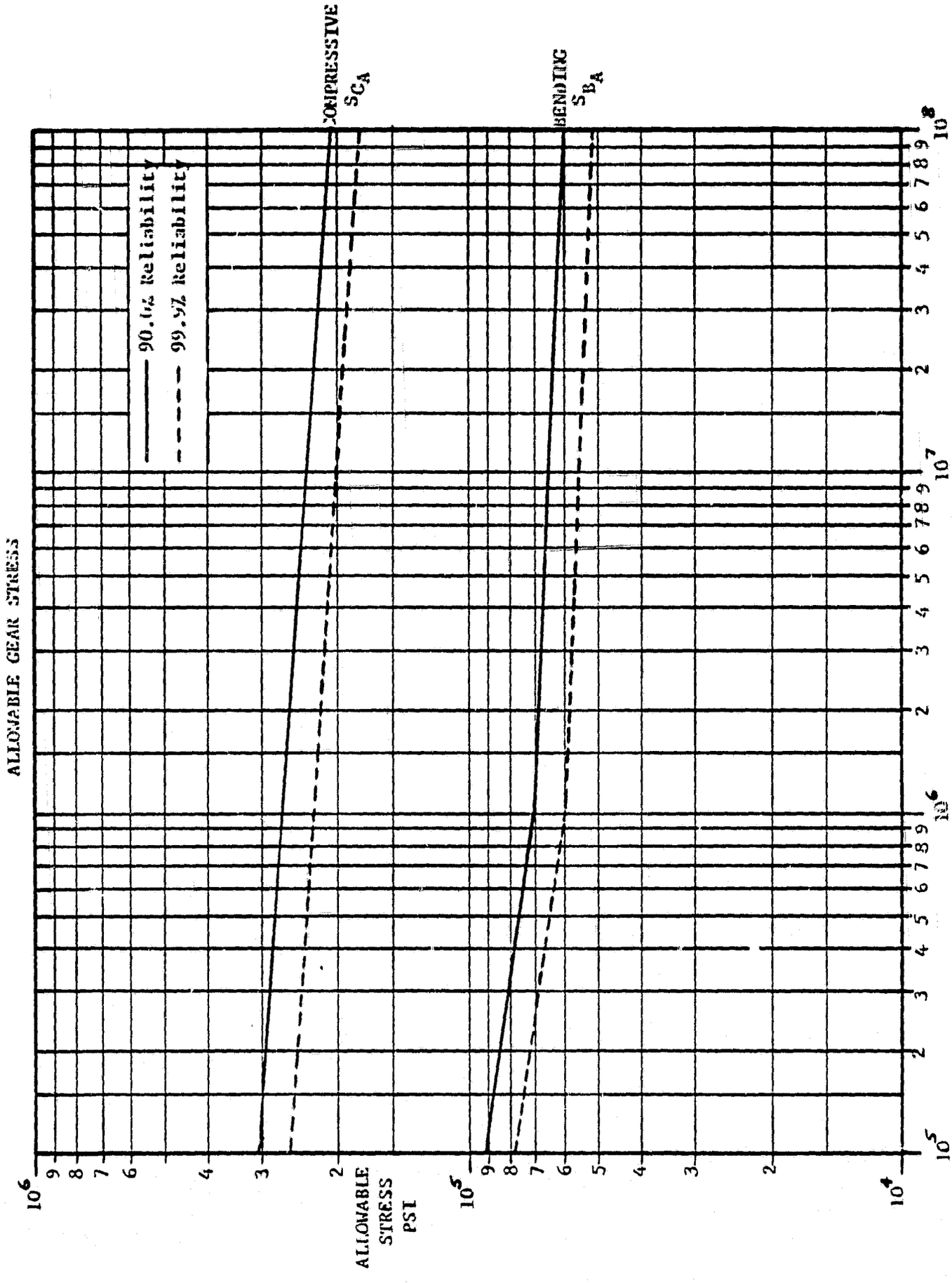

Figure C-1 — ALLOWABLE GEAR STRESS

32 rms surface finish or better. The tolerances specified on pitch diameter runout, spacing error, involute profile error and tooth parallelism error are according to Quality Class 10 per AGMA Standard 390.03, Jan. 1971.

2. LIFE REQUIREMENTS

The 2600 hours of operating life required for the transmission gears is comprised of various durations for different operating conditions as shown in Table IV-5. Operation at maximum torque occurs in the "Maximum Power" condition for gears 1, 2, 3, 4, A, B, F, H, HO, and in the "Maximum Torque-Grade" condition for gears L, LO, S, P, R. Such maximum torque operation was used for design of the gears. Life at the maximum torque condition, equivalent to 2600 hours considering a duty cycle involving all of the various operating conditions, was then calculated using the following formula:

$$L_e = L_1 + \left[L_2 n_2 \left(T_2/T_1\right)^{\alpha} + L_3 n_3 \left(T_3/T_1\right)^{\alpha} + \ldots L_n n_n \left(T_n/T_1\right)^{\alpha}\right] / n_1, (C-1)$$

L_e = equivalent life-hours

L_n = life at various operating conditions-hours

n_n = rpm at various operating conditions

T_n = torque at various operating conditions - lb.in.

α = 8.65 for bending stress for 10^4 to 10^6 tooth contact cycles

α = 29.0 for bending stress for greater than 10^6 cycles

α = 9.0 for compressive stress

This then resulted in the equivalent hours of life as follows:

LIFE AT MAXIMUM TORQUE EQUIVALENT TO 2600 HOURS OF NORMAL DUTY CYCLE

Gear Mesh	(1)(2)	(3)(4)	(4)(B)	(A)(F)	(H)(HO)	(L)(LO)	(S)(P)	(P)(R)
$L_{e_{Bend.}}$	3	3	8.2	53.7	3	26	37.8	37.8
$L_{e_{Compr.}}$	3	3	8.3	24	3	26	40.4	40.4

Since the calculated minimum life at the maximum torque equivalent to 2600 hours of normal duty cycle (using a 1.5 safety factor) equals or exceeds the desired life given on Table IV-5, it is concluded that the gears are adequate for the intended service.

3. STRESS CALCULATIONS

a. Bending Stress

The gear capacity to resist tooth breakage is calculated using the formula:

$$S_{B_C} = W_t P / FJ \qquad \text{(C-2)}$$

S_{B_C} = calculated root tensile or bending stress-psi.

W_t = tangential tooth load - lbs.

P = diametral pitch

F = minimum face width - ins.

J = geometry factor (calculated by computer program)

b. Compressive Stress

The gear tooth surface capacity to resist destructive pitting is based on the "Hertz" stress and is calculated from the formula:

$$S_{C_C} = C_p \, (W_t / dF_e I)^{\frac{1}{2}} \qquad \text{(C-3)}$$

S_{C_C} = calculated mean contact stress - psi

C_p = elastic coefficient = 2290 for steel

W_t = tangential tooth load - lbs.

d = pinion operating pitch diameter - in.

F_e = minimum contact face width - in.

I = geometry factor (calculated by computer program for both pitch line and low point of single tooth loading on the pinion)

The maximum stress at each mesh has been used.

c. Allowable Stresses

The required number of tooth contact cycles for each gear is calculated from the formula:

$$N_{C_R} = 60 \, nL_e \qquad \text{(C-4)}$$

N_{C_R} = required number of tooth contact cycles

L_e = equivalent life - hours

n = rpm

The allowable stresses, S_{B_A} or S_{C_A}, for the required number of tooth contact cycles can be selected from the curves in Figure C-1.

d. Derating Factors

A derating factor (C_d) was calculated by dividing the allowable stresses by the calculated stresses as follows:

$$C_d = S_{B_A} / S_{B_C} \text{ or } S_{C_A} / S_{C_C} \qquad \text{(C-5)}$$

All of the gears are designed for at least 1.5 derating factor as recommended for passenger cars in the AGMA Standard 170.01, Nov. 1976, "Design Guide for Vehicle Spur and Helical Gears" for Quality Class 10 gears.

4. EFFICIENCY

Gear efficiency is discussed elsewhere in other portions of this report. Windage losses of the gears are also given in other portions of this report.

5. SCORING

A flash temperature index was calculated to determine the resistance to scoring of gear teeth surfaces. The calculation was made for contact at the high and low points of single tooth contact on the pinion at each mesh as well as at the tip of tooth and start of active profile per AGMA Standard 217.01, October 1965, "Gear Scoring Design Guide for Aerospace Spur and Helical Power Gears". The formula used is:

$$T_f = T_i + (W_{t_e}/F_e)^{0.75} (50/50\text{-}S) (Z_t n^{0.5}/P^{0.25}) \qquad \text{(C-6)}$$

T_f = flash temperature index - deg. F

T_i = inlet oil temperature - deg. F = 160°

W_{t_e} = effective tangential tooth load - lbs.

F_e = minimum contact face width - in.

S = surface finish after run-in rms = 15

Z_t = scoring geometry factor

n = pinion rpm

P - diametral pitch

The maximum flash temperature index at each mesh is calculated to be well below 276° F (136° C), the temperature above which there is scoring risk.

6. CONCLUSIONS

The results of the calculations, which used a programable calculator and programs tailored to the formulae as described, are shown in Table C-1. All of the gears meet the life and duty requirements of the differential belt transmission within its dimensional restraints.

In addition, special attention has been given to reducing noise, and the use of special materials and manufacturing processes have been avoided.

The design is substantially consistent with automotive practice, and the resulting production gear costs should be similar to production costs of automotive gears.

GEAR STRESS DATA

GEAR	NO. OF TEETH	DIAM. PITCH	FACE WIDTH (MIN) MM	SPEED RPM	OPER. MODE	TORQUE N-m	TANGEN. TOOTH LOAD N	BENDING		COMPRESSIVE		SCORING FLASH TEMP.(2) C°
								CALC STRESS MPa	DERATING FACTOR (1)	CALC. STRESS MPa	DERATING FACTOR (1)	
1	26	20	15.49	21000	MAX POWER	34.11	2045.7	307	1.510	1141	1.510	120.22
2	76		13.46	7184.21		99.69		306	1.575			
3	22	12	18.29	7184.21	MAX POWER	99.69	4240.8	290	1.662	1183	1.546	118.62
4	79		17.78	2000.67		357.99		250	1.642			
4	79	12	17.78	2000.67	MAX POWER	357.99	4266.3	233	1.563	1067	1.651	100.42
B	31		18.80	5098.47		140.48		309	1.525			
A	39	10	5.84	9898.99	MAX POWER	72.35	1448.3	257	1.680	1022	1.566	122.41
F	49		5.33	7878.79		90.90		265	1.641			
H	33	10	7.87	7878.79	MAX POWER	90.90	2153.8	292	1.645	1106	1.646	123.07
HO	52		7.37	5000		143.24		318	1.534			
L	33	10	23.88	1575.76	MAX TORQUE GRADE	285.56	6765.8	302	1.561	1100	1.604	94.17
LO	52		23.37	1000		449.97		315	1.520			
S	27	20	20.32	3275.39	MAX TORQUE GRADE	95.18	1796.2	229	1.969	1009	1.626	79.89
P	26		19.81	1323.75		30.55		234	1.500			
P	26	20	19.81	1323.75	MAX TORQUE GRADE	30.55	1864.2	235	1.491	742	2.511	——
R	81		16.51	1575.76		285.56		211	1.619			

(1) Derating factor equals ratio of allowable stress to calculated stress
(2) Calculated using 71.11° C inlet oil temperature.

TABLE C-1

Table C-1 — GEAR STRESS DATA

APPENDIX D

OIL PUMPS

1. GEAR OIL REQUIREMENTS

Gear Mesh		Mesh. Power Loss (Maximum) KW	HP	BTU/MIN	Oil Flow GPM = .2 (HP)
(1)	(2)	* .14	.19	8.1	.08
(3)	(4)	* .30	.40	17.0	.16
(4)	(B)	.28	.38	16.1	.08
(A)	(F)	.11	.15	6.4	.03
(H)	(HO)	* .18	.23	9.8	.05
(L)	(LO)	.22	.30	12.7	.06
(S)	(P)	.10	.13	5.5 per mesh	.08 total
(P)	(R)	.04	.05	2.1 per mesh	.03 total
					0.57 GPM
				Use	0.60 GPM

* Double oil flow to provide capacity for greater power transfer due to a high speed accelerator clutch.

2. BEARING OIL REQUIREMENT (Maximum Loss)

Bearing	Location	Maximum Power Loss		Oil Flow
		KW	(HP)	GPM = .1(HP)
107	Clutch Shaft	.051	.068	.007
206	" "	.158	.212	.021
203	Motor Shaft	.045	.060	.006
204	" "	.057	.076	.008
WJ162112	Jack Shaft	.048	.064	.006
WJ162112	" "	.024	.032	.003
JH2212	Carrier Shaft	.018	.024	.002
WJ283412	" "	.019	.025	.003
WJ121616	Sun Shaft	.006	.008	.001
WJ121616	" "	.014	.019	.002
141374, 14276	HO Shaft	.046	.062	.006
" "	LO Shaft	.009	.012	.001
L507949,L507910	L Shaft	.023	.031	.003
M86648A,M86610	" "	.009	.012	.001
16009	Torque Sensor	.063	.084	.008
19150, 19281	Pulley A	.290	.389	.039
M84548,M84510	" "	.089	.119	.012
19150, 19281	Pulley B	.189	.253	.025
M84548,M84510	" "	.054	.072	.007
FWJ162117	Planet	.010	.013	.004 (3 planets)
				.165

Use 0.20 GPM

3. CONTROL ACTUATOR OIL REQUIREMENT

Assume operating time from maximum to minimum reduction ratio is 1.5 seconds (specified design requirement = 2.0 seconds). The actuator volume to be filled with low pressure oil is:

$$V = 3(0.5)(r_o^2 - r_i^2)\,\Delta\theta\; W \qquad \text{(D-1)}$$

$$V = 3(0.5)(79.0^2 - 27.0^2)(1.39)(18.8)$$

$$V = 216059\ mm^3\ (13.18\ in^3)\ (.0571\ gallons)$$

$$Q = 13.18\ /\ 231\quad 60\ /\ 1.5 = 2.28\ GPM$$

Note: The high pressure oil is exchanged from one actuator to the other in this operation.

Using a low pressure accumulator (75 PSIG) of 0.25 gallon capacity with 0.5 GPM supply would permit varying the pulley speed over its complete range five times in a rapid sequential fashion without depleting the accumulator.

The high pressure requirement is only that necessary to make up for leakages and for control stability. A high pressure (150 PSIG) accumulator of 0.10 gallon capacity with 0.1 GPM supply appears to be quite adequate.

4. PUMPS, HYDRAULIC OIL

It is proposed to use two gerotor type pumps mounted on the same shaft driven by an electric motor which would be started ahead of and independent of the transmission. One pump will supply 75 PSI oil for the lubrication of bearings, gears and the low pressure oil to the control actuators. The other pump will supply 150 PSI oil to the torque pressure balance regulator and its accumulator. The pump power requirement is:

$$KW_p = Q\,\Delta P\ /\eta_p\ 2300 \qquad \text{(D-2)}$$

Pump "1", $KW_p = .10(150)\ /\ .60(2300) = .011$

Pump "2", $KW_p = 2.0(75)\ /\ .70(2300) = \underline{.093}$

Total Pump Power = .104 KW

Total heat input to oil - design ~ 120 BTU/Min, 147.5 BTU/Min Maximum

Flow = 2.0 GPM, ΔT_o = 120 / (8.34)(.5) 2.0(.85) (D-3)

ΔT_o = 16.93° F

ΔT / ITD = 16.93 / 40.0 = 0.42

Oil Heat Exchanger - Oil in @ 140° F out @ 125° F

Air Flow 330 CFM @ 0.117" H_2O, Air in @ 100° F out @ 118.5° F

ΔP of Oil less than 1.0 PSI

Aluminum Heat exchanger 12.00 x 11.54 x 5.62 inches, weighs 4.0 pounds without fan. Use ram air augmentation to small fan.

Fan Power (HP) = 0.0001573 (CFM) ΔH (inches H_2O) / η_F (D-4)

P_F = 0.0001573 (330)(.117) / .50 = .0121 HP

P_F = 0.009 KW

APPENDIX E

CRITICAL SPEEDS

1. SHAFT - PULLEY A - LUMPED LOADS

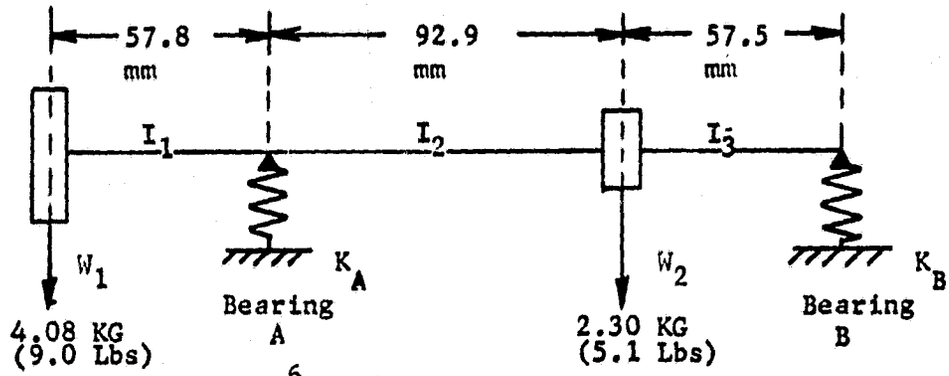

Bearing A, $K_A = 3.24 \times 10^6$ lbs/in 19150 cone, 19281 cup

Bearing B, $K_B = 3.37 \times 10^6$ lbs/in M84548 cone, M84510 cup

$$K_e = K_A + K_B = 6.61 \times 10^6 \text{ lbs/in - Slight Preload only} \qquad \text{(E-1)}$$

Frequency due only to bearing spring rate

$$f_K = \frac{1}{2\pi} (K_e/m)^{\frac{1}{2}}, \qquad m = \frac{W}{g} = (9+5.1)/386 = 0.0365 \ \frac{\text{lbs.sec}^2}{\text{in.}} \qquad \text{(E-2)}$$

$$f_K = \frac{1}{2\pi}(6.61 \times 10^6/.0365)^{\frac{1}{2}}$$

$f_K = 2142$ c/s = 128500 RPM >> 10,000 RPM

Therefore assume solid support at bearings and calculate shaft frequency

$$f = \frac{1}{2\pi} \left[g \frac{(W_1 y_1 + W_2 y_2 + ...)}{(W_1 y_1^2 + W_2 y_2^2 + ...)} \right]^{\frac{1}{2}}, \ \frac{1}{\text{Sec}} \qquad \text{(E-3)}$$

$W_1, W_2 \ldots$ = Loads

$y_1, y_2 \ldots$ = Deflections at Loads, $W_1, W_2 \ldots$

CALCULATION - DEFLECTIONS - CRITICAL SPEEDS - PULLEY SHAFT A

$E = 30 \times 10^6$ psi, I .20 in^4

Due to W_1, using Reference (20)

$$y_{1_1} = \frac{Pb^2 l}{3\,EI} \qquad \text{(E-4)}$$

y_1: $y_{1_1} = \frac{9.0\,(57.8)^2\,(208.2)}{3\,EI\quad(25.4)^3} = +21.23 \times 10^{-6}$, in.

Due to W_2, Reference (21)

$$\theta_1 = \frac{Pab(l+b)}{6l\,EI} \qquad \text{(E-5)}$$

$\theta_{1_2} = 5.1\,(92.9)\,(57.5)\,(150.4 + 57.5) / 6\,(150.4)\,EI\,(25.4)^2$

$\theta_{1_2} = 1.62 \times 10^{-6}$ radians

$$y_{1_2} = \theta_1 b \qquad \text{(E-6)}$$

$y_{1_2} = -3.69 \times 10^{-6}$ in.

$$y_1 = y_{1_2} + y_{1_2} \qquad \text{(E-7)}$$

$y_1 = 21.23 \times 10^{-6} - 3.69 \times 10^{-6} = 17.54 \times 10^{-6}$ in.

y_2:

Due to W_1, $I \simeq .20$ in^4

$$y_{2_1} = \frac{Pbx}{6a\,EI}\,(x^2-a^2) \qquad \text{(E-8)}$$

$$y_{2_1} = \frac{9.0\,(57.8)(57.5)(57.5^2 - 150.4^2) / 6(150.4)\,EI}{(25.4)^3}$$

$y_{2_1} = -13.02 \times 10^{-6}$ in.

Due to W_2

$$y_{2_2} = \frac{Pbx}{6l\,EI}\,(l^2-b^2-x^2) \qquad \text{(E-9)}$$

$$y_{2_2} = \frac{5.1\,(57.5)(92.9)(150.4^2 - 57.5^2 - 92.9^2) / 6(150.4)\,EI}{(25.4)^3}$$

$y_{2_2} = 6.56 \times 10^{6}$ in.

$$y_2 = y_{2_1} + y_{2_2} \qquad \text{(E-10)}$$

$y_2 = -6.46 \times 10^{-6}$ in.

Using Eqn. (E-3)

$$f = \frac{10^3}{2\pi}\left[\frac{386\,(9.0\,(17.54) + 5.1(6.46))}{(9.0\,(17.54)^2 + 5.1(6.46)^2}\right]^{\frac{1}{2}}$$

$f = 791$ c/s = 47460 RPM

2. SHAFT - PULLEY B - LUMPED LOADS

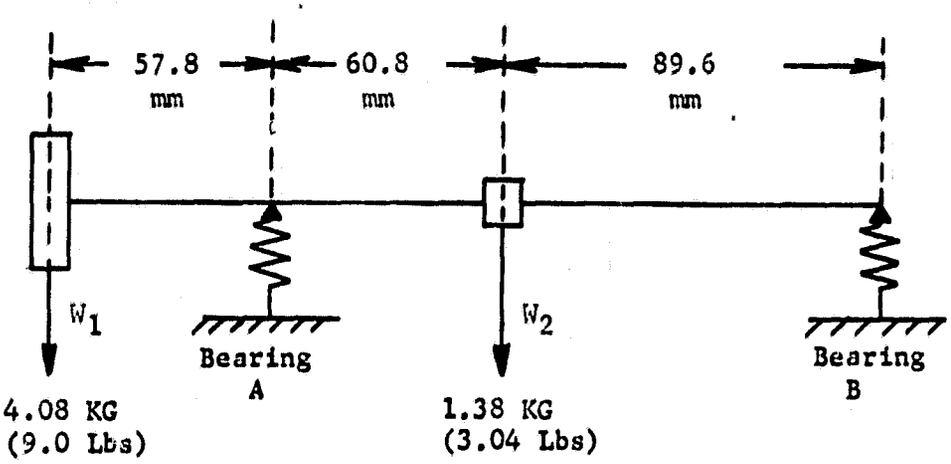

$E = 30 \times 10^6$ psi $I = .16$ in^4

y_1:

$y_{1_1} = 26.36 \times 10^{-6}$ in - scaled from Pulley A calculations

$\theta_1 = 3.04\,(60.8)(89.6)(150.4 + 89.6) / 6\,(150.4)\,E(.16)(25.4)^2$

$\theta_1 = -1.42\ \ 10^{-6}$

$y_{1_2} = -3.24\ \ 10^{-6}$ in

$y_1 = 26.36\ \ 10^{-6} - 3.24\ \ 10^{-6} = 23.12\ \ 10^{-6}$ in.

y_2:

Due to W_1

$$y_{2_1} = \frac{9.0\,(57.8)(89.6)(89.6^2 - 150.4^2) / 6(150.4)\ 30\ 10^{-6}\ (.16)}{(25.4)^3}$$

$y_{2_1} = -9.58\ \ 10^{-6}$

Due to W_2

$$y_{2_2} = \frac{3.04\,(89.6)(60.8)(150.4^2 - 89.6^2 - 60.8^2) / 6(150.4)\ EI}{(25.4)^3}$$

$y_{2_2} = 2.54\ \ 10^{-6}$

$y_2 = 7.04\ \ 10^{-6}$ in

$f = 673$ c/s = 40,350 RPM

3. SUN SHAFT - LUMPED LOADS

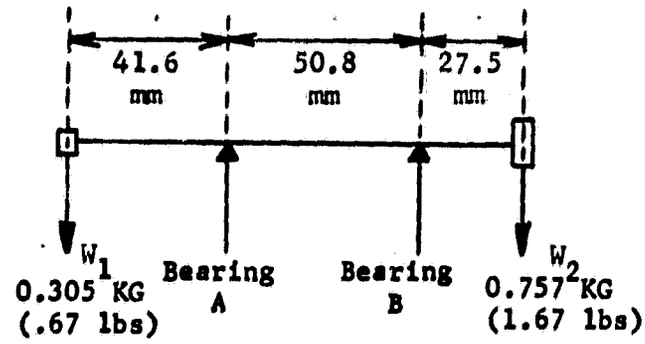

$$I = \frac{\pi}{4}(9.5^4 - 3.5^4) / (25.4)^4 = .015 \text{ in}^4$$

y_1 :

Due to W_1

$$y_{1_1} = \frac{Pb^2 1}{3\,EI} \qquad \text{Same as (E-4)}$$

$$y_{1_1} = \frac{.67(41.6)^2 \;\; 50.8 \;/\; 3(30)\;10^6\;(.015)}{(25.4)^3}$$

$$y_{1_1} = 2.66 \times 10^{-6} \text{ in.}$$

Due to W_2

$$\theta = \frac{Pab}{6\,EI} \qquad \text{(E-11)}$$

$$\theta_1 = \frac{1.67(50.8)(27.5) \;/\; 6(30)\;\; 10^6\;(.015)}{(25.4)^2}$$

$$\theta_1 = 2.679 \;\; 10^{-6} \text{ radian}$$

$$y_{1_2} = r\theta = \frac{41.6}{25.4}(2.679) \;\; 10^{-6} = 4.39 \;\; 10^{-6} \text{ in.}$$

$$y_1 = 7.05 \times 10^{-6} \text{ in.}$$

y_2 :

Due to W_1

$$\theta_1 = \frac{.67\;(50.8)(41.6) \;/\; 6(30)\;\; 10^6\;(.015)}{(25.4)^2}$$

$$\theta_1 = 0.813 \times 10^{-6} \text{ radian}$$

APPENDIX F

SHAFT TORSIONAL VIBRATION

Consider torsional vibration in Pulley A, the belt, Pulley B and the shaft connected to the sun gear which are connected in a series arrangement in the high speed operating mode, as shown in **Figure F-1.** The torsional rigidities of the shafts associated with the flywheel input to pulley B shaft and with the output shaft are very high and are assumed to have a negligible effect on the computation.

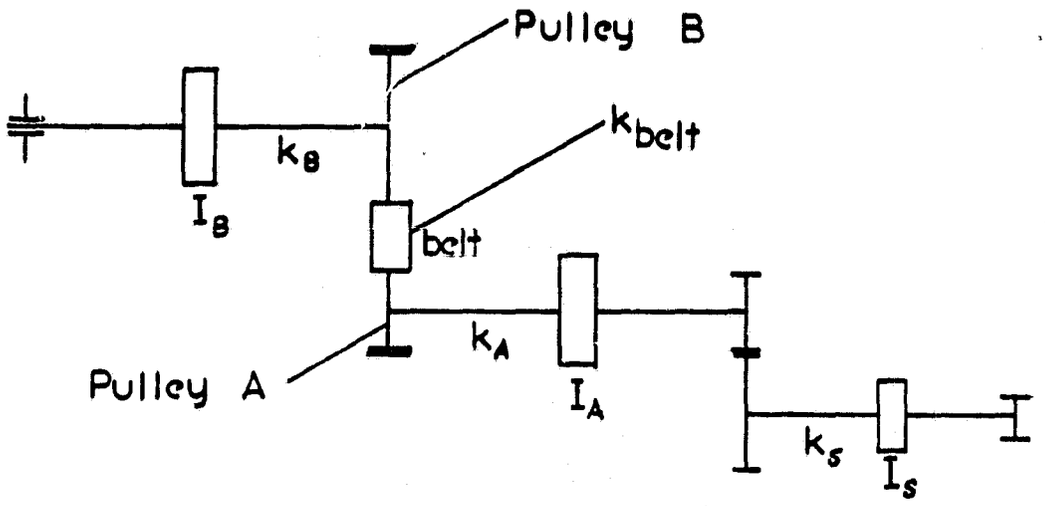

Figure F-1 — SCHEMATIC ARRANGEMENT FOR SHAFT TORSIONAL ANALYSIS

$k = T/\theta = GJ/L$ (F-1)

T = Torque

θ = Angle of twist

G = Shear modulus of elasticity

J = Polar moment of inertia

L = Shaft length

I = Moment of inertia of equivalent disk

Using equivalent moments of inertia, I_A, I_B, I_S, for the elements and torsional spring constants, k_A, k_B, k_S, k_{Belt} in a geared arrangement, the lowest natural

frequency of the system is calculated by obtaining an equivalent spring constant, k_E, and using a lumped torsional system.[22]

$$k_E = 1 / (1/n_A^2 k_A + 1/k_B + 1/k_{Belt} + 1/n_S^2 k_S) \quad \text{(F-2)}$$

$$n_A = N_A/N_B \ , \ n_S = N_S/N_B \quad \text{(F-3)}$$

k_{Belt}: Maximum speed, power

P_O = 75.0 KW, N_O = 5,000 RPM

T_A = 75 N-m (663.75 in.lb) - pulley A

N_A = 9899 RPM, r_A = 51.8 mm

T_B = 145.6 N-m (1288.46 in.lb.) - pulley B

N_B = 5,100 RPM, r_B = 100.5 mm

F_1 = 3050 N (685.7 lb) Belt Tension

F_2 = 1400 N (314.8 lb) Belt Tension

S = 223.7 mm, Belt length between pulleys

n_A = 1.941

Assume belt to extend 0.2% of its length for a load of 11,500 pounds. Determine the angular change, $\Delta\Theta$, of pulley A for an incremental torque, ΔT_A of 1.0 in.lb. Associated incremental force, ΔF_S, increasing the belt length is then:

$$\Delta F_S = (F_1 - F_2) / T_A \quad \text{(F-4)}$$

$$\Delta F_S = (685.7-314.8) / 663.75$$

$$\Delta F_S = 0.559 \text{ lbs/in.lb.}$$

$$\Delta S_A = (\Delta F_S/F)\frac{\Delta L}{L} \ S \quad \text{(F-5)}$$

$$\Delta S_A = (.559/11500)(.002)\ 223.7 = 2.174 \times 10^{-5} \text{ mm/in.lb.}$$

$$\Delta\Theta_A = \Delta S/r_A = 2.174 \times 10^{-5} / 51.8 \quad \text{(F-6)}$$

$$\Delta\Theta_A = 4.20 \times 10^{-7} \text{ radians/in.lb.}$$

$$k_{Belt} = 1/4.20 \times 10^{-7} = 2.38 \times 10^{6} \text{ in.lb./radian}$$

k_A:

$G_A = 12 \times 10^6$ psi , steel

$L_A = 9.61$ inches

$J_A = 0.20$ in^4

$$k_A = G_A J_A / L_A = 12 \times 10^6 (.20)/9.61 = 0.250 \times 10^6 \text{ in.lb./radian} \qquad \text{(F-7)}$$

k_B:

$G_B = 12 \times 10^6$ psi , steel

$L_B = 3.62$ in.

$J_B = 0.25$ in^4

$k_B = G_B J_B / L_B = 12 \times 10^6 \ (0.25)/3.62 = 0.829 \times 10^6$ in.lb./radian

k_S:

$G_S = 12 \times 10^6$ psi , steel

$L_S = .40$ in. (Gear F to Gear H)

$J_S = 3.0$ in^4

$k_S = 12 \times 10^6 \ (3.0)/.40 = 90 \times 10^6$ in.lb./radian

Since $k_S >> k_A$, neglect k_S.

k_E:

$k_E = 1 \ / \ (1/1.941^2 \ (.250) \ 10^6) + (1/(0.829) \ 10^6) + (1/(2.38) \ 10^6)$

$k_E = 0.372 \times 10^6$

$I_A = I_p + I_s + I_g = 0.093 + 0.007 + 0.009$, p = pulley, s = shaft, g = gear (F-8)

$I_A = 0.109$ in.lb.sec^2

$I_B = 0.093 + 0.006 + 0.003$

$I_B = 0.102$ in.lb.sec^2

Lumped Torsional System

$$f = \frac{1}{2\pi}\left[k_E \ (I_A + I_B) \ / \ I_A \times I_B\right]^{\frac{1}{2}} \qquad \text{(F-9)}$$

$$f = \frac{1}{2\pi}\left[0.372 \times 10^6 \ (0.109 + 0.102)/(0.109)(0.102)\right]^{\frac{1}{2}}$$

$f = 423$ c/s = 25390 RPM >> 10,000 RPM

APPENDIX G

UNBALANCE LOAD OF CLUTCH PLATES

USING INVOLUTE SPLINE ENGAGEMENT

Assumptions:

(1) Base analysis on an electric clutch

(2) Use ASA B5.15-1960 - 30 Degree Pressure Angle - Flat Root Side Fit Involute Class 1 Fit (Loose Fit) Tables.[23]

(3) Four Driven Plates - 0.050 inch thick

Pitch Diameter = 4.8000 inch, 12 teeth 2.5/5 Pitch

Internal - Space Width - Max. Actual : 0.6323 inch
Min. Eff. : 0.6283 inch

External - Class 1 Fit - Max. Eff : 0.6263 inch
Min. Actual : 0.6222 inch

TABLE 3[23] - Effective Clearance Min : 0.0020
Max. : 0.0052

Use Radial Movement = 0.0061 inches

(4) Five Driving Plates - 0.050 inch thick

Pitch Diameter = 1.9167 inch, 23 teeth, 12/24 Pitch

Internal - Space Width - Max Actual : 0.1340 inch
Min. Eff : 0.1309 inch

External - Class 1 Fit - Max Eff : 0.1293 inch
Min. Actual : 0.1262 inch

TABLE 2[23] - Effective Clearance Min : 0.0015 inch
Max : 0.0041 inch

Use Radial Movement = 0.0047 inches

Analysis:

1. Base calculation on plate diameters of 4.8000 inch and 4.0625 inch respectively. Assume all plates are positioned in one direction relative to the rotating axis. Calculate the unbalance by increasing the plate radius by the clearance and changing the plate density to reflect the weight change. Thus, for the four driven plates:

$$R = (P.D. + 2\Delta R)/2 \qquad \text{(G-1)}$$

$$R = [4.8000 + 2(0.0061)] / 2 = 2.4061 \text{ inches}$$

$$W = \rho t n \pi R^2 = 0.286\ (0.050)\ 4\pi\ (2.4061)^2 = 1.04034 \text{ pounds} \qquad \text{(G-2)}$$

One half of the plate, W_h, has an additional weight of

$$\Delta W = 2\ R \rho t n\ \Delta r = 2(2.400)(0.286)(0.050)\ 4(.0061) \qquad \text{(G-3)}$$

$$\Delta W = 0.00167 \text{ pounds}$$

The other half, W_L, loses this weight

Thus:

$$W_h = 1.04034/2 + 0.00167 = 0.52184 \text{ pounds}$$

$$W_L = 0.51850 \text{ pounds}$$

The equivalent densities, ρ_h, ρ_L, may then be obtained

$$\rho_h = (0.52184)\ 2/\pi\ (2.4061)^2\ (0.050)\ 4 = 0.28692 \qquad \text{(G-4)}$$

$$\rho_L = 0.28508 \text{ lbs/in}^3$$

2. Centrifugal Forces and Unbalanced Load

Calculate the force F_y, in the y direction due to centrifugal force on one half of the disc having weight, W_h.

$$F_y = m \omega^2 r \sin\theta \qquad \text{(G-5)}$$

$$\Delta F_y = \omega^2 r [\sin\theta]\ \Delta m \ , \quad \Delta m = [\rho/g]\ n t\ r\ \Delta\theta\ \Delta r \qquad \text{(G-6)}$$

Integrating over 180 degrees

$$F_Y = \int dF_Y = 2\omega^2 [\rho/g]\ n t \int_0^R r^2 dr \int_0^{\pi/2} \sin\theta\, d\theta \qquad \text{(G-7)}$$

$$F_Y = 2/3\ [\rho/g]\ n t\ \omega^2 R^2 \qquad \text{(G-8)}$$

The unbalanced load is

$$F_{y_h} - F_{y_L} = [2/3]\, m t \omega^2 R^2 [\rho_4 - \rho_L]/g \qquad \text{(G-9)}$$

At 21000 RPM, ω = 2199 radians/sec, 4 driven plates

$$F_{y_h} - F_{y_L} = [2/3]4(0.050)(2199)^2\ (2.4061)^3\ (0.28692-0.28503)$$

$$F_{y_4} - F_{y_L} = 42.8 \text{ pounds}$$

A similar calculation for the 5 driving plates gives

$$F_{y_h} - F_{y_L} = 29.7 \text{ pounds}$$

Maximum unbalance of plates = 42.8 + 29.7 = 72.5 lbs

3. Plate Arrangement to Obtain Balance Load

The amount of perpherial material per plate may be calculated that corresponds to the unbalanced force. For the driven plates using steel at a density of 0.286 lbs/in^3, this amounts to a volume of 0.00125 in^3 or an area of 0.0249 in^2, having a thickness of 0.050 inch at the periphery of the plate. If this amount or slightly more material were removed from each of the plates, the unbalance per plate is doubled or more. However, by then arranging the four plates — locating the removed material at every 90 degrees would then give a dynamic balanced centrifugal load which should stay balanced due to each plate seeking its maximum unbalanced position.

IV. Buttress Plate - Centrifugal Unbalance

The external buttress plate moves on splines in the current configuration to engage the clutch plates. Calculating the unbalance in the same fashion as given above shows an unbalance load of about 32.4 pounds maximum — at 21000 RPM. This unbalance should be reduced significantly

if it is possible to pilot and move the plate over a cylindrical shaft surface and use the splines to engage the plate of the assembly only. Reducing the clearance to give a maximum eccentricity of 0.001 inch would then reduce the eccentric buttress load to 6.9 pounds at 21000 RPM.

VIII. REFERENCES

(1) Scott, David, International Viewpoints, "DAF Simplifies Belt-Drive Automatic", Automotive Engineering, March 1975, p. 14.

(2) Ibid, "Belt-Drive Automatic Programmed for Economy", Automotive Engineering, August 1978, p. 98, 99.

(3) Ibid, "Belt-Drive CVT for '82 Model Year", Automotive Engineering, February 1980, p. 136-141.

(4) Gogins, L.G. & Russell, C.P., "Mechana-Power: A New Approach to Infinitely Variable Transmissions (Domestic and Foreign Patents in Process), SAE 76 0586.

(5) "Development of an Automotive Hydromechanical Transmission", Weseloh, W.E., et al, Orshansky Transmission Corp., SAE 780688.

(6) Cordner, M.A. & Grimm, D.H., "Hybrid Propulsion System Transmission Evaluation, Phase I, Final Report", Sundstrand Aviation, PB-210057, 25 February 1972.

(7) Baudoin, P., Regie Nationale des Usines Renault, "Continuously Variable Transmissions for Cars with High Ratio Coverage", SAE 790041.

(8) Roark, Raymond J., Formulas for Stress and Strain, McGraw-Hill Book Co., 4th Edition, 1965, Table X, Formula 48.

(9) Shipley, Eugene E., "How to Predict Efficiency of Gear Trains", Gear Design & Application; Nicholas P. Chironis, Editor, McGraw-Hill, 1967, p. 244-249.

(10) Ibid, Benedict, G.H., Kelley, B.W., "How Various Operating Conditions Affect Friction of Gear Teeth", Gear Design & Application, p. 246-249.

(11) Anderson, Neil E., Loewenthal, Stuart H., "Spur-Gear-System Efficiency at Part and Full Load", NASA TP-1622, AVRADCOM TR 79-46, p. 8, 9.

(12) SKF Engineering Data, SKF Industries, Inc., 1968, Form 587-A, 15M, 7-68.

(13) Ibid, Anderson, Neil E., Loewenthal, Stuart H., p. 10.

(14) "Magnesium: The Ultimate Weight-saving Metal?", SAE March 1980, Vol. 88, No.3, p. 66.

(15) Hillquist, R.K., "Sound Measurement Standards for Surface Transportation Vehicles," Noise Control Engineering, May-June 1979.

(16) Von Hey de Kampf, G.S., "Damping Capacity of Materials", Proceedings, ASTM, Vol. 31, Part 2, 1931.

(17) Hermann, J., "The Effect of the Casing on Noise Radiated from Gear Boxes and Constructive Measures for its Reduction", Doctorate Thesis, Rhein Westphalia Technical High School.

(18) Timoshenko, S., Strength of Materials, Part II, Advanced Theory and Problems, 2nd Edition, D. Van Nostrand Co., Inc., 1941, Deflection of Curved Bars, p. 79-82.

(19) Marco, S.M., Starkey, W.L. & Hornung, K.G., "A Quantitative Investigation of the Factors which Influence the Fatigue Life of a V-Belt" Trans, ASME, Journal of Engineering for Industry, Feb. 1960, p. 47-58.

(20) Spotts, M.F., Design of Machine Elements, Prentice-Hall, Inc., 5th Edition, 1978, Figure 1-15, Item 14, p. 24.

(21) Ibid, Spotts, M.F., Figure 1-15, Item 7, p. 23.

(22) Vierck, R.K., Vibration Analysis, 2nd Edition, Harper & Row, Pub., p. 311,312.

(23) Involute Splines, Serrations & Inspection, ASA B5.15 - 1960, ASME Publisher.